AFGL-TR-77-0248

ERROR ANALYSES OF OPERATIONAL SATELLITE
SOUNDINGS OF VERTICAL TEMPERATURE PROFILES

Wayne D. Mount
B. Richard Fow
Donald E. Gustafson
William Ledsham

Geo-Atmospherics Corporation
Box 177
Lincoln, Massachusetts 01773

Final Report
12 January 1977 to 30 September 1977

31 December 1977

DDC
RECEIVED
MAR 13 1978
B

SECURITY CLASSIFICATION OF THIS PAGE (When Data Entered)

REPORT DOCUMENTATION PAGE	READ INSTRUCTIONS BEFORE COMPLETING FORM

1. REPORT NUMBER	2. GOVT ACCESSION NO.	3. RECIPIENT'S CATALOG NUMBER
AFGL-TR-77-0248	DF248610	

4. TITLE (and Subtitle)	5. TYPE OF REPORT & PERIOD COVERED
ERROR ANALYSES OF OPERATIONAL SATELLITE SOUNDINGS OF VERTICAL TEMPERATURE PROFILES.	Final, 12 January ~ 30 September 1977
	6. PERFORMING ORG. REPORT NUMBER
	GAC-78-CR-001

7. AUTHOR(s)	8. CONTRACT OR GRANT NUMBER(s)
Wayne D. Mount, B. Richard Fow, Donald E. Gustafson* and William Ledsham	F 19628-77-C-0118

9. PERFORMING ORGANIZATION NAME AND ADDRESS	10. PROGRAM ELEMENT, PROJECT, TASK AREA & WORK UNIT NUMBERS
Geo-Atmospherics Corporation Box 177 Lincoln, Massachusetts 01773	62101F 7670-09-03

11. CONTROLLING OFFICE NAME AND ADDRESS	12. REPORT DATE
Air Force Geophysics Laboratory Hanscom AFB, Massachusetts Francis Valovcin/Monitor/OPI	31 December 1977
	13. NUMBER OF PAGES
	184

14. MONITORING AGENCY NAME & ADDRESS(if different from Controlling Office)	15. SECURITY CLASS. (of this report)
	Unclassified
	15a. DECLASSIFICATION/DOWNGRADING SCHEDULE

16. DISTRIBUTION STATEMENT (of this Report)

Approved for public release; distribution unlimited.

DDC RECEIVED MAR 13 1978 B

17. DISTRIBUTION STATEMENT (of the abstract entered in Block 20, if different from Report)

18. SUPPLEMENTARY NOTES

* Scientific Systems, Inc.
1640 Massachusetts Avenue
Cambridge, Massachusetts 02138

19. KEY WORDS (Continue on reverse side if necessary and identify by block number)

Satellite	Infrared Transmittance
Remote Probing	Water Vapor
Temperature Retrievals	Underlying Surface
Infrared Radiance	Temperature Profile Errors

20. ABSTRACT (Continue on reverse side if necessary and identify by block number)

Satellite observations have the ability to determine meteorological conditions over inaccessible or unfriendly territory. The Defense Meteorological Satellite Program (DMSP) has two satellites (Bird 8531 and 9532) that provide infrared radiance data on a routine basis for operational applications at the Air Force Global Weather Center (AFGWC). Multi-spectral infrared radiometers operating at →next page

DD FORM 1473 1 JAN 73   EDITION OF 1 NOV 65 IS OBSOLETE

cont. identical wavelengths on each of the satellites are used to interrogate different depths in the atmosphere to derive air temperature profile information. AFGWC has a sophisticated computer program that operates upon satellite radiance observations using their 12-hour forecast temperature fields as a first guess to derive a measure of the temperature profile. Errors are especially noticeable in the lower troposphere near the earth's surface and in the tropopause region. This report describes an analytical and a statistical approach to isolate the largest error sources and to suggest promising avenues for operation improvement. A research version of SOUNDER, the AFGWC operational computer program, was formulated and used to systematically analyze physical, computational, and hardware contributions to errors in the retrieval of temperature profiles. It was found that radiance observations from Bird 8531 were higher (warmer) than for Bird 9532 in seven of the eight sensor channels. The present operational criteria used to eliminate low level clouds or hot surface are so restrictive that many of the most significant types of atmospheric temperature profiles are also eliminated. Water vapor contributions to errors can be large in the tropics, worthy of consideration in mid-latitudes, and insignificant in the polar regions. Temperature retrieval errors due to water vapor are most pronounced at the 700 mb level. Underlying surface effects are not properly taken into account. These surface effects provide the greatest single error source for AFGWC's operational routines for satellite temperature retrievals in the lower troposphere. It is shown that these surface effects have an influence on all sensor channels and are related to the low level atmospheric stability conditions. Statistical models were developed and compared with the minimum information technique in current use at AFGWC for temperature retrievals. Significant error reductions are possible using the statistical methods. It appears that statistical coefficients derived from one week of data can be used with confidence during the subsequent week to derive temperature profiles from multi-channel satellite radiance data.

PREFACE

We want to express our gratitude to Mr. Francis Valovcin,
Mr. Vincent Falcone, Dr. Jean King and Dr. Robert McClatchey of Air
Force Geophysics Laboratory and Captain William Smith and Captain
Thomas Kyle of the Air Force Global Weather Central for valuable
discussions and use of their data bases.

Contents

7

11

1 INTRODUCTION

1.1 GENERAL

1.1.1 Overview

Meteorological observing station density increases have improved weather analysis and forecast accuracy. Many uninhabited regions of the world exist, especially over ocean and polar regions, that can be interrogated remotely from satellites to obtain weather information. The Defense Meteorological Satellite Program (DMSP) has provided routine observations of weather phenomena on a scale never before attainable. Improvements in the aviation weather variables of cloud, fog, and significant weather depiction have been obtained. The advent of multi-frequency infrared radiometric sensors, operating on absorption/emission bands of atmospheric constituents, has opened new horizons for remotely probing the vertical structure of the atmosphere. This has been especially true for remotely probing the vertical temperature profile which plays an important role in specifying atmospheric stability that is so important to numerical weather prediction. Performance of present methods for remotely deriving temperature profiles from satellites has been questioned. Even for cloud free lines of sight, large errors exist in attempting to retrieve air temperatures from satellite radiance data. These large errors are especially noticeable in the lower troposphere near the surface and in

15

the tropopause region separating the troposphere from the stratosphere. It is the source of these large errors and the identification of promising corrective methods that received emphasis in this study.

Two methods of approach taken in this study included analytical and statistical techniques. An analysis was made of Air Force Global Weather Central's (AFGWC) "SOUNDER" computer program package for operationally retrieving temperature profiles from 12-hour forecast and satellite data inputs. A Geo-Atmospherics Corporation (GAC) research version of SOUNDER was developed and used to perform a sensitivity analysis of the response of SOUNDER to accurate and contaminated data, error source discrimination criteria, solution convergence procedures, sensor noise and errors, water vapor, and underlying surface effects. A statistical analysis was made on a large two week February 1975 northern hemisphere data base at Air Force Geophysics Laboratory (AFGL). Data files of cloud free satellite soundings and "nearby ground truth" grid point temperature analyses were generated and used to derive and verify stepwise regression equations for retrieving air temperatures from satellite data.

Serious sources of large errors were identified, especially those due to underlying surface effects, and promising methods for error reduction were demonstrated. Significant reductions in the rms error at

all levels in the atmosphere were obtained with the statistical models. The remainder of this report provides background information, details of SOUNDER, discussion of analytical and satistical results, and a list of conclusions and recommendations.

1.1.2 Background

The problem of obtaining vertical temperature profiles from passive satellite sensors has been the object of much study for almost 20 years. Kaplan [1] first suggested that spectral measurements in the 15μ m CO_2 band could be used for temperature soundings. The first experimental verification came 10 years later with the launch of the Nimbus 3 satellite. Since that time, a number of other satellites capable of such measurements have been launched, including the SSE package utilized in the DMSP.

The ability to perform accurate soundings on a world-wide basis is an important element in meeting the desire of the Air Force to achieve a continuous world-wide weather analysis and prediction capability. Temperature profiles are also an element in predicting likelihoods of cloud type and cover.

1.1.3 Approaches to Temperature Inversion

Two basic approaches are used for temperature inversion. These may be classified as:

    (1) Atomistic Approach

    (2) Holistic Approach

The atomistic approach is based on the use of micromodels. All known physics is used, including equations of radiative transfer, hydrostatic equation and Planck's equation. Mixing ratios of the various atmospheric constituents are computed and explicit calculations are made to include the effects of temperature on liquid water content. Computations are based either on physical laws or empirically derived relations. Modifications are made on the microsystem level in order to obtain a better microsystem (subsystem) model. The minimum-information method[2] is an example of an atomistic method of temperature retrieval. Other examples are Chahine's method[3] and Smith's nonlinear iterative method.[4]

The holistic approach utilizes an information model. Models are built up which _best_ fit the needs of the application at hand. For the temperature inversion problem, holistic methods are statistical in nature and are based on achieving the best inversions as determined via testing on an independent data base. Examples of holistic inversion methods are the statistical eigenvector method (Smith and Woolf)[5] and regression analysis.

It should be mentioned that some methods are a combination of atomistic and holistic methods. For example, the "full statistical" method (Fritz et al.)[6] uses both transmittance functions and temperature and radiance covariance matrices. It should be pointed out, however, that the minimum-information method is not a holistic approach even though it is usually thought of as a special case of the "full statistical" approach. This is due to the fact that the scalar "noise-to-signal power" ratio is selected on the basis of expected calibration errors and expected errors in the guessed radiances (Smith, Woolf and Fleming).[2] In the holistic approach, this parameter would be chosen, for example, to minimize the mean-squared prediction errors in the vertical temperature profiles, using an independent data base for performance testing.

18

Based on this discussion, it is clear that the essential difference between the two methods is the way in which models are built up. Every temperature inversion technique requires a model which relates the measured radiances and the vertical temperature profile. The model may or may not include other parameters, such as season, latitude, scanning pattern, initial forecast field, and so forth. The essential difference in the methods is that, in the atomistic approach the model is developed based on physical models using little or no actual data. On the other hand, the holistically-derived model is based on analysis of a significant amount of actual data for which independent verification may be obtained.

Neither the atomistic nor the holistic approach offers a panacea for all problems and the choice of method depends upon both the nature of the problem and the availability of a representative data base. For initial development, an atomistic approach is almost mandatory, since little or no actual data is available. However, as data becomes available, the use of a holistic method should be considered.

The development of methods for temperature retrieval has, in fact, followed this path. The most widely used technique is the minimum-information technique, used in conjunction with the empirical correction technique of Weinreb and Fleming.[7] Empirical and physical models are used for computation of the transmittances. Several hybrid techniques were then tested. Fleming and Smith[8] compared the iterated "full statistical" method to the iterated minimum-information method, the iterative nonlinear method of Chahine[9] and a general nonlinear iterative method. Experimental evaluation indicated that the "full statistical" method gave the best overall performance. This is an interesting result since this is the only method, of the four analyzed, which included statistical information based on actual data in the model.

In another related study, Crosby and Weinreb[10] compared the performance of the "full statistical" method and the minimum-information method for December-January data. Their results indicated that minimum information retrievals were uniformly worse, with rms differences of up to $1°K$ in the region between 200 and 300 mb and about $1/2°K$ above 300 mb. However, there was also a degradation of about $1°K$ at 800 mb.

19

Malkevich, et al.[12] used empirical orthogonal functions in a linear regression model to estimate temperature profiles. The empirical functions were found by using the kernel function of the integrated form of the equation of radiative transfer.

Recently there has been an increasing interest in the use of statistical methods. Smith and Woolf[5] used a statistical eigenvector method for estimation of vertical profiles of temperature, moisture and cloudiness. Comparisons with the minimum-information method indicated that the rms error in predicting cloud-free brightness was significantly reduced with the statistical eigenvector method. Klein, Kyle and Smith[12] compared the minimum-information and statistical eigenvector methods on operational SSE data and concluded that, on the basis of the data studied, neither could be strongly recommended over the other. The statistical eigenvector solution was better for tropical soundings and in the lower troposphere. At mid-latitudes, the minimum-information solution was better between 250 and 500 mb but poorer elsewhere.

In yet another study, Smith[13] investigated the effect of measurement noise on both the minimum-information and statistical eigenvector retrievals. Both were found to be very sensitive to noise, if the model did not account for the noise. The sensitivity was substantially reduced when the noise was accounted for, however.

1.2 METHODS OF ANALYSIS

1.2.1 Theoretical Model for Temperature Retrieval through a Cloudless Atmosphere

For a non-scattering cloud-free atmosphere in local thermodynamic equilibrium, the integral form of the radiative transfer equation is

$$N(\nu) = B[\nu, T(p_s)] \, \tau(\nu, p_s)$$

$$- \int_0^{x(p_s)} B[\nu, T(p)] \, \frac{d\tau(\nu, p)}{dx(p)} \, dx(p) \tag{1.1}$$

where

> $N(\nu)$ = outgoing spectral radiance within a spectral window centered at frequency ν
>
> $B[\nu,T]$ = Planck radiance for temperature T at frequency ν
>
> $\tau(\nu,p)$ = transmittance of the atmosphere above pressure p
>
> $x(p)$ = arbitrary monotonic function of p
>
> p_s = atmospheric pressure at the earth's surface

The objective is to solve (1.1) for T(p) given a finite set of radiance measurements $N(\nu_1)$, $N(\nu_2)$,....$N(\nu_k)$. One significant problem in (1.1) is the nonlinear dependence of $B[\nu,T(p)]$ on $T(p)$:

$$B[\nu,T(p)] = \frac{C_1 \nu^3}{\exp\left[\dfrac{C_2}{T(p)}\right] - 1} \tag{1.2}$$

where C_1, C_2 are known constants. The problem may be linearized by noting that, in the infrared region and at terrestrial temperatures, the variation of B due to changes in ν is much less than the variation due to T.

The variables may be separated by first computing the brightness temperature $T_B(\nu)$ from (1.2):

$$\begin{aligned} T_B(\nu) &= B^{-1}[\nu,N(\nu)] \\ &= \frac{C_2 \nu}{\ln\left[\dfrac{C_1 \nu^3}{N(\nu)} + 1\right]} \end{aligned} \tag{1.3}$$

The variables may then be separated by normalizing the measured spectral radiance to the black-body equivalent at a reference frequency ν_r:

$$N_r(\nu) \triangleq B[\nu_r, T_B(\nu)] \tag{1.4}$$

Then a normalized version of (1.1) may be solved:

$$\begin{aligned} N_r(\nu) &= B[\nu_r, T(p_s)]\tau(\nu,p_s) \\ &\quad - \int_0^{x(p_s)} B[\nu_r, T(p)] \frac{d\tau(\nu,p)}{dx(p)} \, dx(p) \end{aligned} \tag{1.5}$$

21

In this form, the equation is linear in $B_r(p) = B[\nu_r, T(p)]$. Once $B_r(p)$ has been found, the temperature profile estimate is found by using Planck's equation:

$$T(p) = B^{-1}[\nu_r, B_r(p)] \tag{1.6}$$

1.2.2 Minimum Information Method

In the minimum information method, (1.5) is written in a perturbed form by using the initial guessed profile. Denoting the first guess profile by $T_0(p)$, we have from (1.5):

$$N_0(\nu) = B[\nu_r, T_0(p_s)]$$

$$- \int_0^{x(p_s)} B[\nu_r, T_0(p)] \frac{d\tau(\nu, p)}{dx(p)} \, dx(p) \tag{1.7}$$

Then it is assumed that $T_0(p_s) = T(p_s)$ by virtue of the fact that accurate surface temperature estimates are available from the "window channel" measurements. With this assumption, the perturbed equation is

$$\Delta N(\nu) = N_r(\nu) - N_0(\nu)$$

$$= \int_0^{x(p_s)} \Delta B[\nu_r, T(p)] \frac{d\tau(\nu, p)}{dx(p)} \, dx(p) \tag{1.8}$$

where

$$\Delta B[\nu_r, T(p)] = B[\nu_r, T(p)] - B[\nu_r, T_0(p)] \tag{1.9}$$

Now by using numerical quadratures, (1.8) can be written in the form

$$n_i \stackrel{\Delta}{=} N(\nu_i)$$

$$= \sum_j \Gamma_{ij} b_i; \ i = 1, 2, \ldots, M \tag{1.10}$$

where

$$b_j = \Delta B[\nu_r, T(p_j)] \tag{1.11}$$

and Γ_{ij} is computed as a function of $x(p)$ and the integration rule. In practice x is chosen to be proportional to $p^{2/7}$, which gives essentially

22

equally-spaced intervals. Then, using trapezoidal integration:

$$\Gamma_{ij} = 0.5 \begin{cases} \tau_{ij} - \tau_{i,j+1} & ; \; j=1 \\ \tau_{i,j-1} - \tau_{i,j+1} & ; \; 1<j<L \\ \tau_{i,j-1} + \tau_{i,j} & ; \; j=L \end{cases} \tag{1.12}$$

where $\tau_{ij} = \tau(\nu_i, p_j)$ and p_j is ordered monotonically increasing with j. Thus j=1 corresponds to the top of the atmosphere (10 mb in this study), while j=L denotes the 1000 mb pressure level. For DMSP, L = 70.

It is convenient to write (1.10) in vector form as

$$n = \Gamma b \tag{1.13}$$

where n is an M-dimensional column vector of radiance variations, b is an L-dimensional column vector of brightness temperature variations and Γ is the matrix of transmittance functions. Since, in practice, L > M, the problem of inverting (1.13) to find b is ill-conditioned and the solution is non-unique. However, once a solution for b is found, the temperature profile can be found by using (1.1), (1.9), and (1.6).

In order to find an appropriate value of b, consider the following generalized least squares problem. We wish to find b to minimize

$$J(b) = b^T E^{-1} b + (n-\Gamma b)^T R^{-1} (n-\Gamma b) \tag{1.14}$$

where E and R are positive definite symmetric matrices. The value of b which minimizes J(b) is

$$\hat{b} = E\Gamma^T (\Gamma E \Gamma^T + R)^{-1} n \tag{1.15}$$

This equation may be interpreted in terms of Bayesian estimation theory if several assumptions are made. Assume that b is a zero mean Gaussian random variable with covariance matrix E. Similarly assume that $n - \Gamma b$ is a zero-mean Gaussian random variable with covariance matrix R. Then $\hat{b}$ is the conditional mean of b given n and is also the minimum-variance estimate of b. Eq. (1.15) is also in the form of the measurement update equation for the celebrated Kalman Filter (Kalman[14]). In practice the values of E, R and Γ will not be known precisely and the random variables will not in general be Gaussian. Nevertheless, this technique can yield quite good performance. In the vertical temperature retrieval

23

literature, (1.1) forms the basis of the "full statistical" method
(cf. Fritz et al.[6]) and is generally used several times in an attempt
to iteratively converge to the correct solution.

The minimum information method uses a special case of (1.15)
and is found by setting

$$E = \sigma_E^2 I, \ R = \sigma_R^2 I. \tag{1.16}$$

Then

$$b_{mi} = \Gamma^T (\Gamma\Gamma^T + \gamma I)^{-1} n \tag{1.17}$$

where $\gamma = \sigma_R^2/\sigma_E^2$ is the "noise-to-signal" power ratio. This solution was
considered by Foster (1.15) who noted that it corresponded to a maximum
entropy ensemble in which there is a minimum of information regarding the
statistical characteristics of the random variables b and n. This is
equivalent to the assumption of isotropic scattering about the mean for
each random variable and further that the random variables, under the
Gaussian assumption, are independent.

Twomey[10] investigated problems of this type and suggested
the use of a trial solution. The final solution would then be constructed
to minimize the deviation from the trial solution. The elements of this
process are present in both the "full statistical" and the minimum-informa-
tion solutions. As $E \to 0$ (or $\gamma \to \infty$) for fixed R, $b \to 0$ and the estimated
temperature profile approaches the initial guessed profile. This also
holds if $R \to \infty$ with E held fixed. In this case either the confidence in
the initial guessed profile is high or the measurements are extremely bad.

The opposite situation occurs when confidence in the initial guess
is low ($E \to \infty$, with R fixed) or the measurements are extremely good ($R \to 0$,
with E fixed). In either case $\gamma \to 0$ and $\hat{b}$ is obtained via the pseudoinverse:

$$\hat{b} = E\Gamma^T (\Gamma E\Gamma^T)^{-1} n \tag{1.18}$$

Note that $n = \Gamma\hat{b}$, thus satisfying (1.13), and in addition the
weighted cost

$$J(b) = b^T E^{-1} b \tag{1.19}$$

is minimized.

This method is also closely related to the method of Backus and
Gilbert[17] who investigated the non-uniqueness problems associated with

determination of fine geophysical structure from gross earth data measurements. In their method, they find a solution $\hat{b}$ which minimizes the quadratic cost

$$(\hat{b}-b_0)^T \; W^{-1} \; (\hat{b}-b_0) \tag{1.20}$$

where b_0 is the guessed brightness profile and W is a positive-definite symmetric weighting matrix. They also constrain the estimated measurements to correspond to the actual measurements:

$$\hat{n}(\hat{b}) = \tilde{n} \tag{1.21}$$

where $\tilde{n}$ denotes the vector of actual radiance measurements. The solution is found by using the following iteration:

$$\hat{b}^{(k+1)} = \hat{b}^{(k)}$$
$$+ \; WG^{(k)\;T} [G^{(k)}WG^{(k)T^{-1}}] \cdot$$
$$[\tilde{n} - \hat{n}(\hat{b}^{(k)}) - G^{(k)}(b_0 - \hat{b}^{(k)})] \tag{1.22}$$

where

$$G^{(k)} = \left. \frac{\partial \hat{n}}{\partial \hat{b}} \right|_{\hat{b}^{(k)}} \tag{1.23}$$

Note that $G^{(k)} \approx \Gamma$ from (1.13). This iteration is thus similar in form to the "full statistical" approach except that an additional term $G^{(k)}(b_0 - \hat{b}^{(k)})$ is present. However, the fundamental difference is that $\hat{n}(\hat{b}) \to \tilde{n}$, while in the full statistical or minimum-information approach (1.21) is never satisfied. It is interesting to note that in their numerical studies, Backus and Gilbert simplified (1.22) by assuming $b_0 = \hat{b}^{(k)}$. This is precisely what is done in the iterated "full statistical" and minimum-information methods, namely, at each step, the best estimate of the initial profile is set to the estimate on the previous iteration. With this assumption, the method of Backus and Gilbert reduces to (1.18) under the assumptions $W = E$ and $G^{(k)} = \Gamma$. It is interesting to note that their method does not explicitly account for statistical uncertainty in the measurements as do the "full statistical" and minimum-information methods.

The minimum-information solution is seen to offer a compromise between using the initial guess profile and matching the guessed and measured radiances. The virtue of using the first guess profile is that erroneous atmospheric waves which may be generated as a result of ill-conditioning are suppressed. However, this smoothing effect can lead to biases in the troposphere under partially cloudy conditions. [2]

The DMSP temperature retrievals are performed in the SOUNDER program, in which up to five iterations of (1.17) are made. Using the notation

$$C = \Gamma^T (\Gamma \Gamma^T + \gamma I)^{-1}$$

the iterations proceed as follows. On the kth iteration

$$T^{*(k)} = T^{*(k-1)} + C[\tilde{n} - \hat{n}^{(k-1)}]$$

where T^* is the brightness temperature computed from the temperature profile via Planck's equation, $\tilde{n}$ is the measured spectral radiance vector, and $\hat{n}^{(k-1)}$ is the predicted radiance found from $T^{*(k-1)}$ and the radiative transfer model. The surface temperature estimate is not iterated. The iteration terminates when the radiance deviation in each channel falls below a preset threshold. In DMSP, all thresholds are set equal. It should be pointed out that this may lead to problems, since the uncertainty associated with each channel is not the same. Inspection of individual iterations reveals that channels 1,2,3 are almost invariably the last to meet the threshold requirement, which is in intuitive agreement with the fact that expected errors for these channels are greater. This may induce errors larger than necessary in the temperature estimates above 200 mb.

1.2.3 Regression Analysis

The use of regression analysis is a powerful tool in analyzing the relationships between sets of variables of different types. In the present problem, we are interested in analyzing the relationship of vertical temperature profiles, actual measured spectral radiances, initial forecast fields (first guess fields) and the TTPACK analysis.

The several objectives of the analysis were:

(1) Investigate the information content of the initial forecast field and spectral radiances relative to vertical temperature profiles.

26

(2) Perform a validation study of the minimum-information technique relative to an optimum linear processor.

(3) Develop methods for improving the minimum-information technique.

(4) Perform analyses to determine robustness of estimators.

It was decided that regression analysis would be used for developing statistical models rather than principal components (statistical eigenvector methods) for several reasons. First, a weakness of the principal components methods is that it depends on the units of measurement. If a variable is measured in such small units that its numerical values dominate those of the other variables, the first principal component will essentially reflect the behavior of this variable. This is sometimes handled by normalizing each variable to zero mean and unit variance. However, the correct weighting to be given to each variable is not clear, since it depends on the nature of the problem. The most significant variables might be given higher weighting. In the sounding problem, this is equivalent to saying that accurate temperature retrievals may be more important in certain pressure regions than in others. Secondly, by working in the natural units of the problem, the results are made easier to interpret. Thirdly, the first few principal components computed by Smith and Woolf[5] and Smith[13] looked sufficiently similar to the transmission functions to indicate that regression models may be competitive in practice. Finally, the objectives of this study were limited to investigation of the minimum-information solution and methods of improvement rather than investigation of the many possible alternatives to temperature retrievals.

1.2.3.1 Regression Models

Two different regression models were utilized in an attempt to assess the performance of the minimum information solution. For temperature, the estimate for the ith level is

$$\hat{T}_i = \sum_{j=1}^{13} \alpha_{ij} T_{oj} + \sum_{k=1}^{8} \beta_{ik} r_k + \gamma_i; \quad i = 1,\ldots,13$$

where T_{oj} is the first guess at the jth level and r_k is the measured spectral radiance for the kth channel. The coefficients α_{ij}, β_{ik} and γ_i are determined by means of a stepwise regression technique in which only the most significant

27

coefficients are retained in the model. The units for temperature are °C and the units for the radiances are ergs $(cm^2 - sec - ster - cm^{-1})^{-1}$.

For estimating heights, the model is

$$\hat{H}_i = \sum_{j=1}^{13} \delta_{ij} H_{oj} + \sum_{k=1}^{8} \varepsilon_{ik} \tau_k + \tau_i; \quad i=1,\ldots,13$$

where H_{oj} is the first guess height (in ft) at the jth level. The regression coefficients δ_{ij}, ε_{ik} and τ_i are found by the same stepwise regression method used for the temperature estimates. The regression method used was performed by the program RLSEP, which was available at AFGL as part of the International Mathematical Statistics Library (IMSL).

It is important to point out that the regression method implicitly takes into account empirical linear correction techniques, such as the method of Weinreb and Fleming. [7] In this method the observed systematic disagreeement between temperature inversions and RAOBs is reduced by employing a linear correction to the spectral radiances. With the usual relation between brightness temperature and radiances given as

$$b = Cn,$$

Weinreb and Fleming proposed adding a term to n to give

$$b' = C(n + \delta n)$$

The value of δn was then found using a least squares fit to a set of actual RAOB data. This method is used in the AFGWC SOUNDER program. The necessity of using such a technique is an indication of the use of statistical methods in present use and of the usefulness of statistical techniques in general.

1.2.3.2 Stepwise Regression

In computing linear regression models, it is important to determine the effect of using different subsets of independent variables. It is desirable to use only those variables which significantly reduce the regression errors. Overfitting can lead to models which are overly sensitive to noise. Stepwise regression provides a partial automation of the variable selection process. It is based on a technique which in the process of computing an ordinary regression on m predictors obtains, at essentially no extra expense, m intermediate regressions which are useful in determining functional relationships between the dependent variable (temperature or height)

and several selected subsets of the total set of independent variables, or predictors. In the simplest case, one variable is added at each step. There are several meaningful statistical criteria which may be used to determine which predictor variable to add to the model:

> (i) add the predictor whose F-to-enter statistic has the largest value.
>
> (ii) add the predictor that gives the greatest decrease in the residual sum of squares.
>
> (iii) add the predictor which gives the greatest increase in the multiple correlation between the dependent variable and the predictors.

The F-to-enter statistic for a predictor is the F-statistic for testing the significance of the regression coefficient the predictor would have if it were added. All four of these criteria are, in fact mathematically equivalent; however the F-to-enter statistic was used in programs utilized in this study.

In addition to adding variables it is also desirable to provide for removal of variables. It may happen that recently added variables may in combination render a variable entered at an earlier state statistically insignificant. Removal of variables is based on an F-to-remove test. In the stepwise regression procedure, the test for removal of predictors is first made for each predictor already in the model. If a predictor is removed, the program proceeds to the next step. If no predictor is removed, the step continues with the addition of a predictor. The stepwise regression procedure terminates when no predictor is either deleted or added at a step. The details of the stepwise regression procedure may be found, for example, in Draper and Smith.[18]

1.2.4 Discussion of DMSP Analysis

A simplified information flow diagram for the DMSP minimum-information technique is shown in Fig. 1.1, depicting the major inputs, outputs, computing blocks and parameters.

As a result of investigating the minimum-information techniques and discussions with AFGL and AFGWC personnel, several possible sources of error have been defined. In approximate order of decreasing significance

29
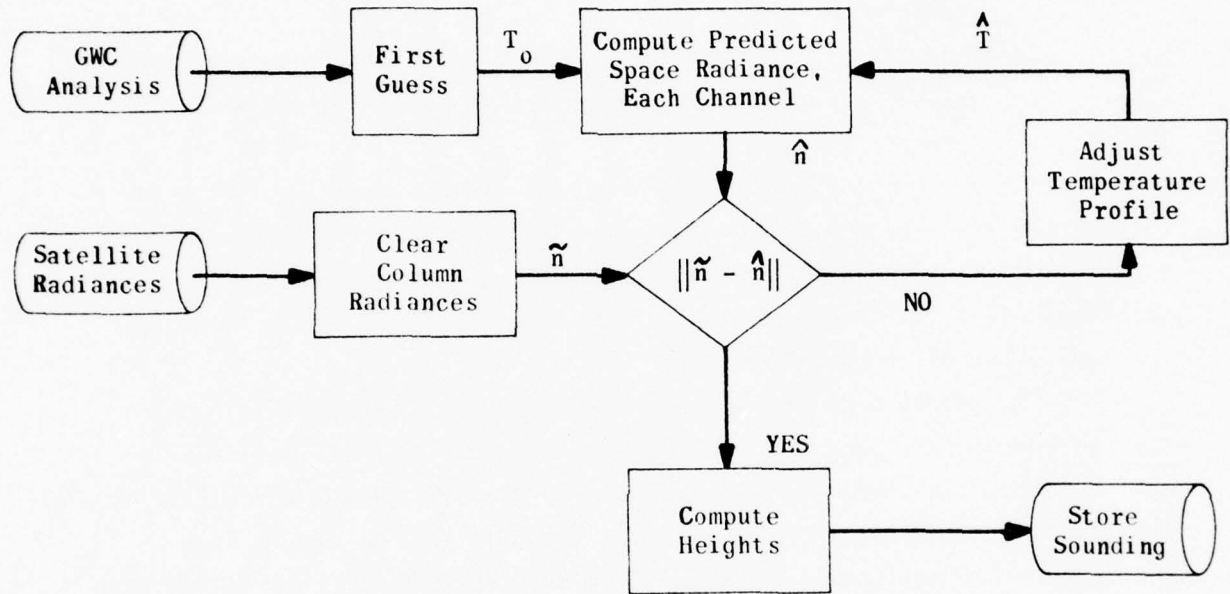
Figure 1.1 Information Flow For Minimum-Information Technique

they are:

   (1) <u>Clouds</u>. Currently, the DMSP software selects a
       single candidate sounding from each 240 nautical mile
       grid point to generate the clear column radiance file.
       This candidate is chosen purely on the basis of the ratio
       of the observed radiance of an upper air channel to the
       window channel. While this test is employed to eliminate
       cloudy areas, discussions with AFGL personnel indicated that
       considerable cloud contamination may occur. Future work will
       be necessary to define and evaluate cloud contaminant reduc-
       tion techniques, such as the adjacent field method.

   (2) <u>Water Vapor Correction.</u> The transmittance functions of
       the atmosphere are not updated for the contribution of
       water vapor arising from changes in the temperature of the
       profile (via a constant mixing ratio assumption) as the algorithm
       proceeds.

   (3) CO_2 <u>Transmittance</u>. Errors in τ_{CO_2} cause errors in the
       inversion process since this parameter is used directly
       in the inversion. At present, no temperature dependence is
       assumed.

   (4) <u>Temperature Profile Adjustment</u>. The principal sources of
       error here appear to be the problem of determining the trans-
       mittance matrix Γ accurately and defining a more complete
       error model.

   (5) <u>Empirical Corrections</u>. This technique is used to correct
       for bias before the inversion is performed.

   (6) <u>Channel Width/Frequency</u>. Errors in assumed channel center
       frequency and width cause errors in the computed temperature
       profile.
       Other possible sources of error include level conversion,
       layer spreading, and earth location.

The minimum-information solution which is being used for temperature
inversion is a prime candidate for a source of a significant percentage of the
observed errors. One of the assumptions employed in the model is that the

31

errors associated with each IR channel have equal variances. (cf. Section 1.2.2). The accuracy of this assumption is questionable. Another assumption, which is more questionable, is that the temperature estimation errors associated with each pressure level are of equal variance. It is further assumed in the model that all errors (both radiance measurement and temperature inversion) are uncorrelated. This assumption does not appear to be met in practice.

The transmittance matrix Γ is formed by taking differences of the transmission functions, so that errors in the transmission functions translate directly in errors in the transmittance matrix. One source of error is the assumption that Γ is independent of temperature. Also, Γ is determined using models of water vapor transmittance, ozone transmittance and CO_2 transmittance and thus is dependent on accuracy of all of the models.

The minimum-information solution may be modified by doing several things. First, the adequacy of the noise models should be validated. This has been done by performing statistical analyses on the data available at AFGL. Covariance matrices for both the measurements and estimation errors have been estimated.

The matrix Γ can also be adjusted to achieve better performance. Two criteria can be used; (1) variance matching, (2) whiteness tests. Variance matching is easier to perform, but whitening the residuals (difference between measurement (radiance) and estimated measurement (brightness temperature), is a more powerful approach. A hybrid approach which is similar to whitening the residuals is used in the sequel to study the properties of the minimum-information method.

Another problem with the minimum-information method is that it is, in its present form, an ad hoc approach. From a Bayesian point of view, only a single iteration need be taken since the model is linear with no dynamics and a single vector measurement. This problem has been addressed implicitly in this study by comparing minimum-information retrievals with statistical non-iterative methods.

32

2 MINIMUM INFORMATION TECHNIQUE AT AFGWC

The minimum information technique is part of an AFGWC software system called E-package or EPKG. Most of the subprogram components of the system are written in the language of FORTRAN V and in the particular dialect which is resident on the UNIVAC 1100 Series Operating System. Extensive use has been made of the unique features of FORTRAN V and 1100 Operating System in the EPKG. Because of this, implementation of the EPKG on other systems would be a very involved process and difficult, particularly if undertaken by one not familiar with the UNIVAC Operating System and FORTRAN V.

The procedures, calculations, etc. which constitute the minimum information technique are embodied in the main program SOUNDER and its associated subprograms of the EPKG. An annotated flow diagram showing the major procedural and computational steps in SOUNDER is given in section 2.1. The functions of the simpler subprograms called by SOUNDER are described on the flow diagram. The functions of the more complex subprograms are described in sub-sections of 2.1 verbally, diagrammatically or by a combination of these forms.

2.1 MAIN PROGRAM SOUNDER

The following annotated flow diagram shows the major pro-
cedural and computational steps in SOUNDER which relate to the im-
plementation of the minimum information technique. The operations of
SOUNDER which deal with the locating or addressing and storage and
retrieval of data from the AFGWC data bases are not shown. The
decision criteria described as well as the values quoted for constants
and test variables were those in use in the operational version at AFGWC
as of 1 April 1977.

Various levels of detail have been used in describing the
operations in SOUNDER and its subprograms. The general guidance used
in determining the level of description detail was the specificity and/or
uniqueness of the operation to the implementation of the minimum in-
formation technique at AFGWC. For example, subprogram elements
ITERAT, H2OTAU, and COFWGT are described in considerable detail as
they constitute the essence of the minimum information technique. On
the other hand, subprogram elements THKNES, MANTMP, and TRPFIN
which employ techniques familiar to most meteorologists for the deter-
mination of thicknesses, the height and temperatures of mandatory

34

levels and the location of the tropopause from lapse rate changes are described very briefly. In between these two extremes are subprogram elements INITMP and SMOOTH which, although for the most part use conventional meteorological procedures, also have a few somewhat unique but critical functions in the implementation of the minimum information technique.

START

Determine
month of
year

READY-
RADIANCE
FILE

EPKG
STATISTICS
FILE
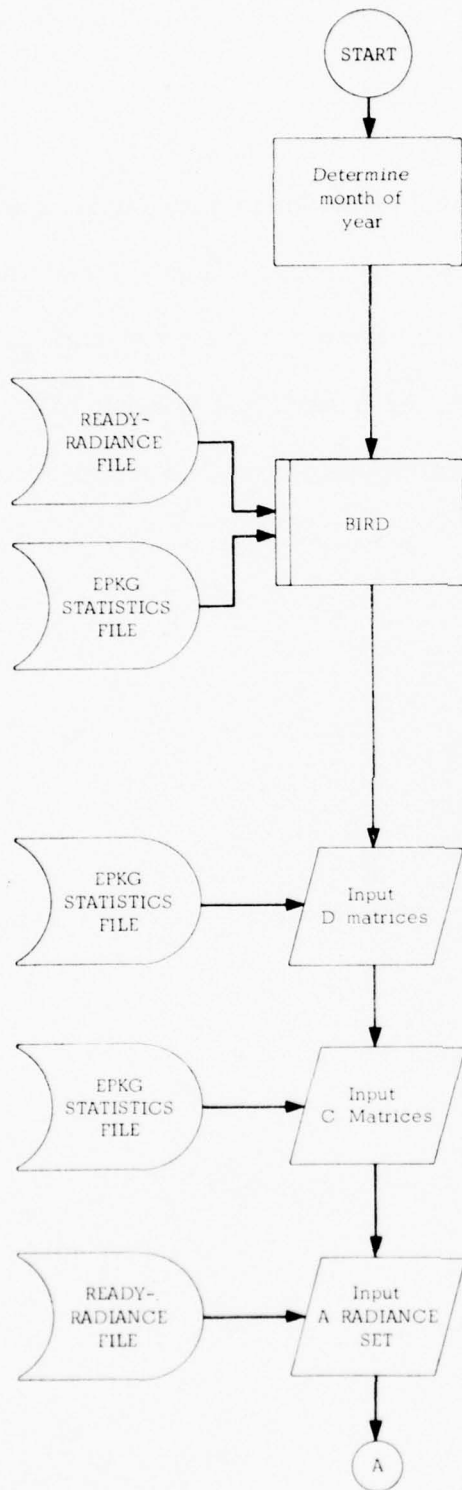
BIRD

Determine satellite index number for
current bird, number of radiance sets
to be processed and read in first
guess statistics for the bird.

EPKG
STATISTICS
FILE

Input
D matrices

Read in D matrices which are used to
compute a statistical correction to be
added to the satellite measured
radiances. [7]

EPKG
STATISTICS
FILE

Input
C Matrices

Read in C matrices for C Matrix
temperature retrieval technique.

READY-
RADIANCE
FILE

Input
A RADIANCE
SET

The data items contained in the radiance
set are described in Table 2.1.

A

36

A

THROW

Abnormal Return — YES → 8 / NO

TRAMIS

SMOOTH ↔ INITMP

Abnormal Return — YES → 8 / NO

B
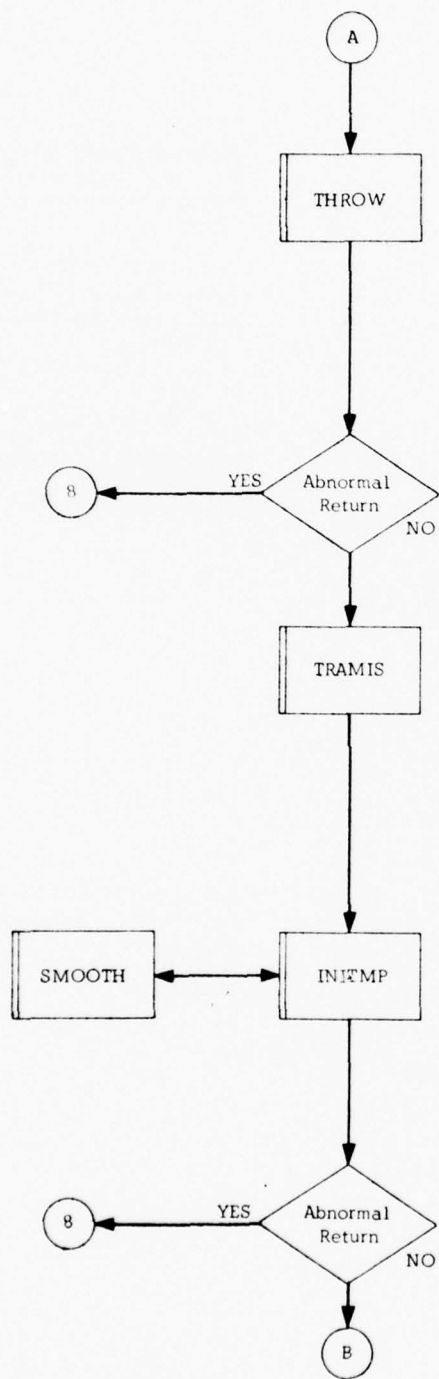
Subroutine THROW performs the following functions:

1 - Terminates analysis of a sounding whose underlying surface was land

2 - Terminates analysis of a sounding whose zenith angle exceeds 60°

3 - Determines zenith angle index number of stored CO_2 transmission function

Subroutine TRAMIS determines the drum sector addresses of the CO_2 and O_3 transmission functions for the satellite, month of the year, latitude and zenith angle of the sounding and then inputs these functions from mass storage. A description of the stored transmission functions is given in Table 2.2

Subroutine INITMP uses stored climatological profiles and AFGWC analysis temperature fields to construct first guess profiles. Subroutine SMOOTH smoothens the transition from the climatologically derived and analysis sections of the first guess profile.

37
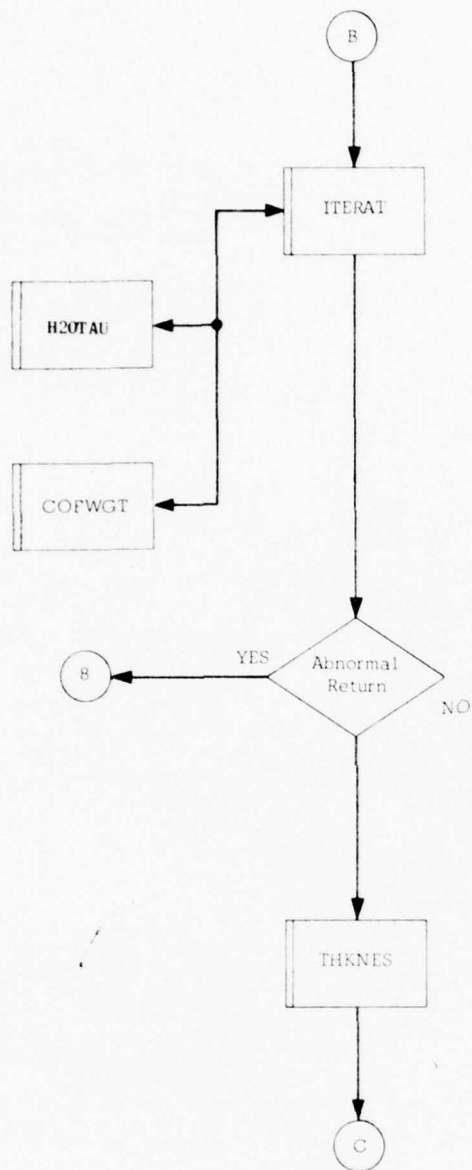
Subroutine ITERAT executes the specific procedures of the minimum information technique to retrieve the temperature profiles.

Subroutine H2OTAU calculates the combined carbon dioxide, water vapor and ozone transmission function for channels 1 through 7.

Subroutine COFWGT generates the coefficient matrix
see Ref. 2 equation 12.

Subroutine THKNES calculates the thicknesses between and heights of the mandatory levels from the retrieved temperature profile and an assumed water vapor profile.

C

Retrieve
Temperatures
by C Matrix
Solution

NO   YES
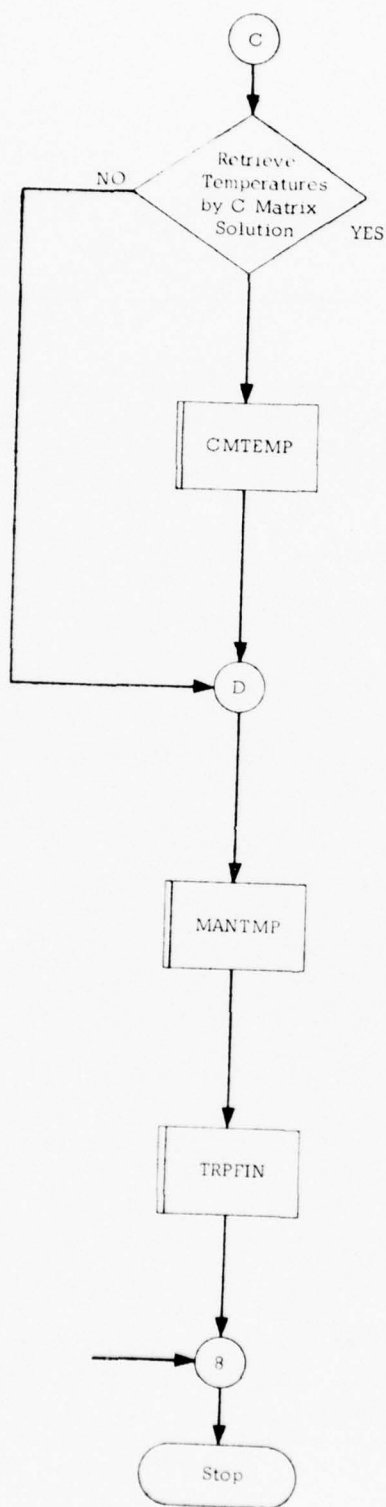
CMTEMP

Subroutine CMTEMP retrieves the
temperature profile by the
statistical C matrix solution
technique.

D

MANTMP

Subroutine MANTMP calculates
temperatures at the mandatory
levels by interpolation between
the computational levels.

TRPFIN

Subroutine TRPFIN determines the
tropopause level in the final
temperature profile.

8

Stop

39

Table 2.1   Data Items in a Radiance Set of the READYRADIANC   File

Name	Description
Latitude Belt No.	An integer from 1 to 45 denoting the 4 degree latitude belt in which the sounding was made. North Pole is belt no. 1, South Pole is belt no. 45
Longitude	Longitude of sounding
Latitude	Latitude of sounding
Minutes	Minutes after the hour of sounding
Hemispheric Indicator	Indicator which shows the hemisphere of the sounding
3D-NEPH Location	The 3D-NEPH box no, I and J coordinates of sounding
Julian Hour	Julian hour of the sounding
Channel Radiances	Measured radiances for the eight channels
Zenith Angle	Zenith angle for the measured radiances
Terrain Height	Terrain height at the location of the sounding
Surface Indicator	Indicator denoting the type of surface (sea, land, ice) underlying the sounding
Mandatory Level Analysis Data	AFGWC analysis temperature and D values for the fifteen mandatory levels from 1000 mb. to 10 mb.

Name	Description
Tropopause Data	AFGWC analysis tropopause temperature and pressure
Dummy Block Station Number	A number which identifies the satellite from which the sounding was made and additionally denotes information relevant to the filing of the sounding data

Table 2.2   Description of the Stored Carbon Dioxide and Ozone
Transmission Functions

	Carbon Dioxide	Ozone
No. of atmospheric pressure levels at which transmission from the satellite is specified	70	70
No. of satellites	4	1 *
No. of channels	6	6
No. of atmospheres	6	5
No. of zenith angles	15	1 **

* Ozone transmissions are not satellite specific

** Ozone transmission is specified for 0° zenith angle only

Satellites - WX6530, WX8531, WX9532, WX1534

Carbon Dioxide Atmospheres - 15° N Annual, 30° N Winter
30° N Summer, U.S. Standard
60° N Winter, 60° N Summer

Ozone Atmospheres -   Tropical, Mid-latitude summer,
Mid-latitude winter, High latitude
summer, High latitude winter

42

2.1.1 Subprogram Element INITMP

Subroutine INITMP builds the first guess temperature profile. The temperatures and heights are specified at 70 computational levels which are related to pressure by the equation

$$N = \alpha P^{2/7} + \beta \tag{2.1}$$

where

N = computational level number (integer)

P = pressure (mb)

α = 9.9587402862

β = -1.6716270699

The constants α and β are determined by requiring that

$N = 1$ when $P = .01$ mb.

and $\quad N = 70$ when $P = 1000$ mb.

For the computational levels above 10 mb., temperatures corresponding to one of six climatological atmospheres listed in Table 2.3 are used. The particular climatological profile selected is determined by the month and latitude of the sounding.

For the computational levels which correspond to the mandatory levels from 10 mb. down to 1000 mb., the AFGWC analysis temperatures and D values are used for the first guess temperatures and heights.

43

Table 2.3 Climatological Temperature Profiles Used Above 10 mb.

1.	15° N	or S Annual
2.	30° N	Winter
3.	30° N	Summer
4.	45° N	Spring, Fall
5.	60° N	Winter
6.	60° N	Summer

If a superadiabatic lapse rate results in 850 to 1000 mb. layer, the temperature at 1000 mb. is reduced by 1°C while the temperature at 850 mb. is increased by $.5^{\circ}$C. Successive replications of this procedure are made until the lapse rate in the layer is no longer superadiabatic.

INITMP calculates the temperatures at the computational levels between the mandatory levels. The interpolation algorithm for the temperature at a computational level lying between any two mandatory levels which do not bracket the tropopause is given by

$$T_i = T_m - (T_m - T_{m-1}) * R_i$$

where

$$R_i = \frac{\ln (P_i) - \ln (P_{m-1})}{\ln (P_m) - \ln (P_{m-1})} \qquad (2.2)$$

44

T_i, P_i = temperature, pressure at the computational level

T_m, P_m = temperature, pressure at the first mandatory level below the computational level

T_{m-1}, P_{m-1} = temperature, pressure at the first mandatory level above the computational level

The interpolation algorithms used when the mandatory levels m and m-1 bracket the tropopause are given by

$$T_i = T_{m-1} + (T_t - T_{m-1}) * \frac{\ln (P_i) - \ln (P_{m-1})}{\ln (P_t) - \ln (P_{m-1})} \qquad (2.3)$$

when the computational levels lie above the tropopause and

$$T_i = T_t + (T_m - T_t) * \frac{\ln (P_m) - \ln (P_i)}{\ln (P_m) - \ln (P_t)} \qquad (2.4)$$

when the computational levels lie below the tropopause. T_t and P_t are the temperature and pressure of the tropopause.

2.1.2 Subprogram Element SMOOTH

Subroutine SMOOTH passes a three point smoother thru the first guess temperature profile from level 21 upward to level 10. The purpose of this is to remove any discontinuity that might exist between that portion of the first guess temperature profile obtained by interpolation of the AFGWC mandatory level temperatures and the climatological first guess data used above 10 mb. The smoothing algorithm is given by

$$T_i = W_{1,i} * T_{i-1} + W_{2,i} * T_i + W_{3,i} * T_{i+1} \qquad (2.5)$$

The weights $W_{j,i}$ are given in Table 2.4.

Table 2.4 First Guess Temperature Profile Smoother Weights

i	$W_{1,i}$	$W_{2,i}$	$W_{3,i}$
12	.1	.8	.1
13	.1	.8	.1
14	.1	.7	.2
15	.1	.6	.3
16	.1	.5	.4
17	.1	.4	.5
18	.2	.5	.2
19	.3	.6	.1
20	.2	.7	.1
21	.1	.8	.1

2.1.3 Subprogram Element ITERAT
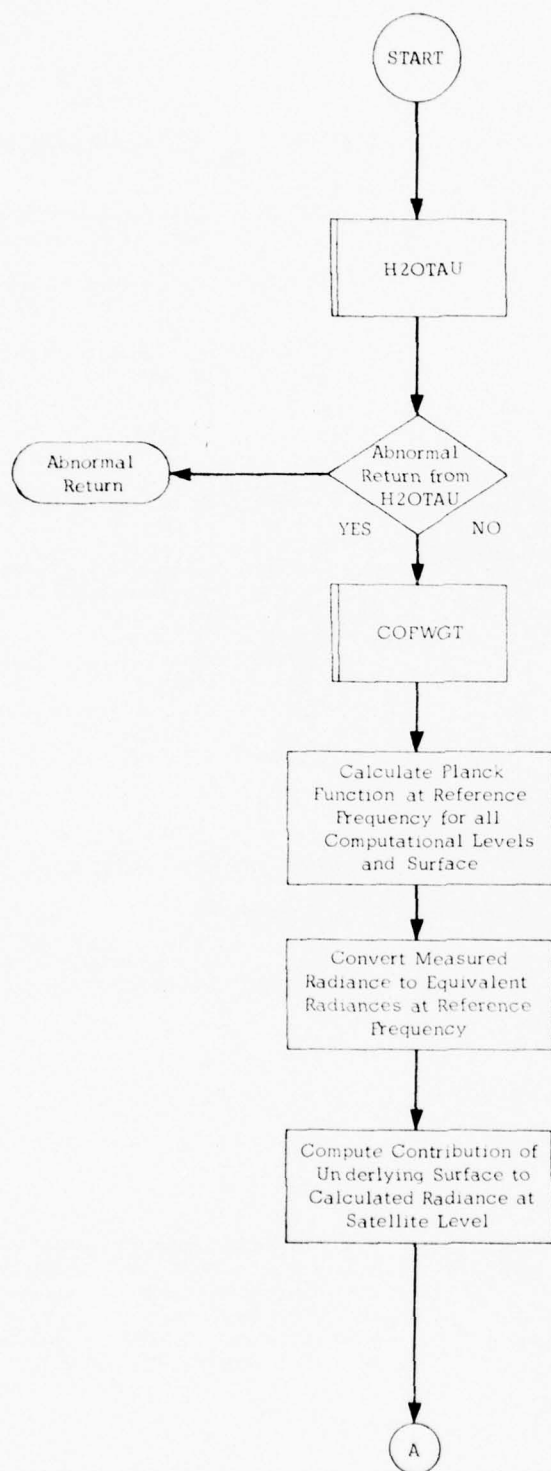
```
                    ┌─────────┐
                    │  START  │
                    └────┬────┘
                         │
                         ▼
                    ┌─────────┐         Calculate transmission functions due to
                    │ H2OTAU  │         water vapor, ozone and carbon dioxide
                    └────┬────┘         at computational levels 1 through 70 for
                         │              channels 1 through 7.
                         ▼
                    ╱─────────╲         If abnormal return from H2OTAU, execute
   ┌──────────┐    ╱ Abnormal  ╲        abnormal return to SOUNDER.
   │ Abnormal │◄──╱  Return from ╲
   │  Return  │   ╲   H2OTAU    ╱
   └──────────┘    ╲─────────╱
                  YES        NO
                         │
                         ▼
                    ┌─────────┐         Compute the coefficient matrix C
                    │ COFWGT  │         (Equation 12, Ref. 2  )
                    └────┬────┘
                         │
                         ▼
              ┌────────────────────┐    Planck function for the surface level
              │ Calculate Planck   │    and computational level 70 (1000 mb
              │ Function at Reference│  level) are equal.
              │ Frequency for all  │
              │ Computational Levels│
              │    and Surface     │
              └─────────┬──────────┘
                         │
                         ▼
              ┌────────────────────┐    Calculate equivalent radiative temperature
              │ Convert Measured   │    for each measured radiance, then calculate
              │ Radiance to Equivalent│ Planck radiance for these temperatures at
              │ Radiances at Reference│ the reference frequency.
              │     Frequency      │
              └─────────┬──────────┘
                         │
                         ▼
              ┌────────────────────┐
              │ Compute Contribution of│
              │ Underlying Surface to │
              │ Calculated Radiance at │
              │  Satellite Level   │
              └─────────┬──────────┘
                         │
                         ▼
                      ┌───┐
                      │ A │
                      └───┘
```

BSFC (NU) = BSURF * TRAN (70, NU)
where

       BSFC (NU) = Calculated radiance at
                satellite level for
                channel NU

      BSURF = Planck Radiance of under-
              lying surface at reference
              frequency and temperature
              of level 70

TRAN (70, NU) = Transmission, surface
to satellite for frequency of channel
NU.

A

```
Compute Atmospheric
Contribution to
Calculated Radiance at
Satellite Level
```
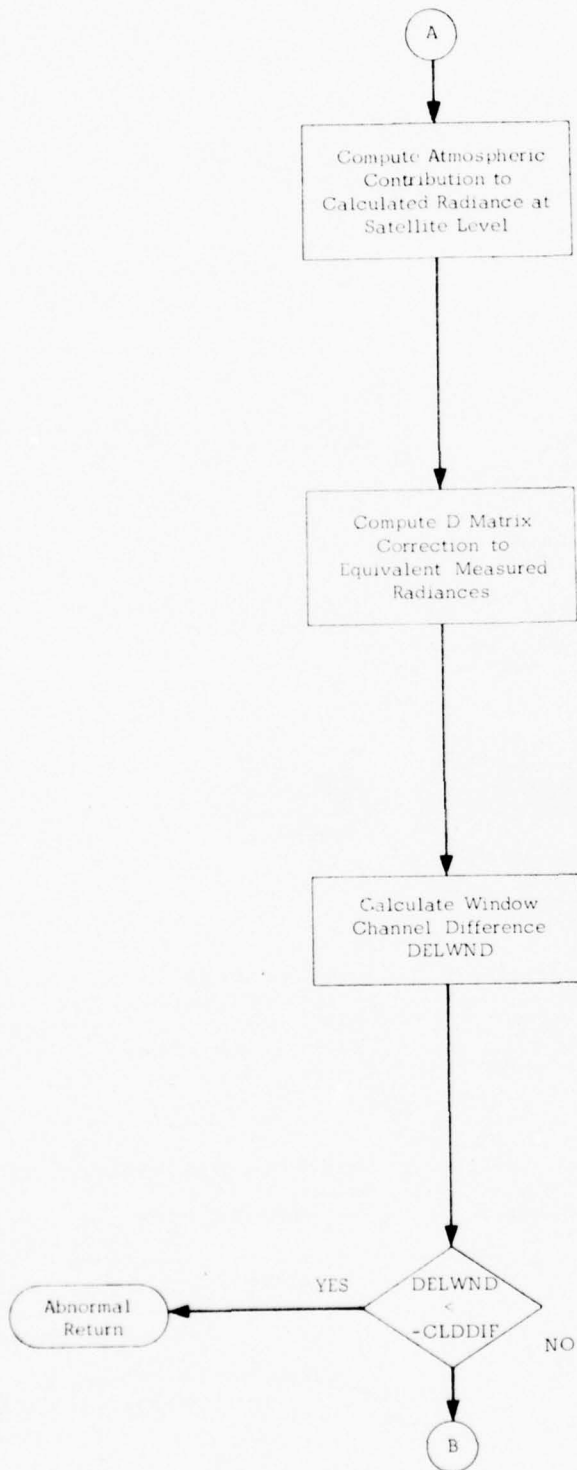
$$CRAD(NU) = \sum_{L=1}^{70} BNUO(L) * DTRAN(L, NU)$$

where

CRAD(NU) = Calculated Atmospheric
Radiance at Satellite level,
channel NU

BNUO(L) = Planck Radiance at the
reference frequency at the
L level

DTRAN(L, NU) = Transmission difference
through the L level at
frequency of channel NU

```
Compute D Matrix
Correction to
Equivalent Measured
Radiances
```

$$DR(I) = DRBAR(I) + \sum_{J=1}^{NA} D(I, J) * (SRAD(J) - RBAR(J))$$

where

DR(I) = Correction to be added to
equivalent measured radiance
of channel I

D(I, J) = "D" matrix

DRBAR(I) = Mean radiance correction
vector

SRAD(J) = Equivalent measured radiance
of channel J

RBAR(J) = Mean radiance vector

```
Calculate Window
Channel Difference
DELWND
```

DELWND = SRAD(NR) - BSFC(NR) - CRAD(NR)

where

SRAD(NR) = "D" matrix corrected
equivalent measured radiance
of window channel NR

BSFC(NR), CRAD(NR) described previously

YES   DELWND < -CLDDIF   NO

Abnormal Return

If the calculated window channel difference
is less than -CLDDIF, the sounding is
assumed to be too cloud contaminated near
the surface for further analysis and an
abnormal return to SOUNDER is executed.
CLDDIF is currently set equal to 1.1.

B

48
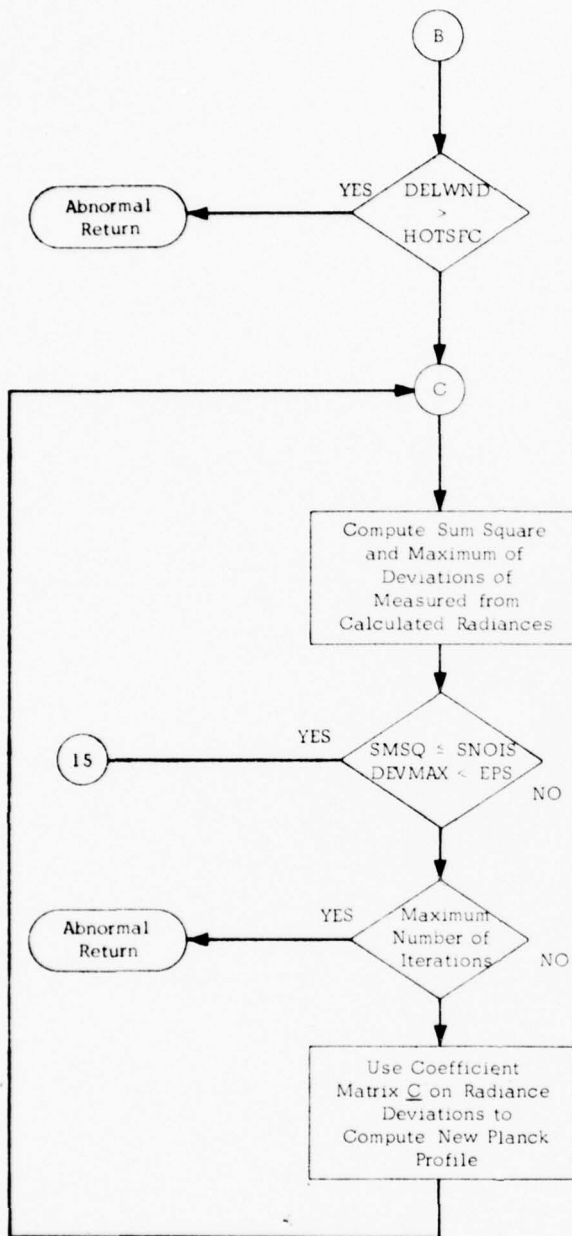
If calculated window channel difference is greater than HOTSFC, execute an abnormal return to SOUNDER as the sounding cannot be processed further either because the underlying surface temperature is too hot or the initial temperature profile guess is bad. HOTSFC is currently set equal to 1.1

If the sum squares of the deviations SMSQ is less than or equal to SNOIS and the maximum deviation DEVMAX is less than EPS, jump to 15 and compute final temperature profile. SNOIS is currently equal to 1.5 and EPS equal to .5.

Abnormal return to SOUNDER if maximum number of iterations have been performed.

The coefficient matrix $\underline{C}$ computed in COFWGT is used on the vector of deviations of calculated from measured radiances to compute a new Planck Function Profile.

49

```
        ( 15 )
           │
           ▼
  ┌──────────────────┐
  │  Compute Final   │
  │ Temperature Profile │
  │ from Planck Function │
  │     Profile      │
  └──────────────────┘
           │
           ▼
   (   RETURN   )          Return to SOUNDER
```

50

2.1.4 Subprogram Element H2OTAU

START

Entry Point = H2OTAU

ESUBS

Subroutine ESUBS
Calculates the saturation vapor pressure, average temperature, and associated temperature functions for the "water vapor layers". The "water vapor layers" start at level 43 and end at level 70.

Calculate
Water Vapor
Path Lengths in
the Layers

Using a fixed relative humidity profile for the water vapor layers (See Table 2.5) calculate water vapor pressure in each layer and the amount of water vapor traversed in the layers given the zenith angle of the sounding.

Calculate
P, T & ρ_w
Terms in Water
Vapor Transmission

Calculate for each of the water vapor layers the pressure, temperature and water vapor path length dependent terms of the water vapor transmission functions.

Calculate
Water Vapor
Transmission for
Window Channel

Calculate the water vapor transmission for the window channel, i.e. channel 7, at computational levels 44 through 70. Levels 1 through 43 set transmission equal to 1.

Calculate Water
Vapor Transmission
for Channels
4, 5 and 6

Initialize transmission for channels 4, 5 and 6 at all computational levels to 1. Calculate water vapor transmission at computational levels 48 through 70.

Water
Vapor Trans.
at Any Level
Negative

Abnormal
RETURN

YES

NO

Test calculated water vapor transmissions. If transmission at any level is negative, execute abnormal return to ITERAT.

A

51

A

Initialize
Transmissions for
Channels 1, 2 & 3

Initialize transmissions for channels 1,
2 & 3 at all computational levels to
CO_2 transmissions.

Initialize
Transmissions at
Levels 1 through 43
for Channels 4, 5 & 6

Initialize transmissions for channels 4,
5 & 6 at computational levels 1 through
43 to CO_2 transmission.

Calculate Intermediate
Transmission Values at
Levels 44 through 70
for Channels 4, 5 & 6

Calculate intermediate transmission
values equal to product of CO_2 and
H_2O transmissions at levels 44
through 70 for channels 4, 5 & 6.

Calculate Final
Transmission Values
All Levels, Channels
1 through 6

Calculate TRAN, final transmission
$TRAN = TRANI * TRANO^{SEC\Theta}$

TRANI = initial or intermediate value
TRANO = ozone transmission
Θ = zenith angle

Trans.
at Any Level
Any Channel
Negative

Abnormal
Return

YES

NO

If transmission at any level for any
channel is negative, execute abnormal
return to ITERAT.

Normal
Return

52

Table 2.5

Relative Humidity Profile in the Water Vapor Layers

Computational Level No.	Average Layer Pressure	Relative Humidity	Computational Level No.	Average Layer Pressure	Relative Humidity
43			57		
	198.860	.158		511.467	.476
44			58		
	214.694	.190		542.359	.491
45			59		
	231.409	.226		574.562	.507
46			60		
	249.034	.257		608.107	.522
47			61		
	267.597	.282		643.029	.533
48			62		
	287.129	.313		679.361	.544
49			63		
	307.658	.343		717.136	.562
50			64		
	329.215	.364		756.388	.588
51			65		
	351.830	.378		797.151	.615
52			66		
	375.533	.391		839.459	.643
53			67		
	400.356	.406		883.348	.673
54			68		
	426.329	.421		928.852	.703
55			69		
	453.484	.452		976.006	.734
56			70		
	481.853	.464			

2.1.5 Subprogram Element COFWGT

START

Calculate Transmission
Differences
DTRAN(K,J)
K = level No.
J = channel No.

$DTRAN(K,J) = TRAN(K-1,J) - TRAN(K+1,J)$
where
$TRAN(I,J) =$ transmission at the
I computational
level and J channel
$J = 1$ through 7

Generate
AA(I,J)

$$AA(I,J) = \sum_{K=1}^{70} DTRAN(K,I) * DTRAN(K,J)$$
$AA = \Gamma\Gamma^T$ term in equation (12)
of Ref. 2

DIAGNL

Diagonalize matrix AA and determine
the matrix of eigenvectors of AA.

AA(5,5) = 0

Set element 5,5 of diagonalized
matrix AA equal to 0.0

Smallest
AA(I,I) < .002
I = 2,6

Find the weakest of channels 2 through
6. Jump to 13 if its value is equal to
or greater than .002.

NO

YES

13

A

54

13 · A

Reduce the Rank of
AA(I,J) by
and Rebuild
Without Weakest
Channel

DIAGNL · Diagonalize new AA matrix

13

Add .001 to
the Diagonal
Elements of AA · Add the scaler γ (equation 12, Ref. 2) to the diagonal elements of AA.

GJR · GJR computes AA^{-1} using a Gauss-Jordan elimination with column pivoting. If an overflow is detected, the last correctly completed row of the reduction is flagged.

Compute
Coefficient
Matrix $\underline{C}$

$$\underline{C} = \sum_{J=1}^{NA} DTRAN(K,JJ)\,AA^{-1}(J,I)$$

NA = Number of rows of AA^{-1}
JJ is a pointer to the active channels.

RETURN

55

2.2 GAC RESEARCH VERSION OF SOUNDER

The Geo-Atmospherics Corporation's (GAC) Research Version of SOUNDER is a modification of the SOUNDER program which was operational at AFGWC on 1 April 1977. Implementation of the minimum information technique in the research version is identical to that in the operational version. Major modifications that were made involved the input/output of data. Exercising GAC's research SOUNDER provides information attainable on weaknesses and strengths of the operational version of SOUNDER.

The GAC research version like the operational version is written in FORTRAN V and must be run on a UNIVAC 1100 Series System. The program requires 44K words decimal to load. The three data files required are the carbon dioxide transmissions, ozone transmissions and the EPKG statistics. A new main program was written which generates a READYRADIANC file from user supplied radiances, first guess temperatures, and heights.

Additional outputs were incorporated into SOUNDER in the research version. They include the normalized measured radiances, radiances calculated from the guess profiles, D matrix corrected radiances, and various differences in these quantities.

The single greatest value in the GAC research version of SOUNDER, however, lies not so much in the revised program itself, but rather in the research capabilities built into the operation and functions of various elements of the program. Research modifications have enabled one to easily modify any of the preselected data or operations incorporated in SOUNDER such as the assumed water vapor profiles and the CLDDIF, HOTSFC, SNOIS and EPS test values.

Other more complex modifications such as the decoupling of underlying surface temperatures from the 1000 mb temperature and provisions for forecast data inputs allow considerable flexibility in deriving operational sensitivity and performance relative to available data inputs.

The GAC research version of SOUNDER is a powerful tool for exploring hardware and software deficiencies and improvements upon routine operational performance.

3 ANALYTICAL ERROR ANALYSIS

3.1 DATA BASES

3.1.1 General

Three data bases used in this study were derived from satellite infrared radiometers, radiosonde observations (RAOB), and Air Force Global Weather Center's (AFGWC) 12-hour numerical forecast field. In operational practice, the forecast data are used to obtain a first-guess temperature profile for use with the multi-channel radiometric data to obtain a retrieved temperature profile using the minimum information technique. This procedure is described in a detailed step by step manner in section 2 of this report. RAOB data were collected for only those locations where a clear (cloud-free) satellite sounding was possible within 60 nautical miles and one hour in time of one another. All satellite data were collected for cloud-free ocean regions only. Data from two satellite birds were available, Bird 9532 and 8531, a morning and noon satellite, respectively.

Characteristics associated with the satellite sensors are given in Table 3.1. Six of the radiometric channels occur on the peak (15.0μ m) or wings of the carbon dioxide molecule absorption/emission band. It can be seen that the higher the channel number the greater the depth of

Channel	Wave-Length (μm)	Wave-Number (cm^{-1})	Band Width (cm^{-1})	Approximate Weighting Function Peak (mb)	Gaseous Species	NESN$_2$ (mw/m^2 : ster·cm^{-1})
1	15.0	668.5	3.5	30	CO_2	0.25
2	14.8	677.0	10	60		0.15
3	14.4	695.0	10	160		0.15
4	14.1	708.0	10	400		0.15
5	13.8	725.0	10	700		0.15
6	13.4	747.0	10	1000		0.15
7	12.0	835.0	8	SFC	WINDOW	0.15
8	18.7	535.0	10	600	H_2O	0.15

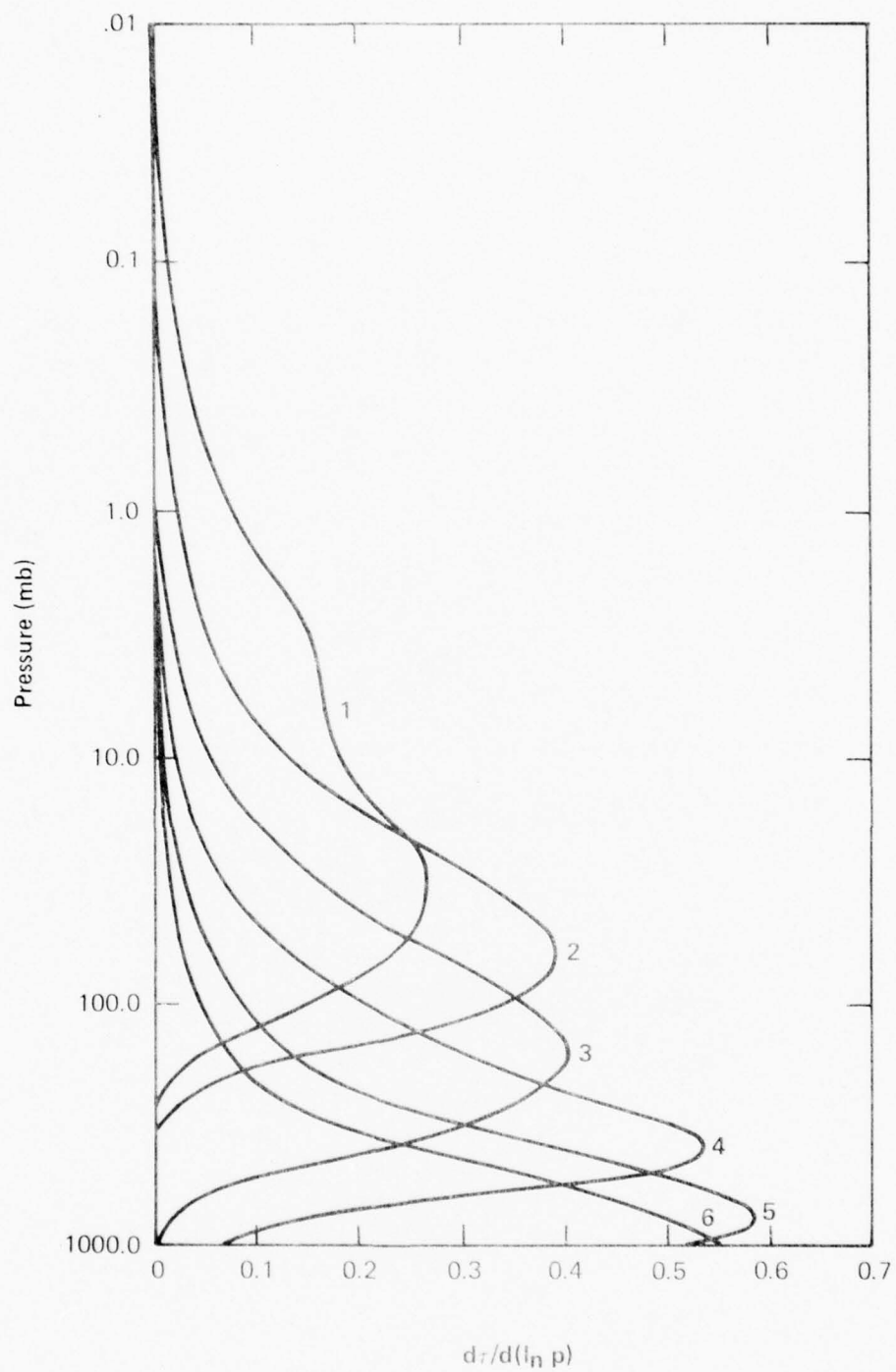Table 3.1 Satellite Sensor Characteristics

Figure 3.1 Distribution of the Weighting Functions
Showing That Portion of the Atmosphere
Which Contributes to Radiation Received
at Each of the First Six Satellite Sensor
Channels

60

penetration or interrogation of atmospheric conditions. This is shown graphically in Fig. 3.1 where the distribution of the weighting function for each of the first six sensor channels shows that portion of the atmosphere that contributes to the radiometric power received at the satellite.

Channel 1 sensor is centered on the peak of the CO_2 band at 15 μ m or 668.5 cm^{-1} wave number and receives radiation throughout a half power band width of 3.5 cm^{-1} with a 0.25 $mw/m^2 \cdot$ ster $\cdot$ cm^{-1} standard deviation of the nominal noise equivalent spectral radiances (NESN). Channel 1 receives upwelling radiation from the top portions of the atmosphere, centered at about the 30 mb level. The band width is increased and the NESN is decreased for all other channels. Channel 6 weighting function peaks at the 1000 mb pressure level whereas channel 7 (12.0 μ m or 835.0 cm^{-1}) operates in a "window" region and receives maximum radiation from the underlying surface. Channel 8 operates on the 18.7 μ m or 535.0 cm^{-1} water vapor line and the weighting function peaks at the 600 mb level. Later in this report it will be shown how water vapor and underlying surface effects contribute adversely to re- trieving atmospheric temperature profiles from satellite radiometric data.

3.1.2 Large Data Base

In order to search for differences that might be attributable to hardware features of the two satellite birds, it was desirable to use a large data base to enhance the chances of each bird viewing similar types of atmospheres. Data from over 3000 satellite soundings over the northern hemisphere were used to derive the mean and standard deviation of radiances measured in each of the eight channels of the two birds. These data were separated into 4 latitude belts and 6 longitude regions. The actual number of cases in each subdivision is given in Table 3.2. In general, the distribution of cases is uniform among the longitude sub-divisions for each bird. This is not the case, however, for the latitude subdivisions. There are about twice as many tropical as mid-latitude cases and about twice as many mid-latitude as polar cases. Over the entire northern hemisphere, the total number of cases are divided nearly evenly between Birds 8531 and 9532. An analysis of these data is given later in section 3.2.

TROPICS - 0 to 26 North Latitude			
	East Longitude		
BIRD	0 to 90	90 to 180	0 to 180
8531	201 cases	262 cases	463 cases
9532	208 cases	204 cases	412 cases
	West Longitude		
	-90 to 0	-180 to -90	-180 to 0
8531	213 cases	300 cases	513 cases
9532	277 cases	79 cases	356 cases

MID-LATITUDE - 26 to 62 North Latitude			
	East Longitude		
	0 to 90	90 to 180	0 to 180
8531	62 cases	135 cases	197 cases
9532	10 cases	141 cases	151 cases
	West Longitude		
	-90 to 0	-180 to -90	-180 to 0
8531	112 cases	123 cases	235 cases
9532	149 cases	18 cases	167 cases

POLAR - 62 to 90 North Latitude			
	East Longitude		
	0 to 90	90 to 180	0 to 180
8531	55 cases	50 cases	105 cases
9532	43 cases	91 cases	134 cases
	West Longitude		
	-90 to 0	-180 to -90	-180 to 0
8531	64 cases	79 cases	143 cases
9532	59 cases	78 cases	136 cases

NORTHERN HEMISPHERE - 0 to 90 North Latitude			
	East Longitude		
	0 to 90	90 to 180	0 to 180
8531	318 cases	446 cases	764 cases
9532	260 cases	436 cases	696 cases
	West Longitude		
	-90 to 0	-180 to -90	-180 to 0
8531	386 cases	501 cases	887 cases
9532	483 cases	175 cases	657 cases

Table 3.2   Number of Cases Used to Generate
Mean Radiances Measured as a
Function of Bird, Latitude, and
Longitude. Data Period 14-28 February
1975.

3.1.3 Coincident Satellite and RAOB Data Base

In order to do an indepth search for the major error sources in the satellite temperature retrieval process, a search was made through the more than 3000 satellite sounding cases to select only those where coincident RAOB's would be available for verification purposes. Out of this large data sample, only 10 cases could be found that matched our coincident requirement, i.e. with the satellite and RAOB sounding within 60 nautical miles and one hour in time of one another.

Table 3.3 gives the geographical location, bird number, and type of low level temperature profile for the 10 coincident soundings within the northern hemisphere. Each bird has 5 cases of nearly simultaneous satellite and RAOB soundings. There is one case in the tropics, 4 cases in the mid-latitudes, and 5 cases in the polar regions. All cases are over the ocean. No observations were available for the North Atlantic Ocean but a variety covering the Pacific and Arctic Ocean and the Mediterranean Sea was obtained.

Plots of the observed RAOB temperature profiles are shown in Figs. 3.2 and 3.11, inclusive, for the 10 soundings. For reference purposes, the AFGWC 12-hour forecast temperatures at mandatory pressure levels are included since these are the values that are used as the

Table 3.3 Location and Number of Research Profiles for Three Categories
of Low Level Atmospheric Stability

Profile Type	Region	Latitude	Longitude	Bird
Dry Adiabatic Profiles	South of Japan	34.5N	138.5E	9532
	East of Japan	38.1N	141.8E	9532
Lapse Profiles	Near Wake Island	19.3N	166.1E	8531
	Mediterranean Sea	34.1N	33.1E	8531
	Sea of Japan	47.4N	141.7E	9532
	Near Finland	65.2N	34.8E	8531
Ground Based Inversion Profiles	Barents Sea	68.2N	53.6E	9532
	Baffin Bay	69.5N	81.0W	9532
	North of Alaska	71.9N	155.5W	8531
	North of Russia	79.8N	75.4E	8531

initial guess temperature profile. These 10 cases were classified according to the low level atmospheric stability conditions between the 850 and 1000 mb pressure levels. Notice that there are four cases where a very stable low level atmosphere exists due to ground based temperature inversion conditions. Two cases exhibit relatively unstable conditions associated with dry adiabatic type profiles. The remaining four cases conform with the more standard type atmospheres found with lapse profiles.
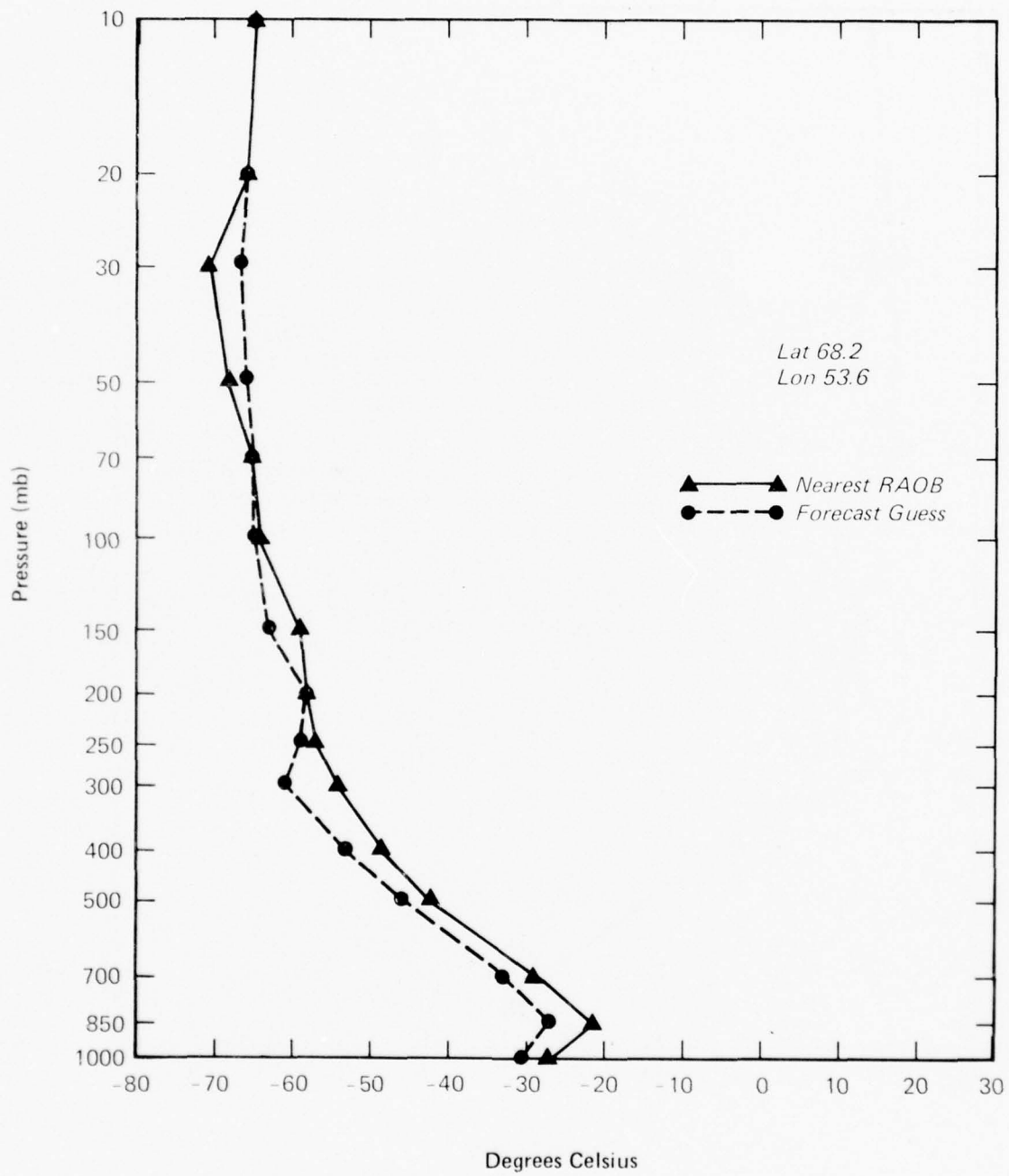
Figure 3.2 Observed and Forecast
Temperature Profile -
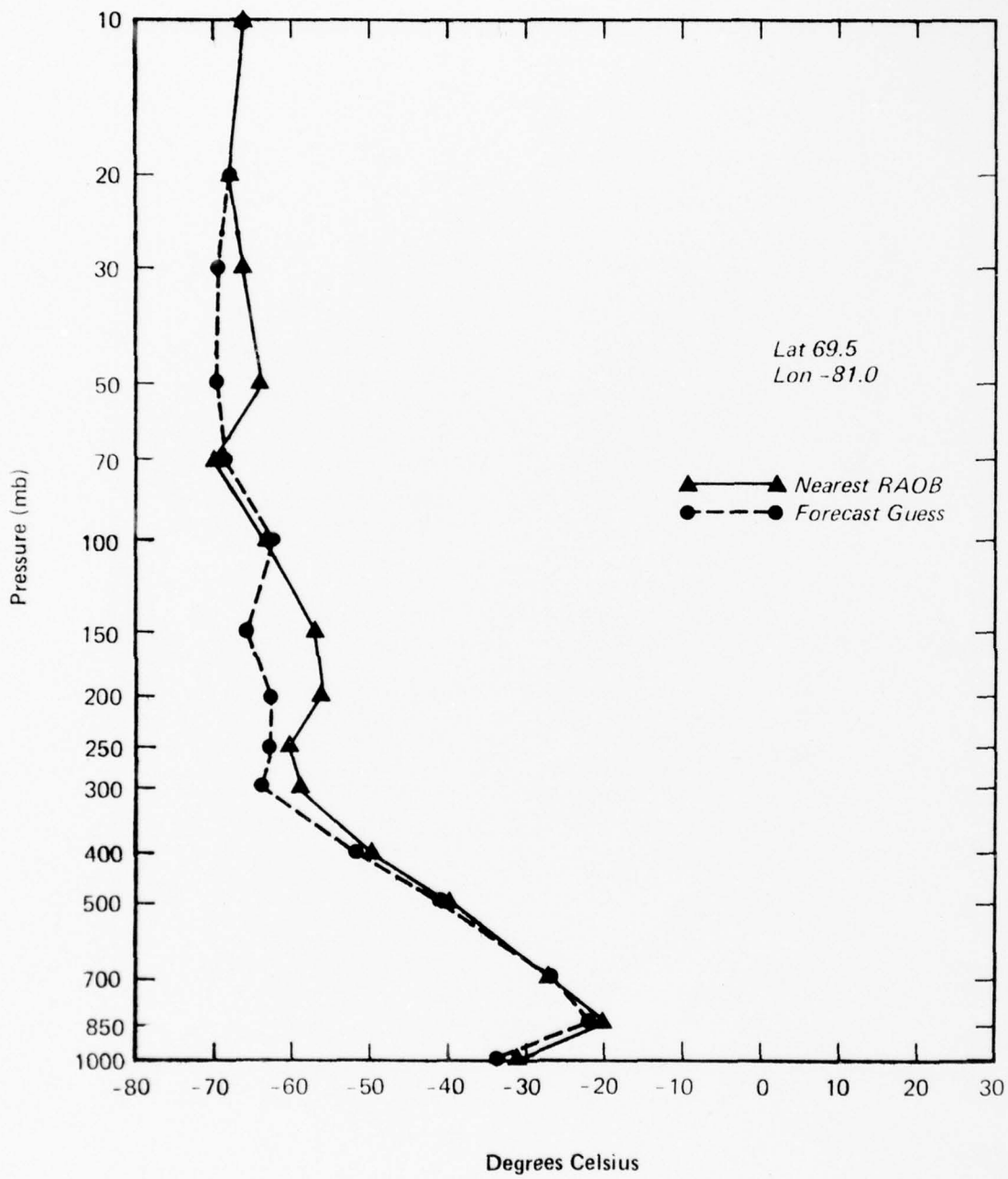68.2 N Latitude 53.6 E
Longitude
February 21, 1975, 0014Z

67

Figure 3.3 Observed and Forecast
Temperature Profile –
69.5 N Latitude 81.0 W
Longitude
February 17, 1975, 1044Z
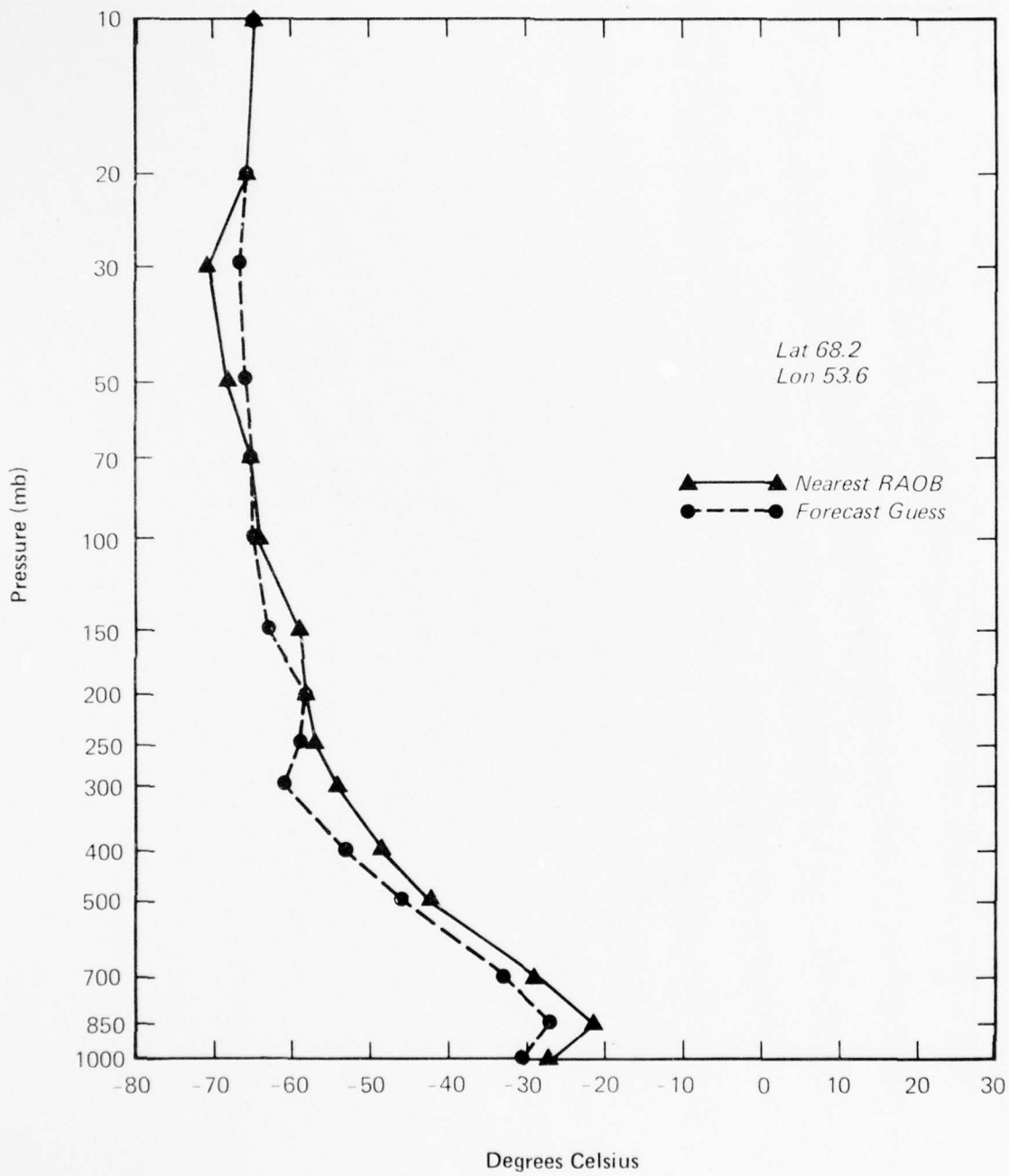
Figure 3.2 Observed and Forecast
         Temperature Profile –
         68.2 N Latitude 53.6 E
         Longitude
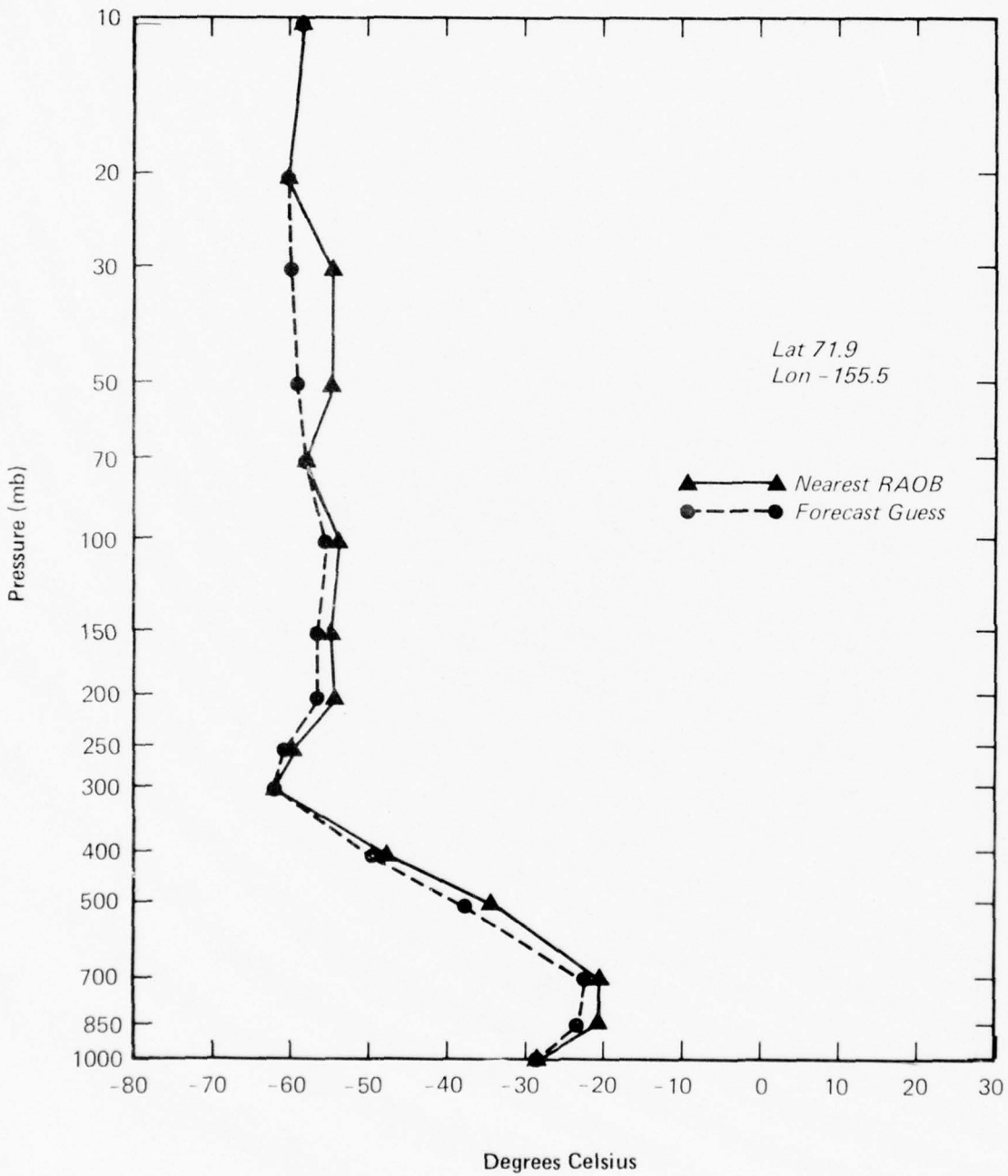   February 21, 1975, 0014Z

Figure 3.4 Observed and Forecast
Temperature Profile –
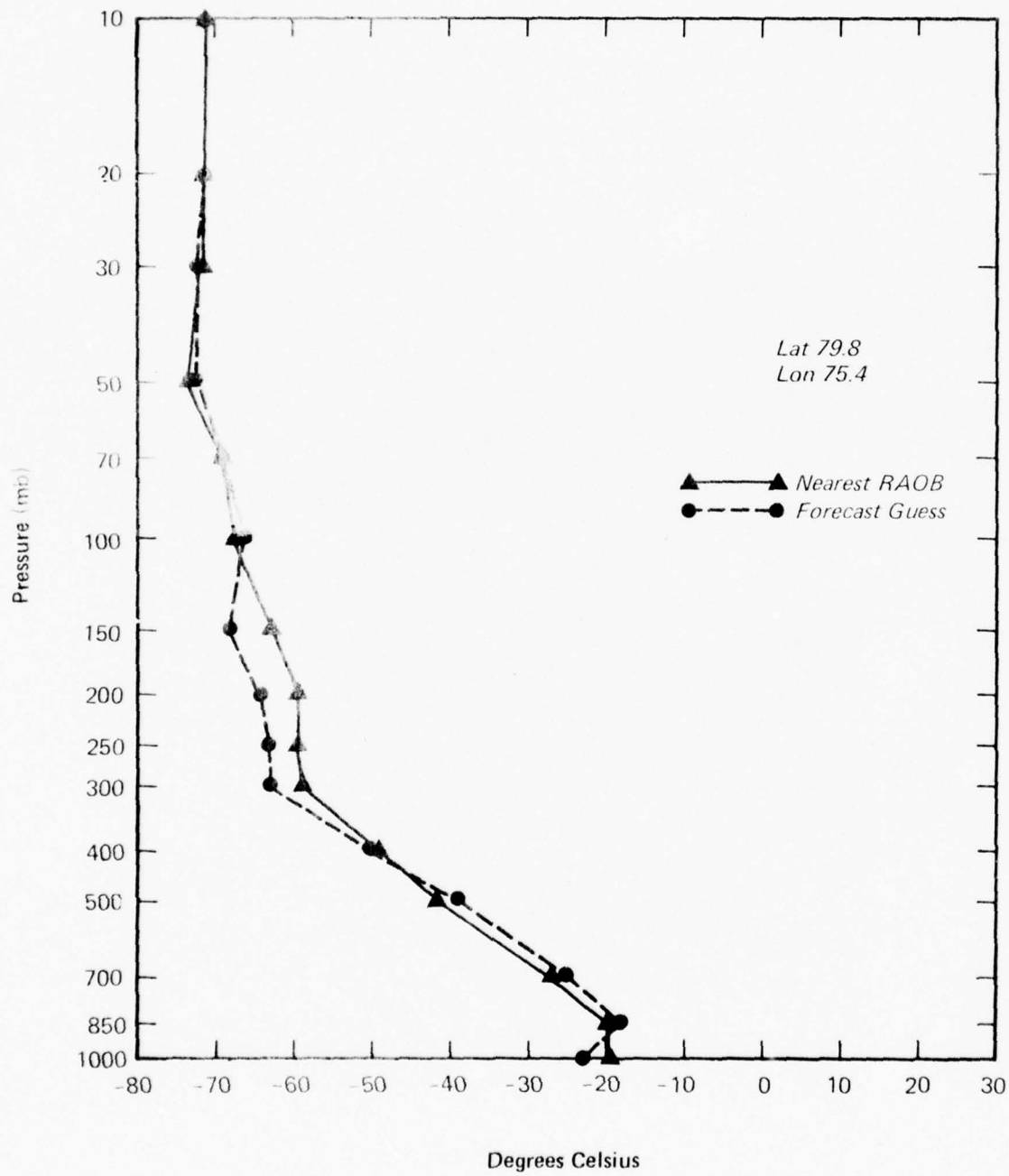71.9 N Latitude 155.5 W
Longitude
February 19, 1975, 2337Z

Figure 3.5 Observed and Forecast
Temperature Profile -
79.8 N Latitude 75.4 E
Longitude
February 20, 1975, 2225Z

Figure 3.6 Observed and Forecast
Temperature Profile –
34.5 N Latitude 138.5 E
Longitude
February 17, 1975, 1004Z

Figure 3.7 Observed and Forecast
Temperature Profile –
38.1 N Latitude 141.8 E
Longitude
February 17, 1975, 1003Z

Figure 3.8 Observed and Forecast
Temperature Profile -
19.3 N Latitude 166.1 E
Longitude
February 16, 1975, 0118Z

73

Figure 3.9 Observed and Forecast
Temperature Profile –
34.1 N Latitude 33.1 E
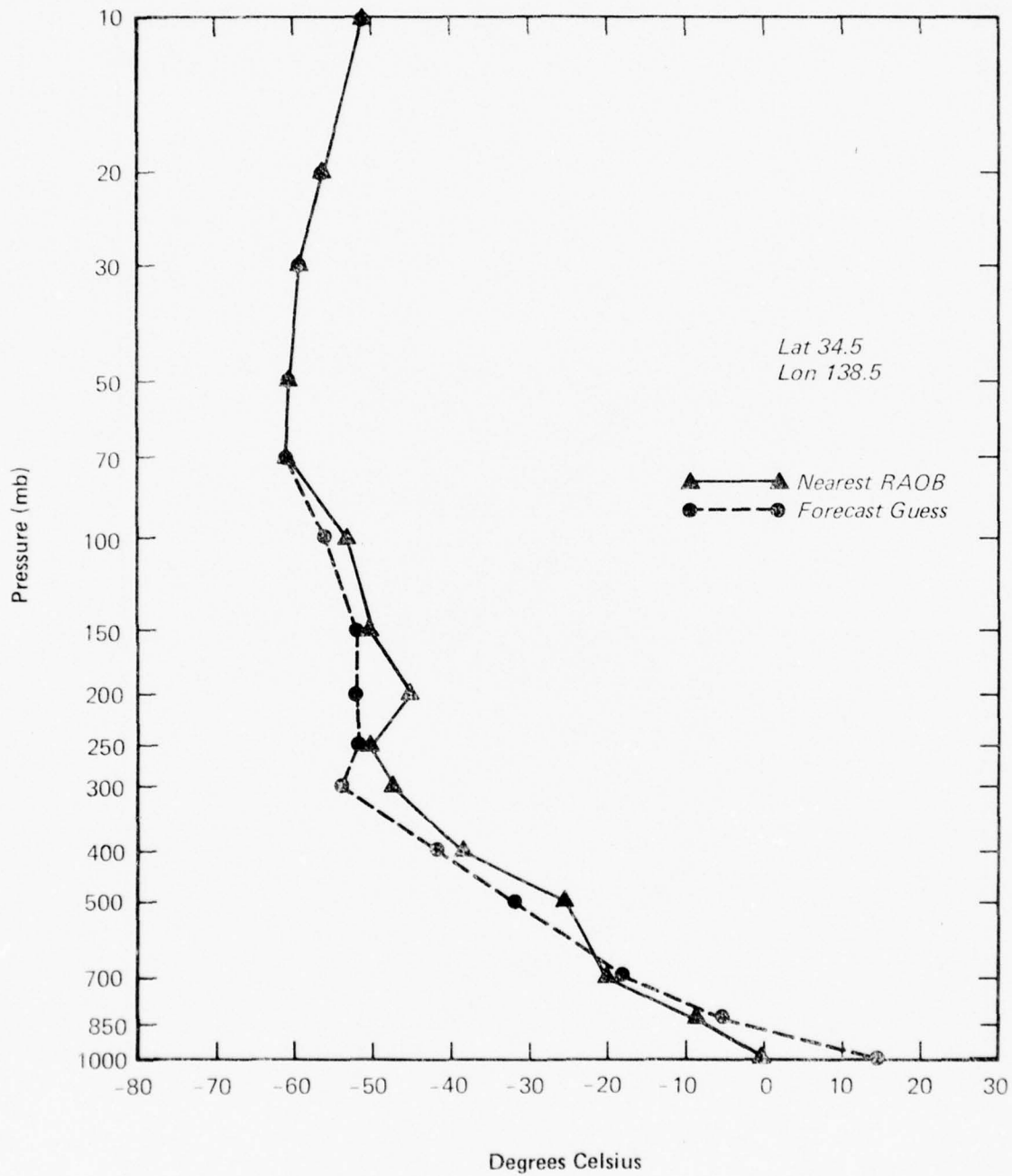Longitude
February 16, 1975, 2212Z

74

Figure 3.10 Observed and Forecast
Temperature Profile -
47.4 N Latitude 141.7 E
Longitude
February 20, 1975, 2142Z

Figure 3.11 Observed and Forecast
Temperature Profile -
65.2 N Latitude 34.8 E
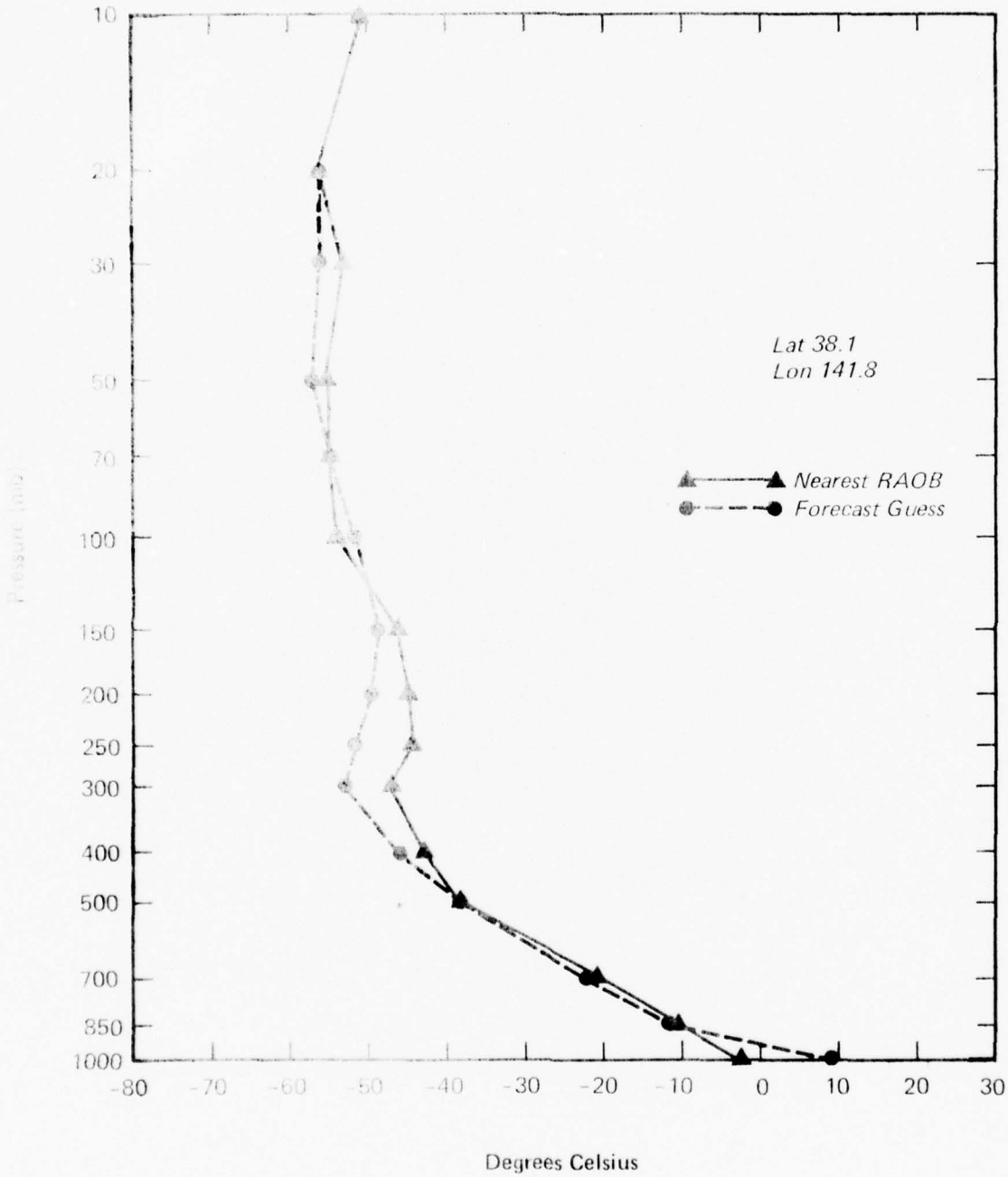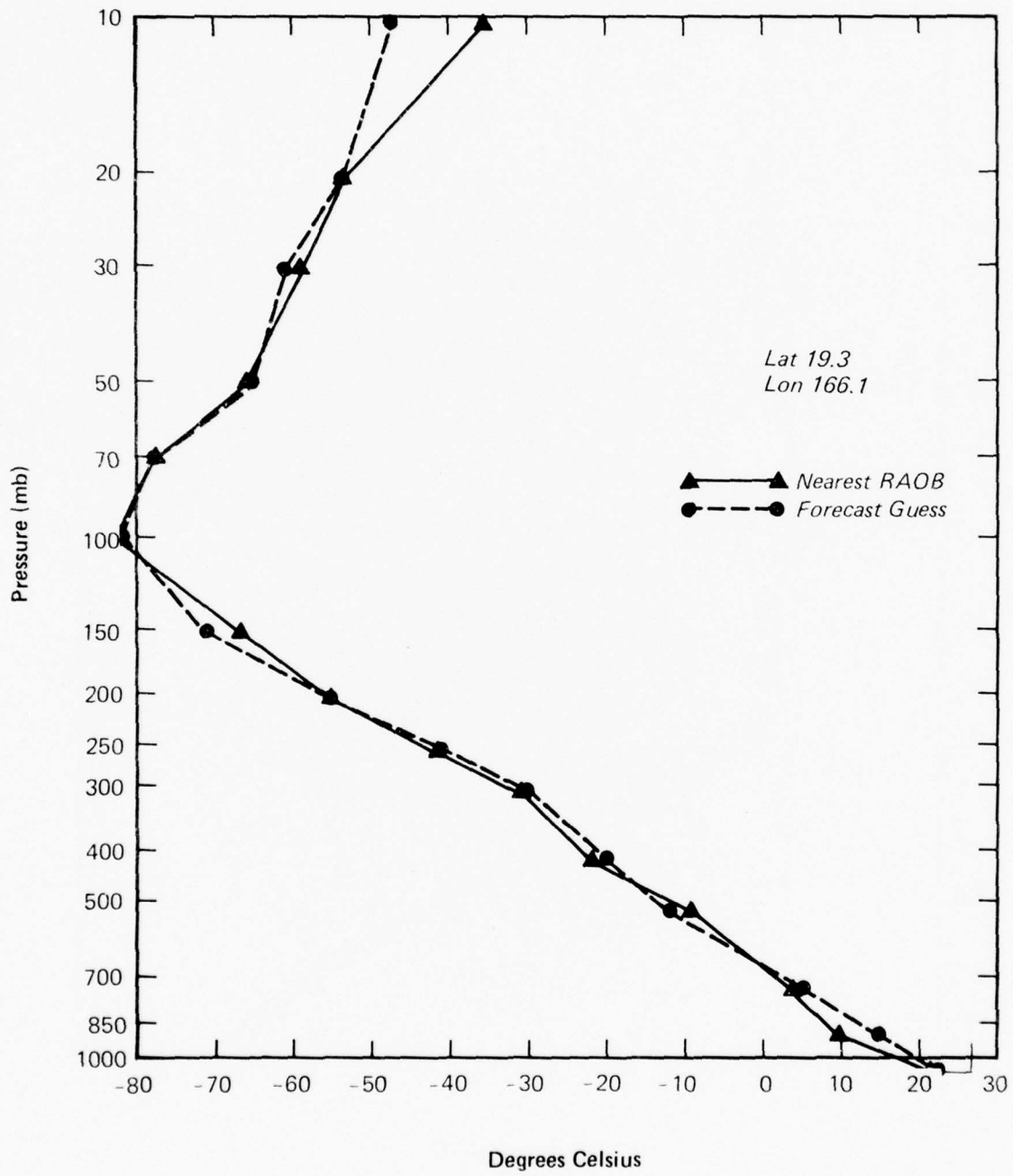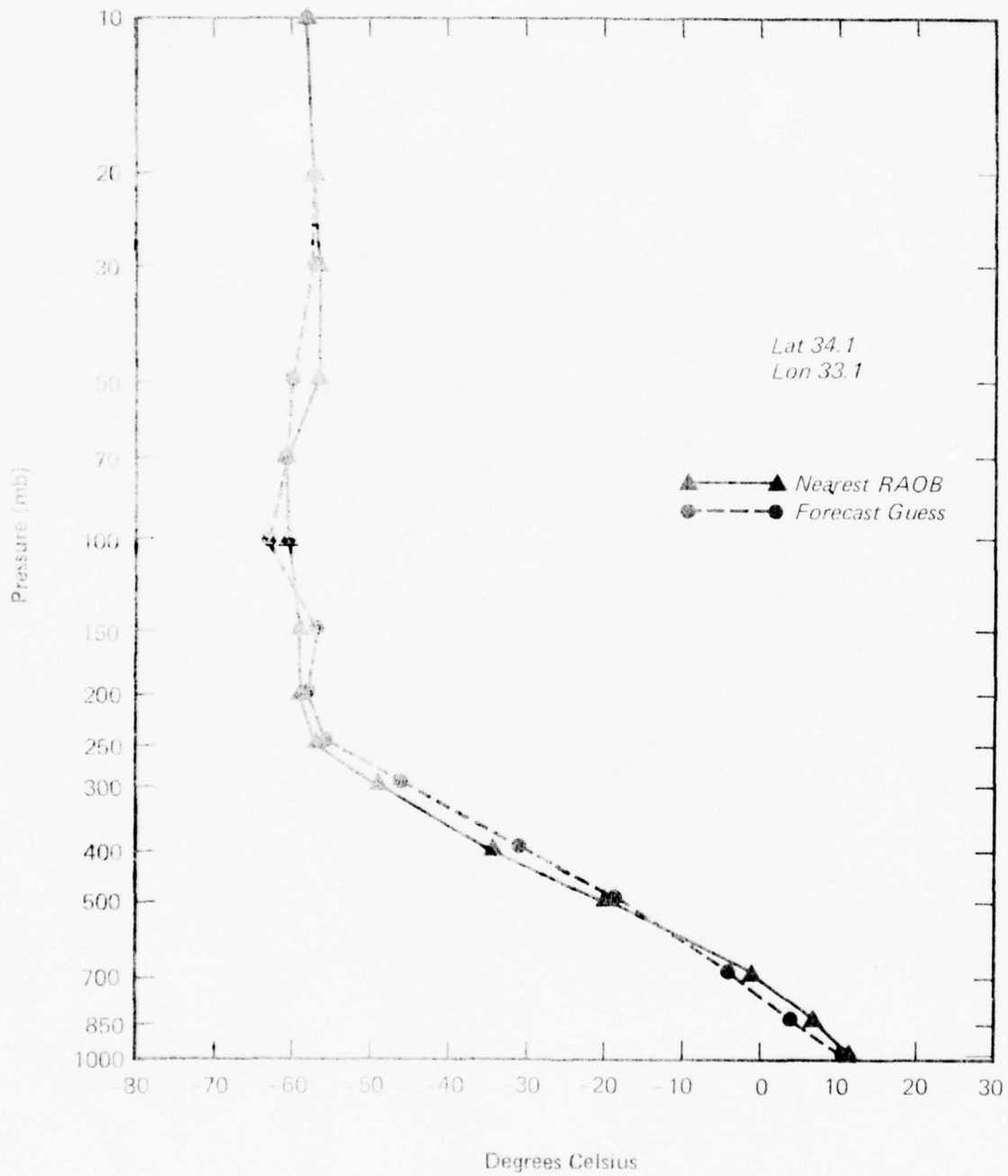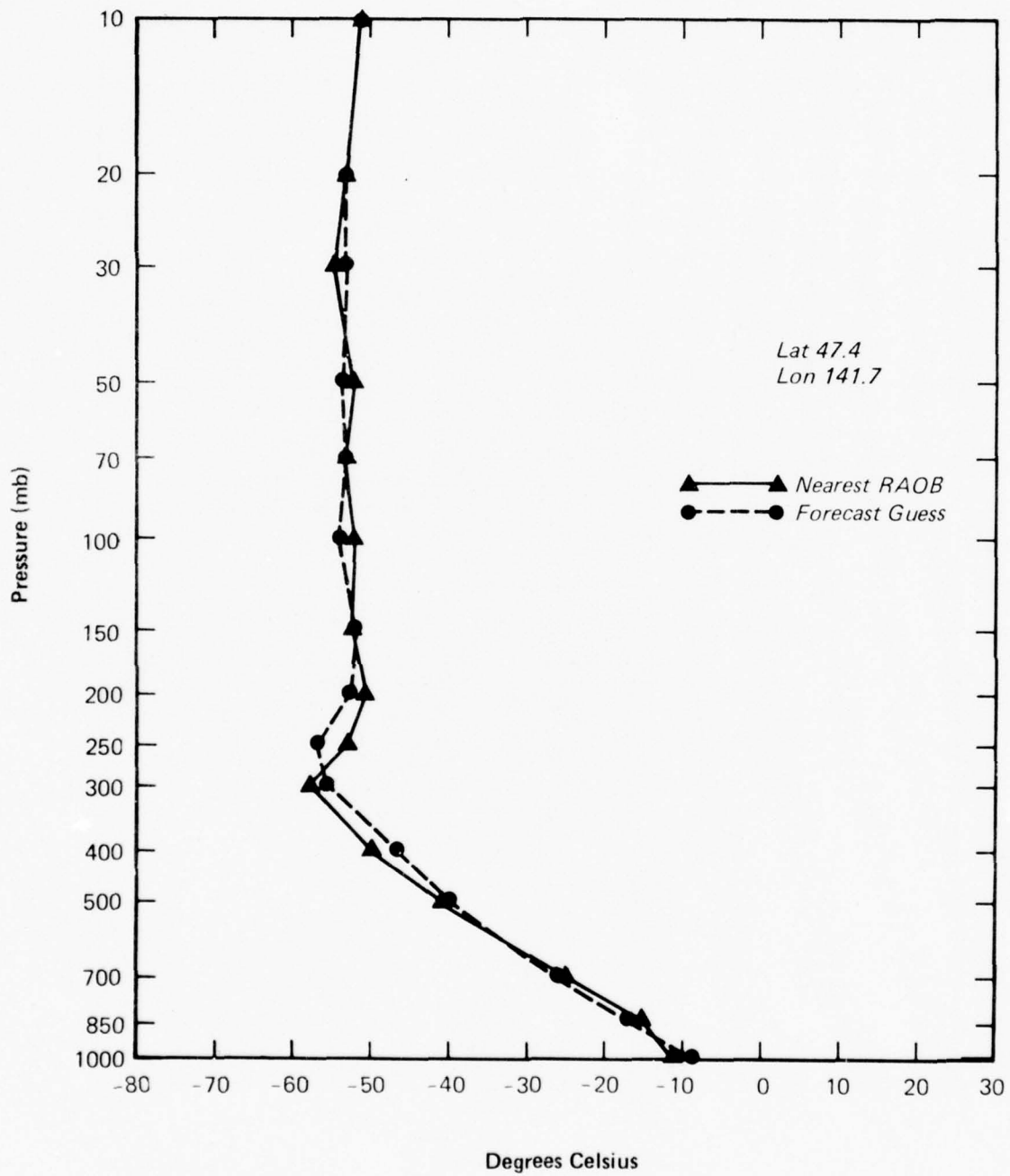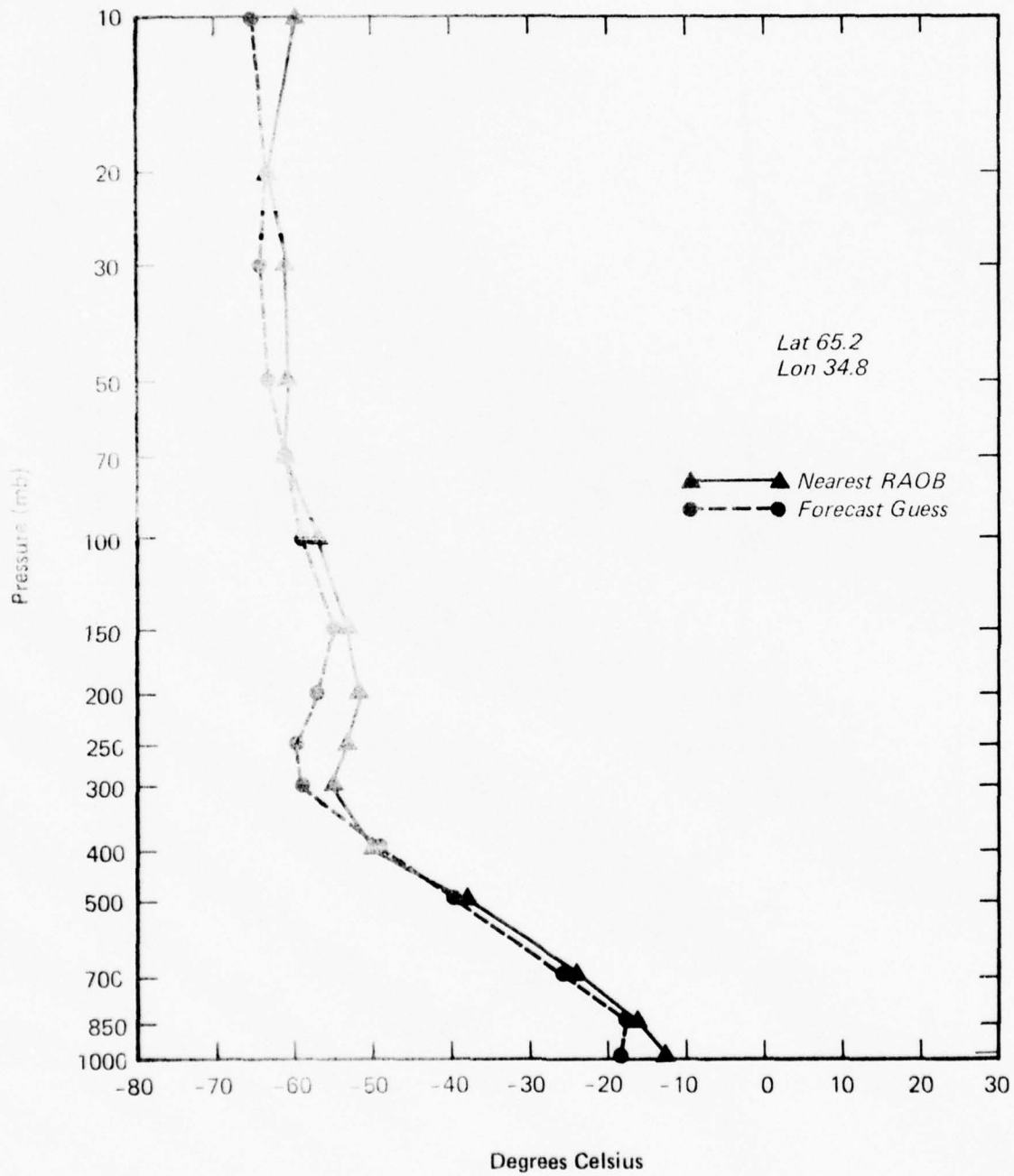Longitude
February 17, 1975, 1040Z

3.2 MEASURED RADIANCES FOR BIRDS 8531 and 9532

If a large enough data sample exists, it should be possible to analyze the measured radiances at each channel from one satellite and compare it with those from another. If the center frequency of a particular channel was off or had drifted, or if the filters had changed so that the band width allowed a different energy spectrum to impinge upon the sensor, or if other satellite hardware aspects changed, then it would be difficult to expect that such changes would be the same for two different satellites. An analysis was made of the mean and standard deviation of the radiances detected for each bird as a function of sensor channel, latitude, and longitude. In particular, comparisons were made to determine the hardware responses for each sensor channel from each bird. Even though one bird is a morning and another is a noon-time sensor, a serious deficiency or equipment degradation should produce noticeable differences in the measured radiances for a particular channel when equipment discrepancies exist between the two birds. Furthermore, before the adverse effects of such things as water vapor or surface effects can be placed within a proper context, it is important to know the mean conditions expected for a particular channel and the normal

variance about that mean.

A representative measure of the mean radiance and standard deviation as a function of channel and latitude is given in Table 3.4 for Bird 8531. In general, channel 3 which has a weighting function which peaks closest to the tropopause has the lowest power (or temperature) and shares with channel 4 the lowest standard deviation of measured radiance. As would be expected, the measured radiant power beginning with channel 4 or greater (with weighting functions peaking at 400 mb or greater) decreases from the tropics to the mid-latitudes to the polar regions. The standard deviation of satellite measured radiance within the tropics is about half of that for extra-tropical latitudes. This should be expected since the most significant day to day atmospheric changes take place within the extra-tropical latitudes.

Since the tropics are relatively quiescent and do not play an important role in most day to day numerical weather forecasts, it becomes important to compare changes that occur between mid-latitudes and polar regions. For the more than 1200 soundings of mid-latitudes and polar regions, the variance of the radiance, measured at each channel that peaks within the troposphere, is nearly the same. That is to say, that whatever differences exist between mid-latitude and polar

TROPICS - 0 to 26 North Latitude

Channel

	1	2	3	4	5	6	7	8
Mean Radiance	57.54	44.82	40.88	54.65	76.31	92.33	117.8	123.6
Standard Deviation	1.47	1.69	.65	2.72	3.83	3.75	2.63	4.27

MID-LATITUDE - 26 to 62 North Latitude

Channel

	1	2	3	4	5	6	7	8
Mean Radiance	56.38	47.83	44.27	49.8	63.81	75.67	91.58	105.22
Standard Deviation	5.	5.06	3.63	2.92	5.8	7.92	13.18	8.06

POLAR - 62 to 90 North Latitude

Channel

	1	2	3	4	5	6	7	8
Mean Radiance	45.5	37.95	35.55	40.65	50.76	58.52	61.56	87.27
Standard Deviation	4.97	5.42	3.87	2.74	4.29	6.93	13.27	8.99

NORTHERN HEMISPHERE - 0 to 90 North Latitude

Channel

	1	2	3	4	5	6	7	8
Mean Radiance	55.59	44.65	41.02	51.47	69.58	83.39	103.32	114.14
Standard Deviation	5.25	4.6	3.54	5.53	10.24	13.42	21.8	14.44

Table 3.4   Measured Radiance Mean and Standard
             Deviation Values for Bird 8531 for 0 to
             180 Degrees East Longitude as a Function
             of Latitude and Sensor Channel

regions, satellite radiometers detect the same signal power variations. This fact will become increasingly more imporant when the effects due to water vapor contributions are discussed in section 3.4, where it will be shown that water vapor cannot possibly account for the variance of radiance observed in the polar regions.

When considering all latitudes and longitudes, it can be shown, as in Fig. 3.12, that the average measured radiance for each Bird is highly correlated with the other, with a correlation coefficient of 0.9978. This implies that within the overall gross sense, observations from one satellite correspond closely with the other satellite.

A comparison was made between the average measured difference in radiance between Birds 8531 minus 9532 as a function of sensor channel and latitude belt, as shown in Figs. 3.13, 3.14, and 3.15. In all cases, for all latitudes, channel 4 radiance for Bird 8531 was lower (colder) than that for Bird 9532. This feature proved to be the exception, however. As latitude of observation increased, so did the difference between measured radiance between Birds 8531 and 9532. In general, Bird 8531 received more radiant power, showed warmer temperatures, than Bird 9532 for ever increasing latitudes. In fact, Fig. 3.16 shows a composite of all satellite soundings at all latitudes and longitudes for each bird as a function of sensor channel. Once again, channel 4 is

odd, showing that the sensor for Bird 8531 reports lower or colder radiances than the same sensor for Bird 9532. On the other hand, all remaining sensor channels of Bird 8531 report higher or warmer values than those from Bird 9532. These results suggest that equipment differences or degradations need to be explored between satellite Birds 8531 and 9532.
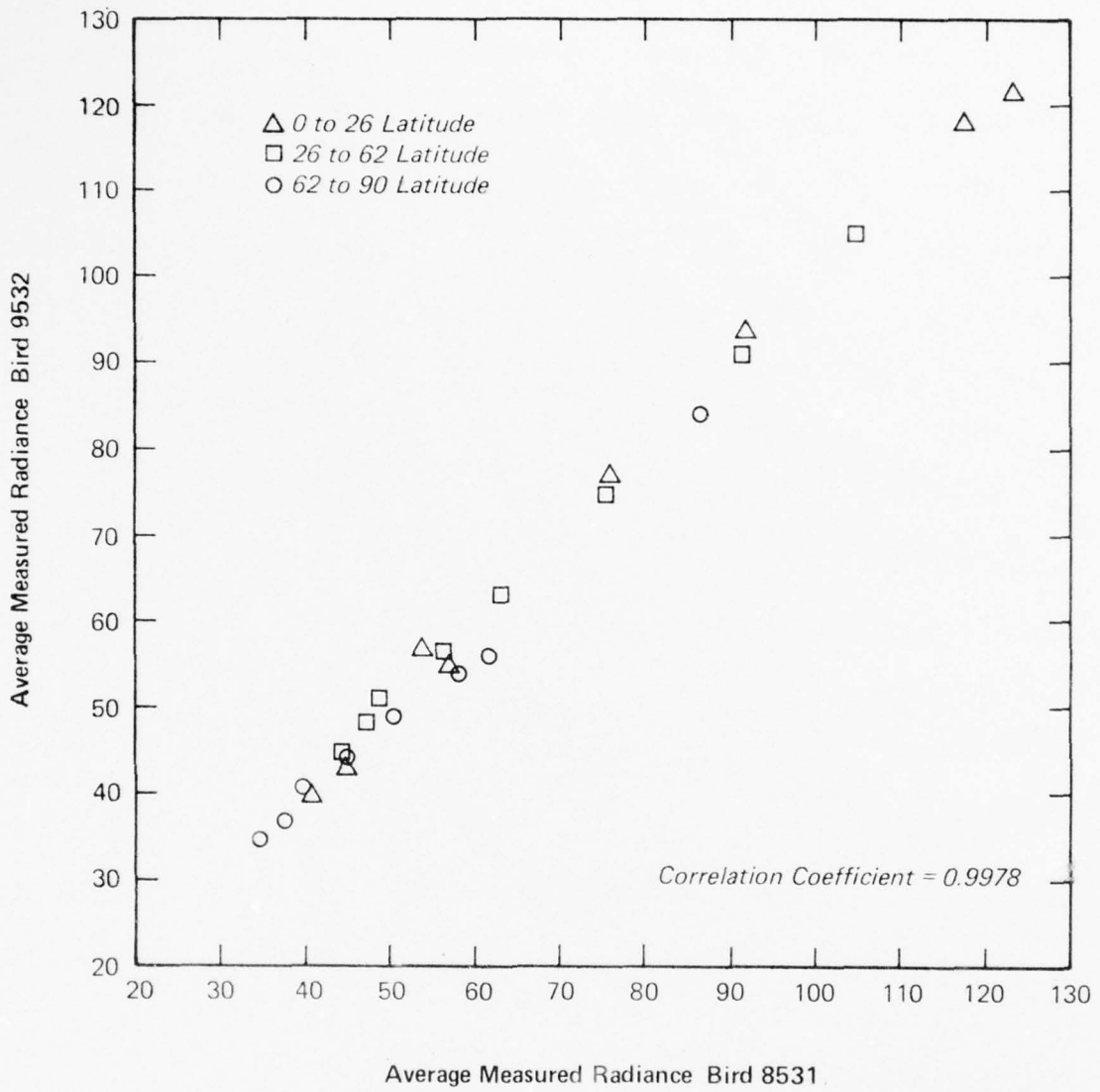
Figure 3.12 Correlation of Radiance
            Measured from Birds 8531
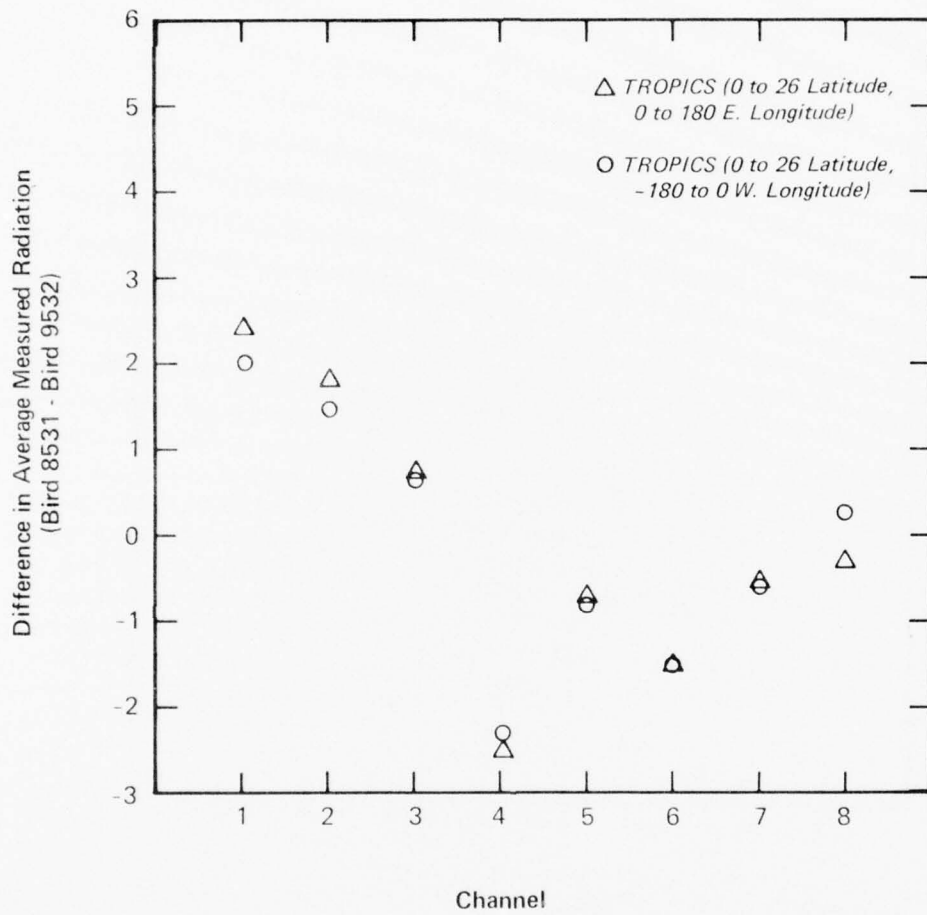   and 9532

82

Figure 3.13 Difference in Radiance
Measured by Both Satellites
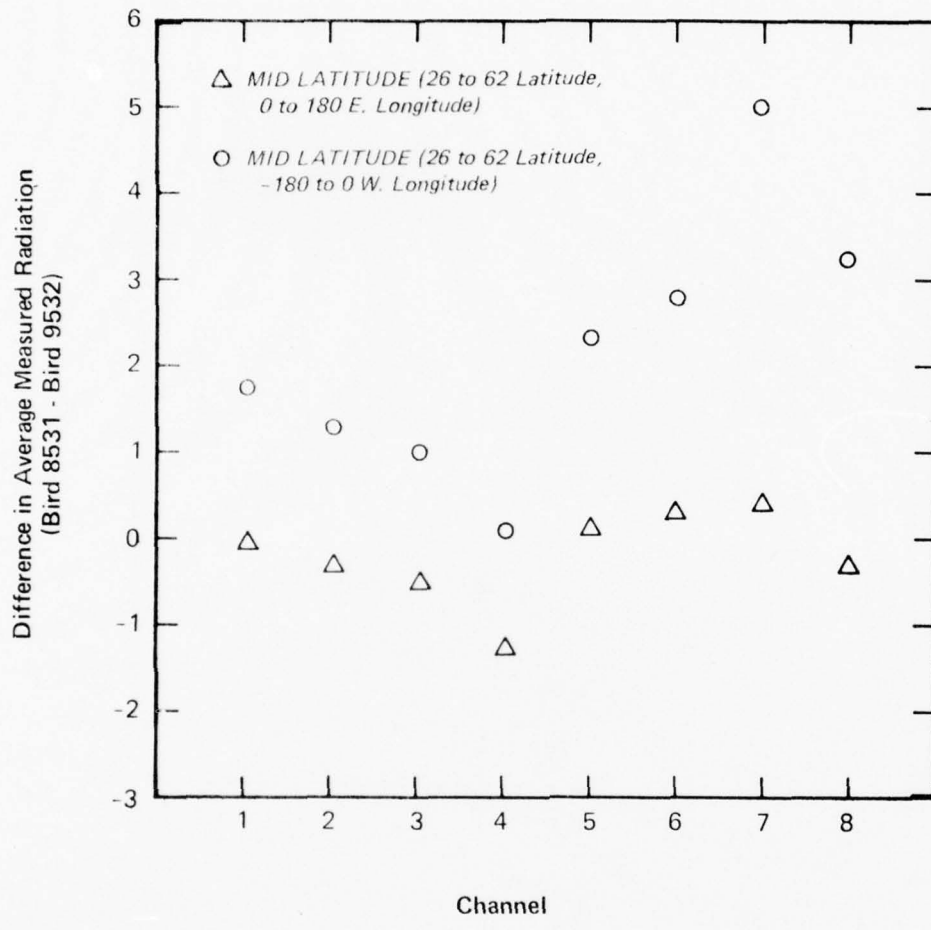in Tropics

Figure 3.14 Difference in Radiance
          Measured by Both Satellites
          in Mid-Latitudes
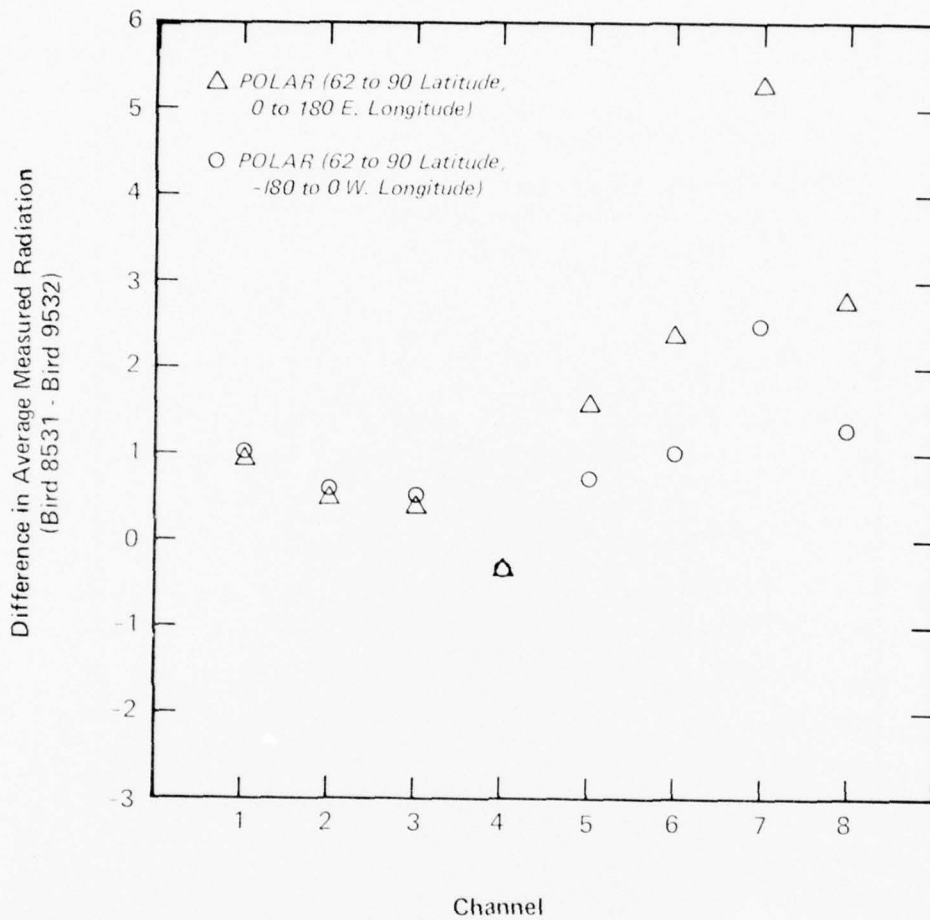
Figure 3.15 Difference in Radiance
Measured by Both Satellites
in Polar Regions
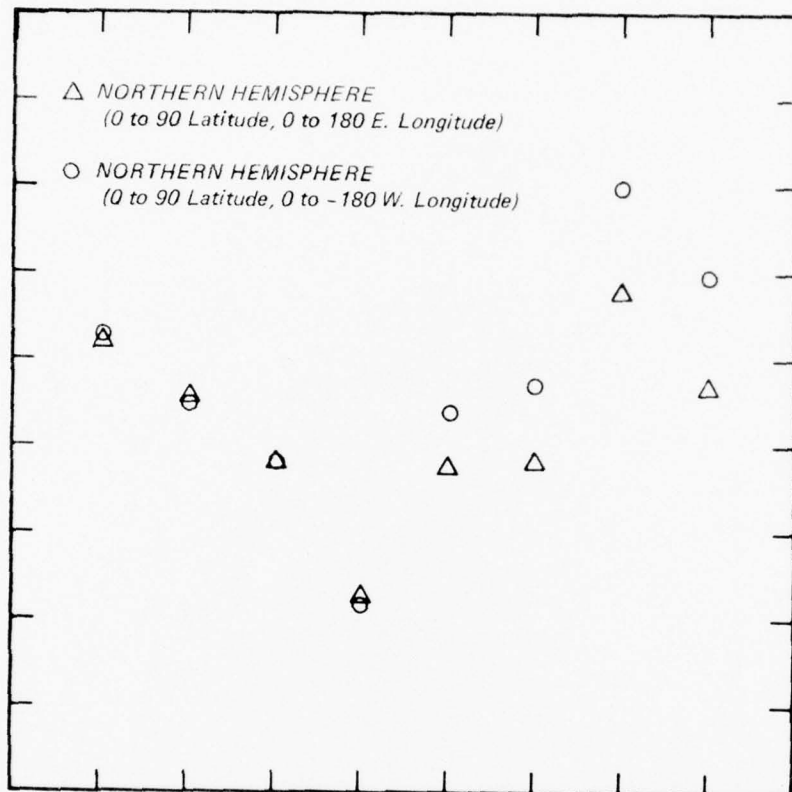
Figure 3.16 Difference in Radiance
        Measured by Both Satellites
        in Northern Hemisphere

86

3.3 DISCRIMINATION CRITERIA

Several types of control parameters are used in the AFGWC computer program SOUNDER that affect acceptance or rejection of a satellite sounding. These control parameters were studied to determine their influence on the number, type, and quality of the satellite radiance observations that are accepted for use in the inversion process. Section 2.1.3, the subprogram ITERAT, discusses in detail functions of the control parameters DELWND, CLDDIF, and HOTSFC. DELWND is the radiance measured for window channel 7 minus the radiance calculated from both the underlying surface and atmosphere. The 1000 mb air temperature is used as the "ground" temperature to compute surface radiation contributions. The value of CLDDIF is used to test for clear radiance and to reject a sounding where clouds might be causing a difference between observed and computed radiance values. The value of HOTSFC is used to reject a sounding when a hot surface exists or a bad first guess temperature profile is made.

Analyses were made on the same data base using values of these parameters that were operational in February 1975 and that are operational today. Results show that SOUNDER with the present values accepts only 1/4 as many cases for completing an inferred profile as

it did in 1975. This was caused by imposing a more restrictive acceptance criteria of 1.1 for both CLDDIF and HOTSFC in the hopes of reducing rather large retrieval errors.

Let us consider the window channel difference values of DELWND in Table 3.5 for the 10 research profiles having coincident satellite and RAOB soundings. In order for any of these soundings to be acceptable for use in the temperature retrieval process, both the low level cloud, CLDDIF, and hot surface, HOTSFC, criteria would have to equal or exceed these DELWND values. With today's operational criteria of 1.1, there is only one case in ten that would be accepted cut of the sample where the nearest (coincident) RAOB was used to calculate surface and atmospheric radiance in the window channel. Furthermore, that one case exists in the tropics where temperature profile data are usually not as critical to the success of numerical analysis and prediction models. Using the 12-hour forecast data in computing the radiances to obtain DELWND, Table 3.5 values show only three of the ten cases would be acceptable to the retrieval process. All three of the acceptable cases, however, have relatively standard type lapse profiles. It appears, therefore, that the discrimination criteria in use today are eliminating those cases having

88

| | | DELWND | |
LATITUDE	LONGITUDE	NEAREST RAOB	FORECAST DATA
BIRD 9532			
69.5	81.0W	-5.2	-2.0
47.4	141.7E	3.5	.8
34.5	138.5E	11.8	-2.3
38.1	141.8E	5.6	-.7
68.2	53.6E	-5.3	-2.1
BIRD 8531			
19.3	166.1E	.2	-1.1
65.2	34.8E	-4.3	2.8
71.9	155.5W	-2.9	-2.9
79.8	75.4E	-1.7	2.8
34.1	33.1E	3.1	4.5

Table 3.5 Low Level Clouds and Hot Surface Discrimination
Values for the Ten Research Profiles

the most significant types of meteorological profiles.

Striking results are shown in Fig. 3.17 where DELWND values are plotted against the observed RAOB temperature gradient from 1000 to 850 mb level for each of the ten research cases. Notice first that the distribution of plots is quite different for Bird 9532 versus 8531. This is due in part to that fact that Bird 8531 has more lapse profile type cases. But of most importance is the 17 mW m^{-2} Sr^{-1} cm^1 range in radiance associated with the type and intensity of low level atmospheric stability. This range in radiance is highly significant especially since, as shown in the next section, it greatly exceeds the range of radiances associated with water vapor contributions in mid and high latitudes and is comparable with the maximum extremes possible within the tropics. It is not the low level temperature gradients per se but rather the effects due to the underlying surface that are important. These surface effects are, however, portrayed by the low level atmospheric stability conditions.

When a ground based temperature inversion exists, the air temperature increases with height. Also under these conditions, the underlying surface is colder than the air temperature. The reverse is true when the atmosphere becomes more unstable and the low level
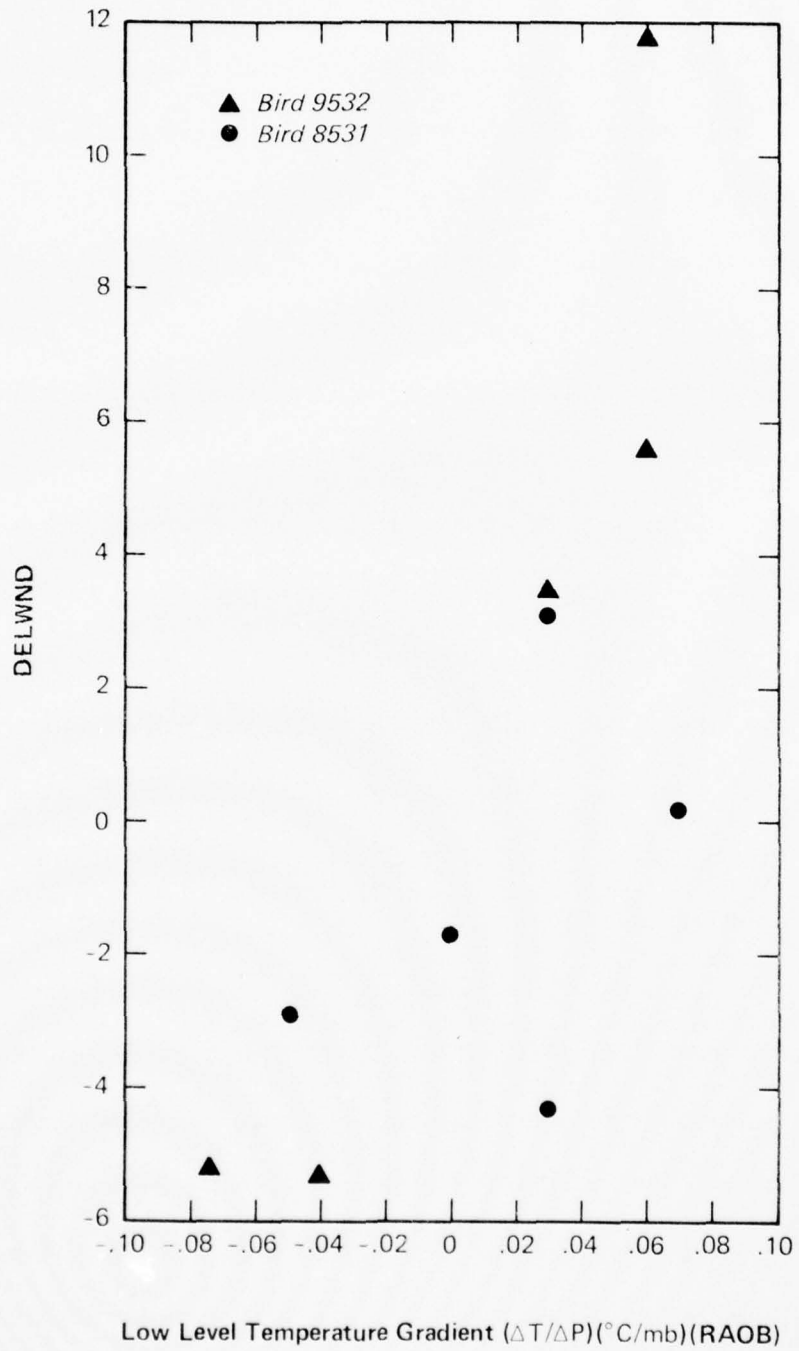
Figure 3.17 Discrimination Criterion DELWND
Related to Low Level Atmospheric
Stability

91

temperature profile approaches or exceeds dry adiabatic conditions. Since the surface radiance contributions are computed using the 1000 mb level air temperatures, significant differences can be expected between measured and calculated when the 1000 mb level air temperature is non-representative of the surface temperature. This becomes more pronounced as the low level atmospheric stability deviates from the standard lapse type profiles. Thus it can be seen in Fig. 3.17 that for ground based inversions, stable atmospheres with a negative change in temperature with pressure, the measured satellite radiance in the window channel is lower (colder) than the calculated ground and atmospheric contributions giving a negative value of DELWND. The reverse is true for those cases when the atmosphere becomes increasingly more unstable. These striking effects due to the underlying surface are discussed in greater detail in section 3.5.

For our purpose here, it must be stated that the existing operational values for CLDDIF and HOTSFC are too restrictive. For example, when the measured surface radiance is lower (colder) than that calculated by an amount exceeding CLDDIF, then no temperature retrievals are presently made from satellite data. The rationale being, if a very low level cloud exists, which could not be detected via

previous discrimination procedures, then the cloud top would produce a lower measured radiance in the window channel than is calculated and thus a cloud-free line of sight does not exist and a temperature retrieval should not be attempted. As shown in Fig. 3.17, this rationale eliminates all the stable cases with low level ground based inversions where the underlying surface air temperature can be considerably lower (colder) than the 1000 mb air temperature. In fact, under these conditions, if a low level cloud did exist, the cloud top temperature would be warmer, not colder, than the underlying surface. For several research profiles with ground based inversions, the ground air temperature is colder than any ambient air temperature up to 10,000 feet (700 mb). Thus restrictive values for CLDDIF eliminate the possibility of temperature retrievals under these conditions. There are times when CLDDIF criteria could eliminate low level cloud cases but these times can only exist during conditions of lapse type profiles. Since the first guess temperature profile, given by the 12-hour forecast field, provides a measured of the low level atmospheric stability, it could be used to improve the discrimination or selection process for satellite soundings worthy of temperature retrievals.

Table 3.6 shows the different combinations of criteria for

CLDDIF, HOTSFC, SNOIS, and EPS used within the GAC research
SOUNDER. From Table 3.5 it can be seen that a value of 5 for CLDDIF
and HOTSFC will allow all cases for Bird 8531 to be retrieved. A larger
value was necessary to accomplish temperature retrievals for all Bird
9532 cases. The purpose here was to insure that all 10 research profile
cases were acceptable for temperature retrievals in order to determine
the effects of SNOIS and EPS on the resultant inverted temperatures.
SNOIS is the ratio of signal to noise of the instrument and is used to
determine if the sum of the square of the deviations between measured
and calculated radiances is small enough to allow convergence for a
solution. EPS is the epsilon value used to monitor the maximum difference
allowable between calculated and measured radiance from any channel.

Table 3.6 Cloud and Hot Surface Discriminants and Solution
             Convergence Values

For Bird #9532 (5 locations)

CLDDIF	5	5	20	20	20
HOTSFC	5	5	20	20	20
SNOIS	3	1.5	3	0.3	0.1
EPS	1	0.5	1	0.1	0.033

For Bird #8531 (5 locations)

CLDDIF	5	5	5
HOTSFC	5	5	5
SNOIS	1.5	0.3	0.1
EPS	0.5	0.1	0.033

These control parameters and how they interface with SOUNDER are discussed in detail in section 2.1.3. In general, it can be said that minor differences were obtained in the retrieved temperature profiles even though a large range of values was used for SNOIS and EPS. Even for a five-fold difference in SNOIS and EPS values, as shown in Fig. 3.18, temperature retrievals at different pressure levels differed by only a few tenths of a degree. On the average, the largest differences occurred in the tropopause region and at about the 70 mb level. None of these differences could account for the source of the larger errors in the satellite retrieval process.
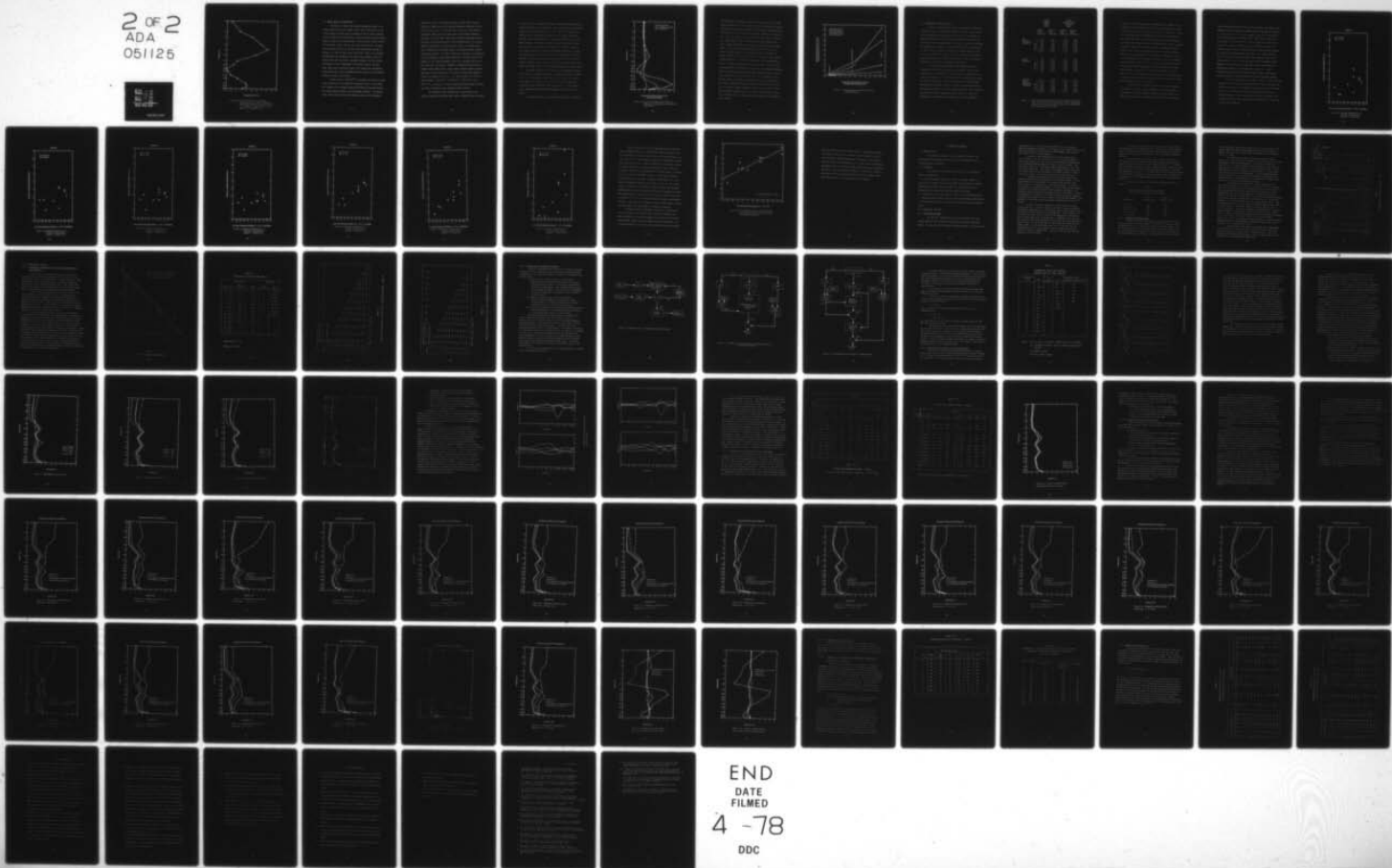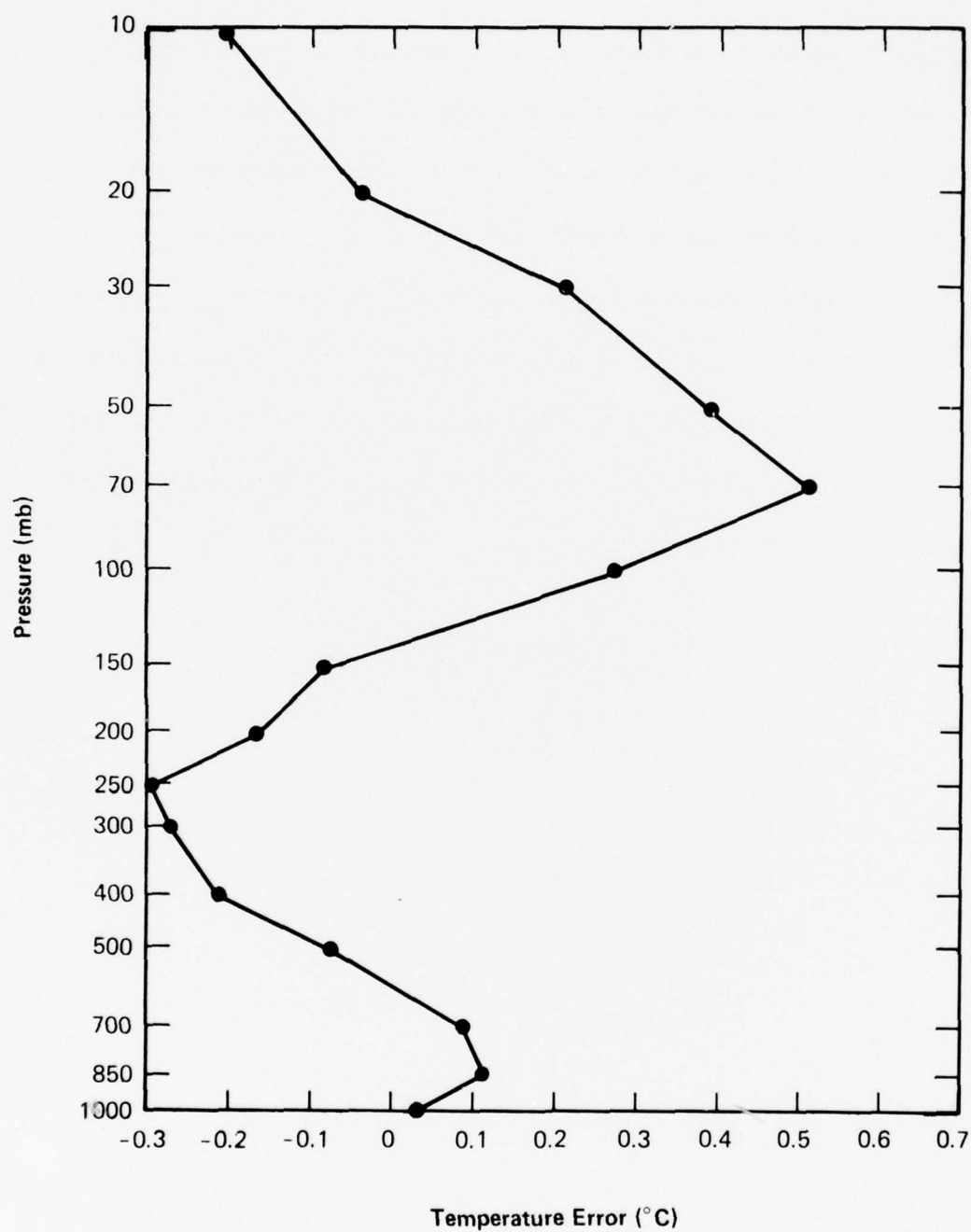
Figure 3.18 Average Difference in Retrieved
          Temperature for Two Sets of SNOIS and
          EPS Values Differing by a Factor of Five
          (i.e. SNOIS = 0.3 and EPS = 0.1, and
          SNOIS = 1.5 and EPS = 0.5)

3.4 WATER VAPOR CONTRIBUTIONS

No attempt is made in the existing operational system to include variable effects due to water vapor. Recall from Table 2.5 that a fixed relative humidity value is assigned to the 28 levels extending from the surface to the 200 mb level. Typical assigned relative humidity values are about 73% near the surface, 65% at 850 mb, 55% at 700 mb, 47% at 500 mb, 32% at 300 mb, and 16% at 200 mb level. For fixed relative humidity values, as the first guess temperatures increase or decrease, so does the water vapor mixing ratio, which is so important in determining the concentration of water vapor molecules which contribute to the final measured or calculated radiance. Via this feature, the warmer low level temperatures in the tropics account for much larger water vapor contributions than do the colder polar temperatures. In this manner the existing SOUNDER routine accounts for major latitude variations of water vapor effects.

A recent study by Weinreb [20] investigated the effects of water vapor contributions on the retrieved temperature profile. It was shown that "changes in the assumed mixing ratio affect the retrieved temperature chiefly through changes in the calculated radiances". Furthermore, it was shown that when the initial forecast guess of the temperature

profile was close to the actual that errors in water vapor estimates resulted in larger errors in the minimum-information technique than the initial forecast guess. On the other hand, when the initial forecast temperature profile guess had large errors, the minimum-information technique, even with water vapor errors, produced temperature profiles that were an improvement upon the initial forecast guess. In essence, Weinreb suggests that, for the most part, errors in estimating water vapor contributions are principal factors in attaining accurate satellite temperature retrievals. In order to place these statements in perspective with the underlying surface effects discussed in the next section, the changes in the computed radiances need to be considered for errors in the water vapor mixing ratio. Weinreb's computational results from a Midway Island RAOB shows a linear relation between radiance changes and errors in the mixing ratio. A 50% error in mixing ratio produced changes in radiance of 3.6, 2.6, 1.1, and 0.2 mW sr^{-1} m^{-2} cm^{1} for sensor channel 7 (835 cm^{-1}), 6 (747 cm^{-1}), 5 (725 cm^{-1}), and 4 (708 cm^{-1}), respectively. It will be shown that these radiance changes are small in comparison with underlying surface effects.

The maximum effects possible due to water vapor on the satellite temperature retrievals were studied. Radiances were calculated

for each of the 10 research RAOB profiles assuming complete saturation (wet) at all levels in the atmosphere. These computations were repeated assuming zero moisture (dry) at all levels. Figure 3.19 presents the difference in the temperatures retrieved via the minimum information technique using totally wet and dry conditions imposed upon the same RAOB sounding. The largest temperature retrieval errors due to water vapor occur in the 850 and 700 mb regions. An oscillation exists in the vertical distribution of retrieved temperature differences such that the surface value is nearly the same sign and magnitude as at 100 mb. Whereas the maximum positive differences around 700 mb give way to negative differences about the 300 mb level. Thus it can be seen how errors in the lower portion of the atmosphere propagate to higher levels.

Very large differences (22.5°C) exist in temperatures retrieved at 700 mb from a saturated and totally dry tropical sounding, as shown in Fig. 3.19. Mid-latitude differences are about half of the extreme values found in the tropics. Even in the polar regions where cold temperatures inhibit high water vapor mixing ratios, a 2°C difference can be expected between retrieved temperatures from a wet and dry profile.

The extreme effects of a totally saturated versus a completely

99

**Retrieved Temperature Difference from
Wet minus Dry Profile**
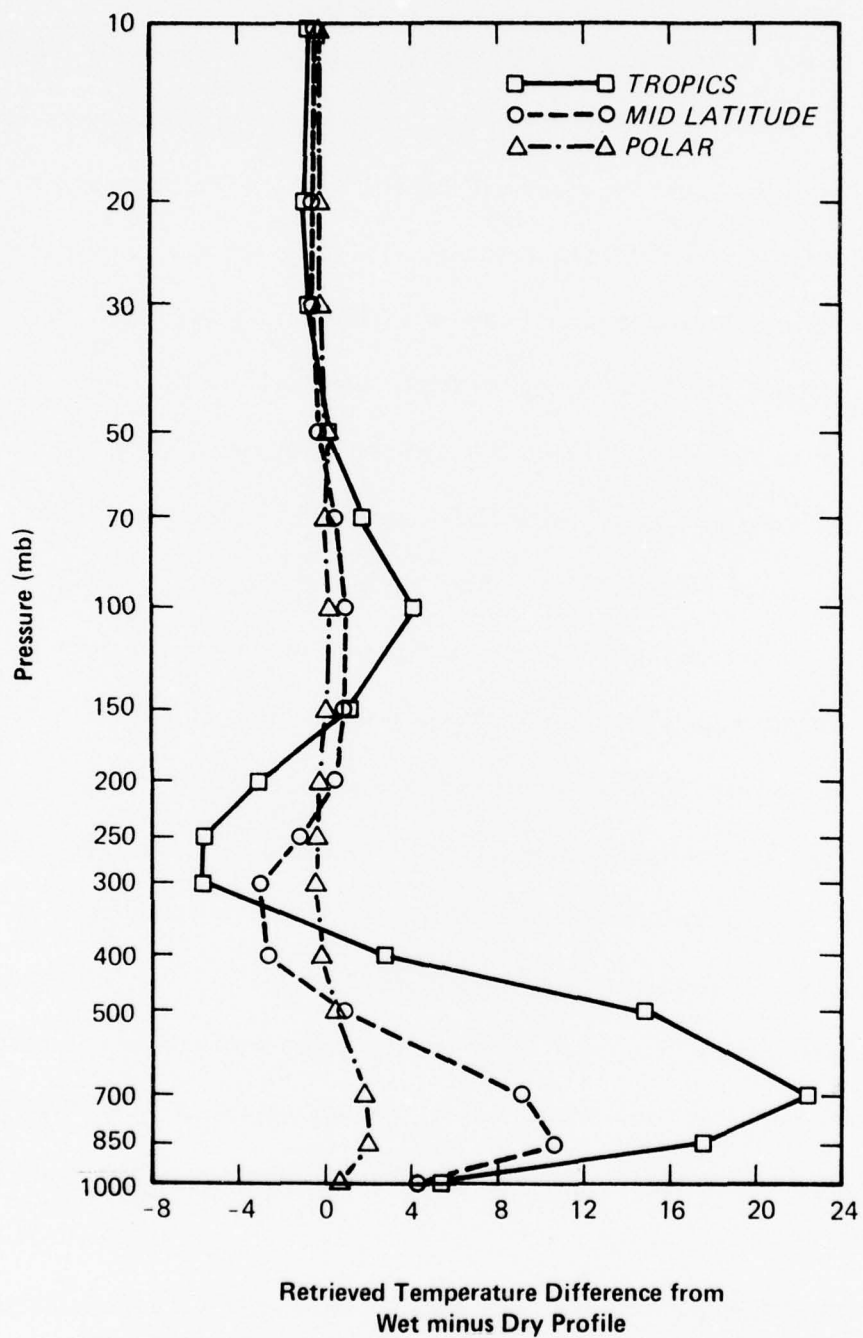
Figure 3.19 Levels in the Atmosphere Where the
Retrieved Temperatures are Influenced by
Water Vapor

100

dry atmosphere on calculated radiance are shown in Fig. 3.20. Radi-
ances calculated from a dry minus those from a wet profile are plotted
against the average of the saturation mixing ratios at mandatory levels
from 1000 mb to 500 mb level. The radiance difference for channels 4,
5, 6, and 7 are plotted at three average saturation mixing ratios that
were derived from a polar, mid-latitude and tropical RAOB profile.
These radiance differences are the extremes possible for water vapor
effects. The greatest radiance difference (19 mW m^{-2} sr^{-1} cm) is
found in window channel 7 for a tropical profile. In general, the
radiance difference due to moisture extremes decreases as the channel
number decreases and the depth of atmosphere under interrogation de-
creases. Radiance differences of less than 5 mW m^{-2} sr^{-1} cm occur
at mid-latitudes for all channels. These values can produce pronounced
errors in retrieved temperatures and efforts should be made to incorpo-
rate satellite derived moisture information into the retrieval process.
Moisture effects are nearly non-existent for the polar regions where
the average saturation mixing ratio between 1000 and 500 mb is less
than one and the radiance difference is less than 0.4 mW m^{-2} sr^{-1} cm.
These radiance differences from a dry and wet profile will be shown
to be small for mid- and high-latitudes when compared with underlying
surface effects.
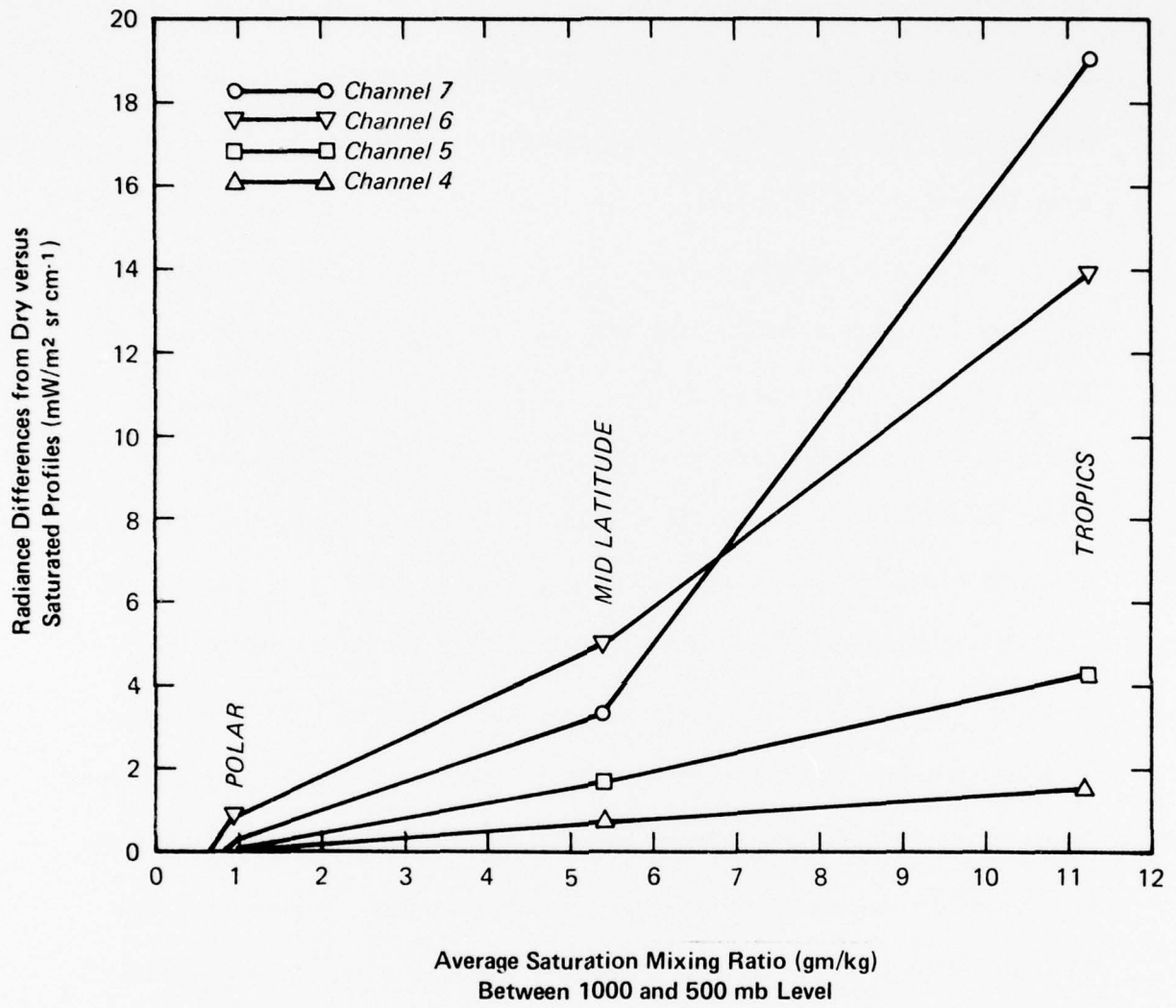
Figure 3.20 Extreme Effects of Water Vapor Upon
Satellite Radiance

3.5 UNDERLYING SURFACE EFFECTS

Section 3.3 described the physics and rationale for effects of underlying surfaces on calculated radiances. In short, it says that for stable atmospheres with ground-based inversions, air temperature increases with height so that the surface temperatures are colder than the 1000 mb level air temperature. The reverse is true for the unstable dry adiabatic type conditions. Presently the 1000 mb air temperature is used to compute surface contributions to satellite radiances. But due to the nonrepresentativeness of these air temperatures in depicting surface temperatures, the largest single source of error in calculated radiances is due to these underlying surface effects.

The ten research RAOB profiles were separated into three categories of ground-based inversions, dry adiabatic, and the more standard lapse type profiles. In order to determine surface effects on each sensor channel, the expected radiance was calculated using first, the coincident RAOB and then the 12-hour forecast temperature data. Differences were obtained between measured and calculated radiances and grouped according to the three stability categories. These radiance differences were added separately for each category to obtain the algebraic and the absolute mean differences, which are tabulated in

| | | USING NEAREST RAOB DATA | | USING TWELVE HOUR FORECAST DATA | |
		Average Mean Difference	Absolute Mean Difference	Average Mean Difference	Absolute Mean Difference
DRY ADIABATIC PROFILES	1	.214	.216	.384	.384
	2	1.706	1.706	4.209	4.209
	3	.541	.541	2.102	2.102
	4	.163	.289	2.231	2.231
	5	3.098	3.098	2.732	2.732
	6	3.546	3.546	.119	.832
	7	8.710	8.710	-1.488	1.488
LAPSE PROFILES	1	- .209	1.844	.582	1.699
	2	.665	2.079	1.585	2.344
	3	.162	1.016	.804	.804
	4	- .740	1.154	- .507	1.004
	5	1.645	1.645	2.109	2.109
	6	.310	.804	.989	.989
	7	.626	2.752	1.766	2.304
GROUND BASED INVERSION PROFILES	1	-2.865	2.865	-2.575	2.575
	2	-1.393	1.393	- .882	1.593
	3	-1.558	1.568	- .372	1.643
	4	-1.864	1.864	- .443	.974
	5	-1.528	1.689	.056	.623
	6	-2.540	2.540	- .512	1.249
	7	-3.799	3.799	-1.045	2.470

(The "Channel" label appears vertically beside the channel numbers 1–7 in each profile group.)

Table 3.7 Difference between measured and calculated radiances for three types of low level temperature profiles. Calculated radiances were made separately using nearest RAOB data and twelve-hour forecast data.

Table 3.7. Thus if the average mean difference has exactly the same magnitude as the absolute mean difference, then differences for each individual case within the ensemble must have the same sign. That is to say that all cases are influenced the same way. This feature is exemplified for almost every sensor channel for both ground-based inversion and dry adiabatic profiles when RAOB data are used to compute radiances. Notice for ground-based inversion conditions, negative values of the average mean difference show that satellite measured radiance is lower (colder) than that calculated. Furthermore, and this is very significant, these effects are prominent in all seven channels, including channel 1 (668.5 cm^{-1}) on the peak of the CO_2 band where the weighting function supposedly terminates well above the underlying surface. The channel 1 average mean difference of -2.865 mW m^{-2} sr^{-1} cm for ground-based inversion cases in the polar regions is more than half the observed standard deviation value that represents the variability for all 518 polar cases.

Influence of the underlying surface is even more pronounced for channels 5, 6, and 7 for dry adiabatic cases which occurred in mid-latitudes. All seven channels show the measured radiance to be higher (warmer) than that calculated. This is due to the underlying

105

surface being hotter than the 1000 mb air temperature. An average mean difference between measured and RAOB calculated radiances for channel 7 is 8.710 mW m^{-2} sr^{-1} cm for dry adiabatic cases and -3.799 mW m^{-2} sr^{-1} cm for ground based inversion cases. This gives a range in the mean values of 12.509 mW m^{-2} sr^{-1} cm. To place this range value in perspective, it can be seen from Fig. 3.20, that this value due to underlying surface effects is more than twice as large as that attainable from extreme mid-latitude water vapor effects, i.e. totally saturated versus a totally dry profile. An analysis for channels 5 and 6 shows similar results. Thus, it can be concluded that the underlying surface effects are more important than water vapor effects in interpreting information from radiance measurements from channels 5, 6, and 7. Properly accounting for these underlying surface effects should greatly improve the ability to remotely measure low level temperature profiles.

Even for standard lapse type profiles, Table 3.7 shows measured radiances on the average are higher (warmer) than those calculated. Although surface effects are recognizable and consistent for lapse profiles they are not as striking as those for ground-based inversion or dry adiabatic conditions. Results using 12-hour forecast temperature data to compute radiances show characteristics similar but not as pronounced as those using RAOB data.

Channel 1

Figure 3.21 Radiance Differences as a
Function of Atmospheric
Stability - Channel One

107

Figure 3.22 Radiance Differences as a
Function of Atmospheric
Stability – Channel Two

Channel 3

Figure 3.23 Radiance Differences as a
Function of Atmospheric
Stability – Channel Three

Channel 4
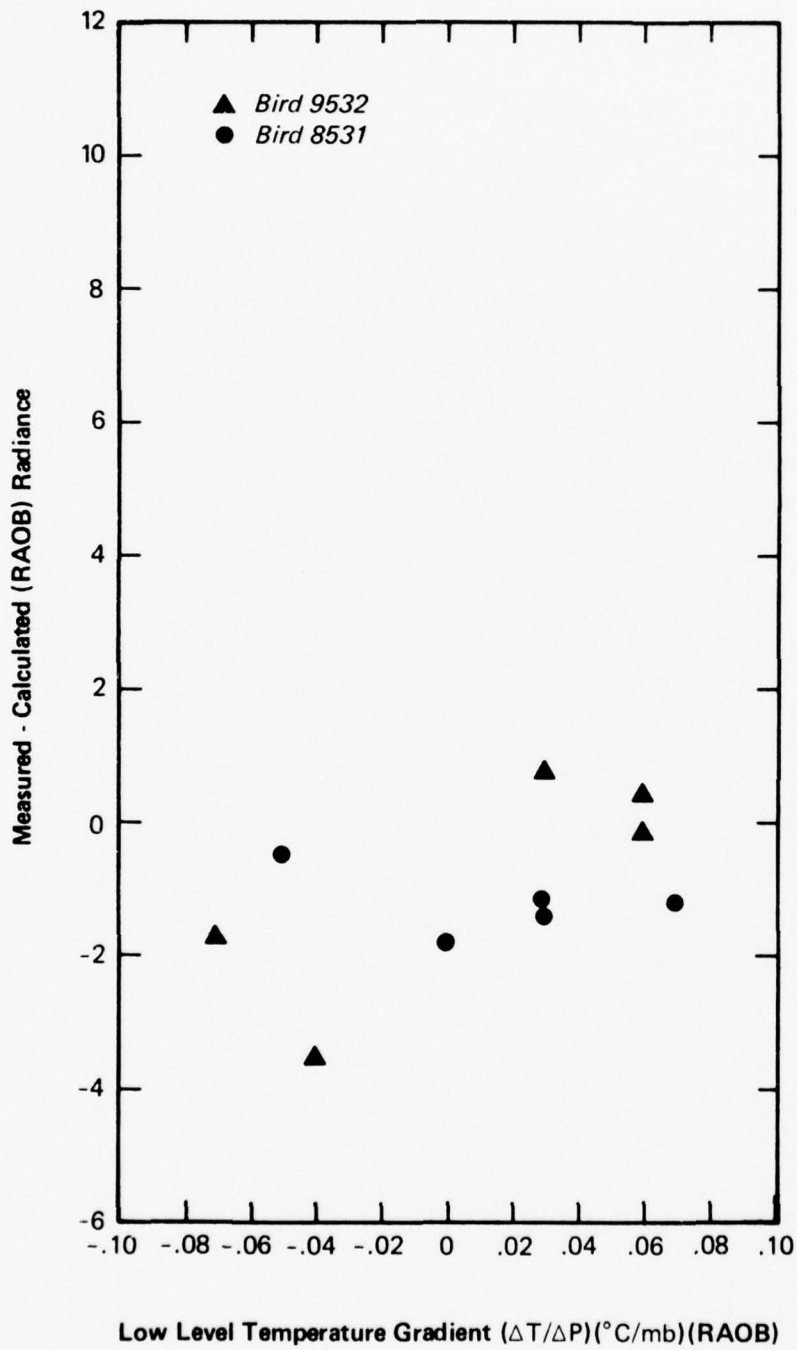
Figure 3.24 Radiance Differences as a
Function of Atmospheric
Stability – Channel Four

Channel 5
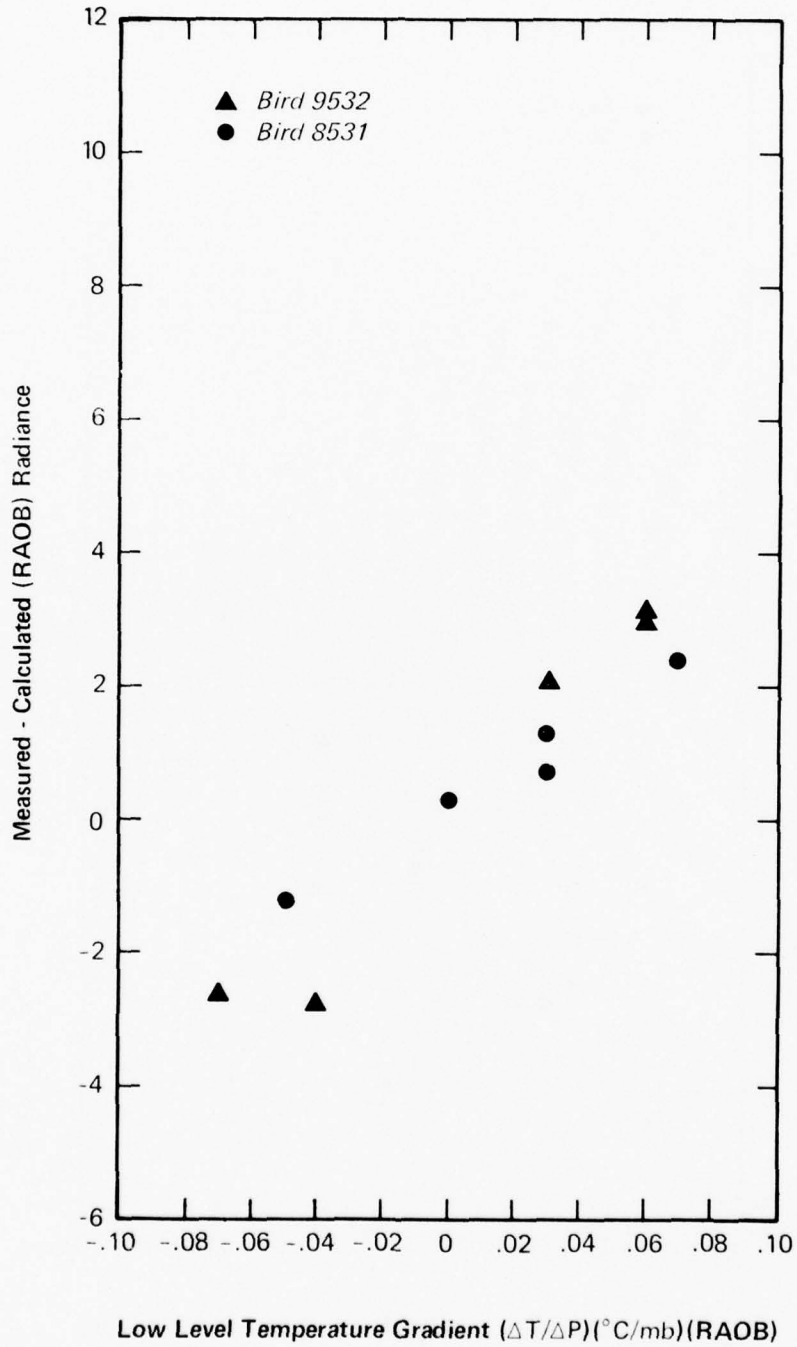
Figure 3.25 Radiance Differences as a
Function of Atmospheric
Stability - Channel Five
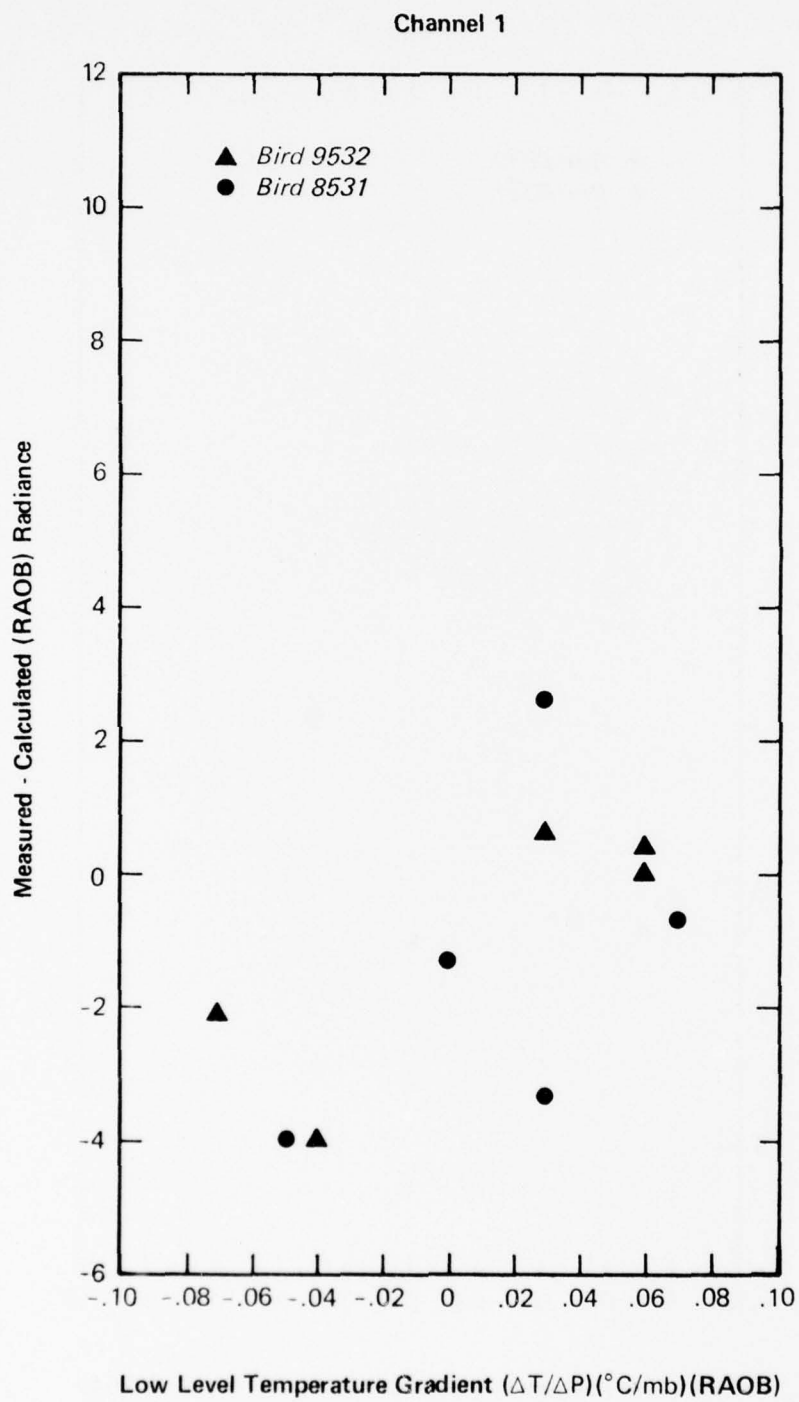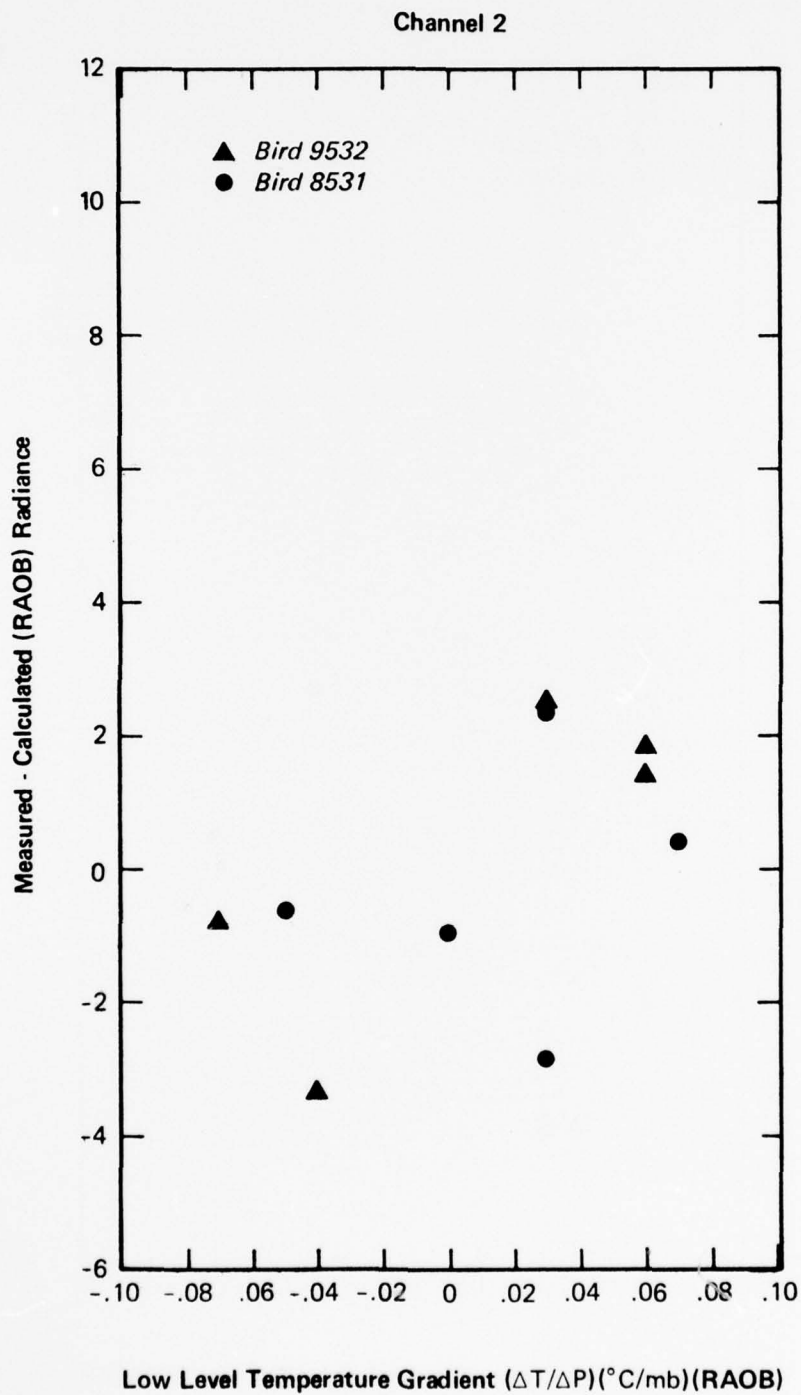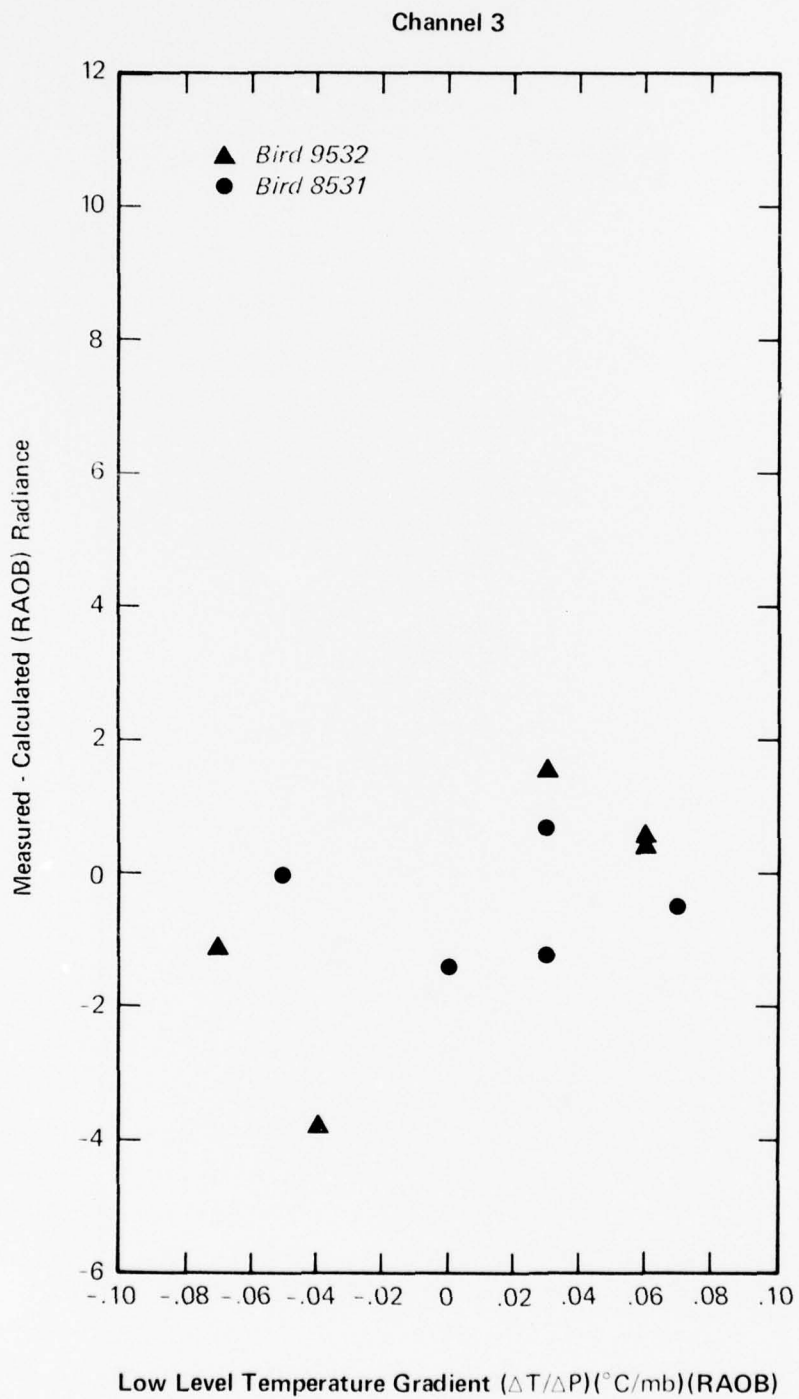
Channel 6
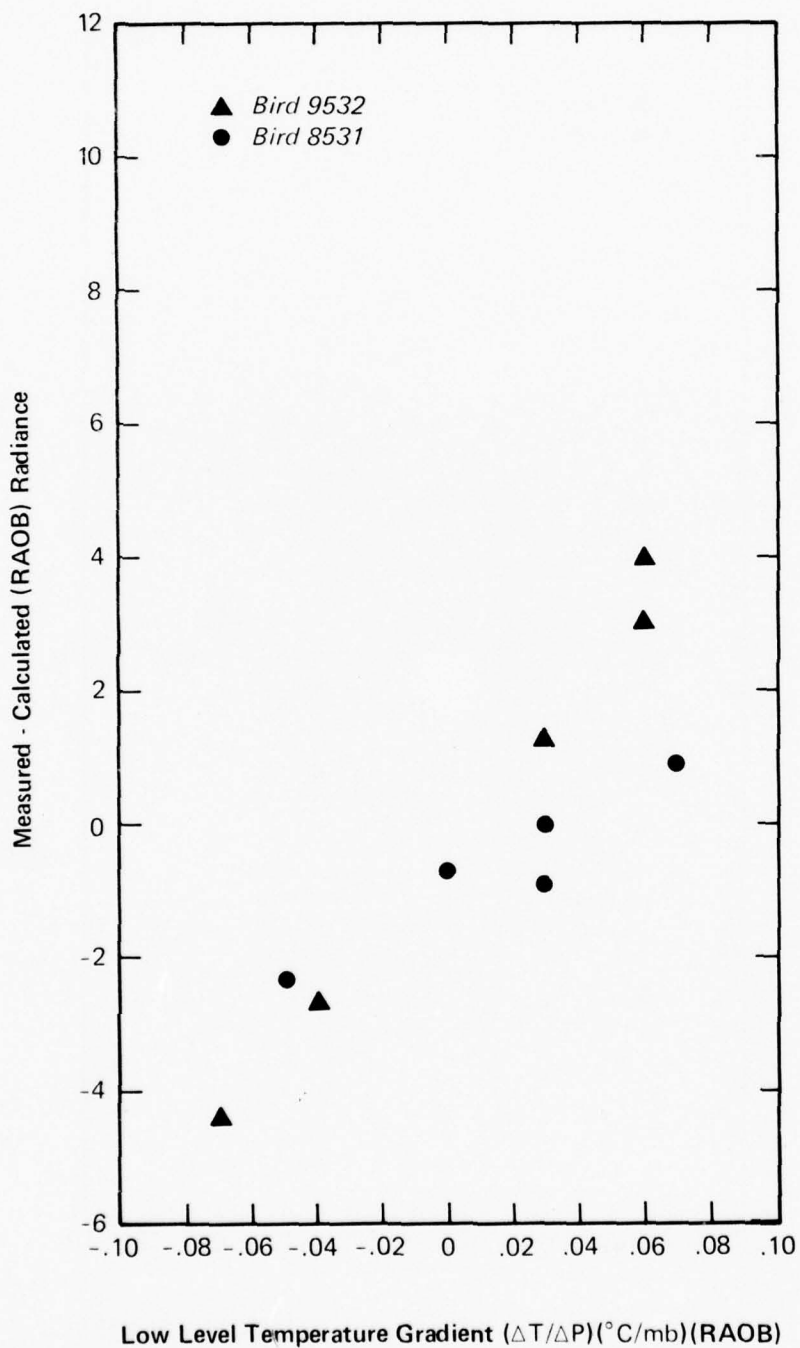
Figure 3.26 Radiance Differences as a
Function of Atmospheric
Stability - Channel Six

Channel 7
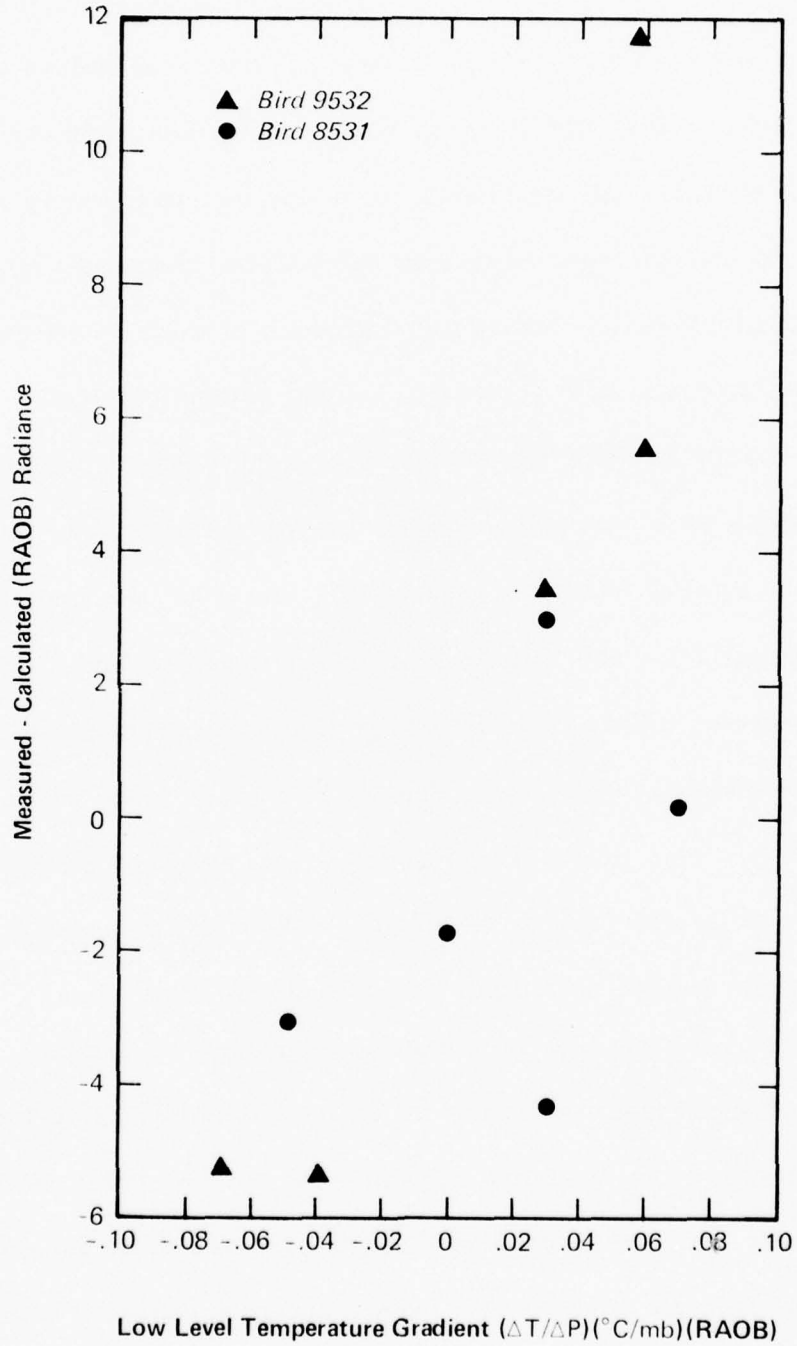
Figure 3.27 Radiance Differences as a
Function of Atmospheric
Stability - Channel Seven

Plots were made to show the relationship between measured minus calculated radiances to corresponding individual values of low level atmospheric stability for each of the seven sensor channels, see Figs. 3.21 to 3.27. All calculated radiances and temperature gradients from 1000 to 850 mb were made from RAOB data. Successively viewing the figures illustrates an increasing influence of surface effects on information contained with increasing sensor channel number. A relationship even exists for both Bird's channel 1 sensor whose weighting function peaks at 30 mb level. Beginning with channels 5, 6, and 7 where the weighting functions peak at 700 mb, 1000 mb, and surface levels, respectively, the difference between measured and calculated radiance becomes highly correlated with low level temperature gradients. The window channel 7 results in Fig. 3.27 show a range of more than 17 mW m^{-2} sr^{-1} cm in the difference between measured and calculated radiances. This error due to underlying surface effects greatly exceeds any other error source investigated for cloud free conditions.

Underlying surface temperatures contribute to outgoing radiation more strongly than accounted for in operational practice today. More importantly, the sign and magnitude of the low level temperature profile appear suitable as aids to correct for these deficiencies. This is shown graphically in Fig. 3.28 where satellite retrieved temperature

114
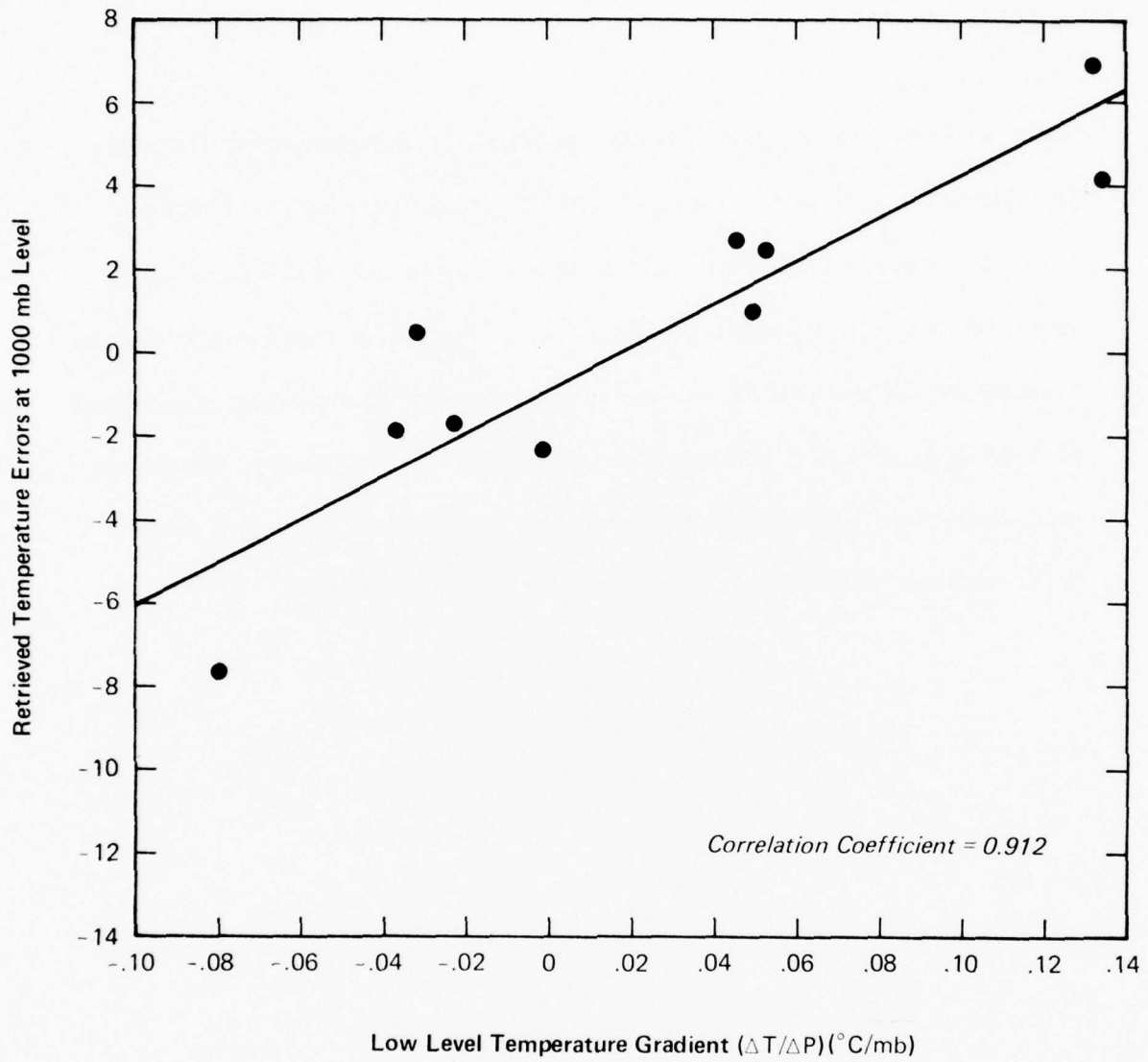
Figure 3.28 Retrieved Temperature Errors at 1000 mb
Level Related to Forecast Low Level Air
Temperature Gradients

errors at 1000 mb level are plotted relative to corresponding temperature gradients provided by the AFGWC 12-hour forecast for 850 and 1000 mb levels. Retrieved temperatures experienced a $15^{\circ}C$ range in errors for the ten research profile cases. It can be seen that retrieved temperature errors at 1000 mb are highly related (correlation coefficient of 0.912) to forecast temperature gradients. In conclusion, objective techniques can and should be developed to account for large underlying surface effects on an operational basis at AFGWC.

4 STATISTICAL ANALYSIS

4.1 INTRODUCTION

The stepwise regression or subset regression analysis was accomplished at Scientific Systems, Inc., under subcontract with the Geo-Atmospherics Corporation.

4.2 OBJECTIVES

The objectives of the project which relate to the statistical analysis problem were:

1. Compare operational soundings of vertical temperature profiles obtained from the infrared Special Sensor (SSE) package aboard the Defense Meteorological Satellite Program (DMSP) with coincident radiosonde observations and available forecast and analysis field data.

2. Investigate the cause and effect of errors in the operational soundings.

3. Develop techniques which minimize the vertical temperature profiling errors.

4. Perform similar analysis for computation of thickness between mandatory levels.

4.3 STATISTICAL DATA BASE

4.3.1 Data Base Structure

The data base selected for use in this statistical study was obtained from the data available at the Air Force Geophysics Laboratory (AFGL). The data covered the Northern Hemisphere during a two-week period

117

from February 14 to 28, 1975 and contained DMSP first guess profiles, DMSP final temperature estimates, Navy TTPACK data, and RAOB (radiosonde) data. All data had passed the tests used in the DMSP SOUNDER program and thus were judged as "clear column" radiances.

The data on tape represented only 4% of the measured data. This saved data is the data for which there is the greatest possibility of no-cloud conditions, so that the clear-column radiance assumption used in the minimum-information solution is made as valid as possible. Each measurement consists of 5 individual radiance measurements per scan line with 5 scans being made. One of these 25 measurements, which is made over the clearest field of view, according to the channel 4/channel 7 radiance ratio test, is kept for use in the temperature or height retrievals.

Statistical data compiled at AFGL on this data base has been analyzed to determine the characteristics of the observed errors. In comparing TTPACK vs. SSE inversions, the following points should be made. Large errors occur predominantly at three pressure levels: (1) surface, (2) tropopause, (3) upper stratosphere. The errors within the stratosphere (primarily at and below 30 mb) are primarily negative and appear to be correlated with an isothermal first guess profile at these levels. Errors at the tropopause do not appear to be related to those in the upper atmosphere. Tropopause errors appear to be most frequent at mid-latitude soundings. The mean error at all levels tracks the inversion coefficient for the $667/cm^{-1}$ channel.

In order to generate a data base, several different selection criteria were used. In order to minimize the effect of spatial horizontal and temporal inhomogeneities, it is desirable that the DMSP soundings correspond closely in space and time with the TTPACK data. Using a threshold of 60 nautical miles and 3 hours, a total of 1067 matches were found (563 for the first week and 504 for the second week). A subsequent set of matches were generated with tighter thresholds but the number of matches was significantly reduced. It was decided that the 1067 matches were large enough in number to make a statistically significant test. At the same time, the thresholds were felt to be sufficiently tight to minimize the effects of spatial and temporal inhomogeneities. Therefore, this basic data base was adopted for use in the study.

118

One objective of this study was to assess the effect of latitude and zenith angle on the regression models. Variations in latitude strongly affect the temperature profile, while variations in zenith angle produce changes in the observed spectral radiances, even for invariant temperature profiles.

The latitudes were partitioned into two sets, one from 0 to 45°N and one from 45°N to 90°N, and the zenith angles (θ) were also partitioned into two sets, one for $0 < \theta \leq 0.7$ radian and one for $\theta > 0.7$ radian. Only two latitude regions were chosen to maintain as much statistical significance as possible. The zenith angle partition was selected to give sets of approximately equal size. It is curious that the data accepted in SOUNDER had a relatively large number of high zenith angles. This is suggestive of an unwanted bias in the computations involved in making the cloud/no cloud decision.

The number of matches for the various partitions are given in Table 4.1.

TABLE 4.1

Number of Matches between DMSP and TTPACK
for Latitude and Zenith Angle Partitions

Description	Week 1 14-21 Feb. 1975	Week 2 22-28 Feb. 1975
all data	563	504
$0 < \lambda < 45°N$	164	332
$45°N < \lambda < 90°N$	399	172
$0 < \theta < 0.7$ rad.	303	275
$\theta > 0.7$ rad.	260	229

4.3.2 Validation of Data Base

In order to perform a meaningful statistical analysis of the vertical temperature sounding problem, it is necessary to acquire a valid "truth" model or data set with which to perform comparison studies. The most common approach is to use radiosonde data, which provides relatively accurate simultaneous measurements of pressure, humidity and temperature and, from ground tracking, altitude. Unfortunately, there were only about

119

50 radiosonde-DMSP final matches using the 3 hr., 60 nm criterion. This number is much too small for performing detailed statistical analysis. However, these data can be used to infer the validity of the TTPACK data for use as "truth".

The TTPACK data are based on an analysis field and include numerical interpolations between radiosondes, including the latest available measurements, using Cressman weighting. In contrast, the DMSP first guess profiles are based on forecast fields and do not include the latest available data. Another advantage of using TTPACK data is that it uses a model which partitions the ground into regions (about 20×20 nm) whereas the radiosonde data are point measurements. Since the DMSP measurements are over regions due to the finite resolving power of the sensors, it is more appropriate to use TTPACK data, if it assumed that the TTPACK errors relative to the radiosonde measurements are small.

This hypothesis was tested using the data supplied by AFGL. The results are summarized in Table 4.2. Inspection of the data reveals that the TTPACK profiles match the radiosonde profiles more accurately than they match the DMSP final profiles and are more accurate than the match between DMSP final and radiosonde profiles. On the basis of statistics for Feb. 14 to Feb. 28, latitude $45°N \rightarrow 15°N$, TTPACK is an unbiased estimator at most levels (perhaps excluding 1000 mb, 30 mb and 50 mb). The rms performance is $\sim 1°K$ at levels below 50 mb with the exception of 300 mb. This is consistent with the fact that a RAOB is a point measurement while TTPACK is an area average. In addition, RAOBs are generally expected to have a .5 to 1°K rms noise. Exact error assignment is impossible due to the small number of samples. This should be contrasted with the 1st guess - RAOB errors. Large mean errors exist between 100 and 500 mb and 1000 mb (magnitude $\sim 1°$, often 2 or 3°K). This trend is also seen in the DMSP-TTPACK errors. The sizes of these samples are more substantial. These means should be regarded as real. The same general trends may be seen in the data for February 14 to 21, latitude 62°N to 90°N.

A similar trend has been found in the height data in TTPACK-RAOB. The mean error is 50 feet below 150 mb. Again the sample is small (10). For levels below 250 mb the mean error is less than 10 feet. Due to the fact that both DMSP and TTPACK represent a spatial average, TTPACK is thus considered to be a representative ground truth.

120

ε_1 = DMSP-TTPACK
ε_2 = DMSP-Radio
ε_3 = TTPACK-Radio

Weeks 1 and 2
λ: 15 N → 45 N
Ω: 115 E → 150 E
273 soundings

Week 1
λ: 62 N → 90 N
Ω: 0 → 180 W
368 soundings

Data matched to within 4 hr, 90 nm.
8531 and 9532 satellites
00 and 12Z
all values in °C.

| | Weeks 1 and 2 | | | | | | Week 1 | | | | | |
| | Mean | | | rms | | | Mean | | | rms | | |
P(mb)	ε_1	ε_2	ε_3	ε_1	ε_2	ε_3	ε_1	ε_2	ε_3	ε_1	ε_2	ε_3
30	-0.1	-2.9	-1.2	2.3	1.6	2.2	-5.3	-1.8	0.5	3.0	2.7	0
50	-1.0	-0.2	-1.4	2.2	3.2	3.5	-0.9	1.3	1.3	3.3	2.6	1.9
100	0.2	-1.3	-0.6	2.6	2.2	1.2	2.8	2.1	-0.5	2.5	2.2	0.3
150	-1.4	-1.2	-0.4	2.0	1.8	0.5	-1.7	-0.3	-0.6	3.7	2.5	0.3
200	-1.8	-2.3	-0.5	2.1	2.6	0.6	-2.6	-1.7	-017	2.7	1.7	0.2
250	-1.8	-1.1	0.2	2.8	3.3	0.8	-1.8	-2.4	-0.8	2.3	1.7	0.5
300	-2.2	-2.4	-0.9	4.3	4.4	2.8	-2.8	-3.5	-0.8	3.2	3.1	0.8
400	-1.8	-3.6	-0.9	2.6	2.4	1.7	0.3	-0.6	-0.7	2.8	2.2	0.6
500	-2.3	-3.5	-0.3	2.8	2.9	1.5	0.9	0.2	-0.5	2.9	3.4	0.1
700	-0.7	-0.4	-0.2	2.5	2.2	1.1	-0.5	-1.2	-0.5	3.2	4.3	0.5
850	0.1	0.7	-0.4	3.1	2.6	0.9	-0.4	-2.0	-0.8	3.9	5.1	0.7
1000	6.1	8.6	1.3	6.1	5.7	1.4	-2.3	-2.0	4.5	7.1	3.7	0
matches	132	25	14	132	25	14	113	25	8	113	25	8

TABLE 4.2

VALIDATION OF TTPACK AS "TRUTH" DATA

4.4 EXPERIMENTAL RESULTS

4.4.1 <u>Statistical Analysis of First Guess Temperatures and Radiances</u>

The rms values and correlations between the 13 first guess temperature levels and the 8 IR channels are given in Table 4.3 and the associated means and the TTPACK means are shown in Table 4.4. Note that channels 5 and 6 have almost identical correlations, implying that they are almost colinear in predictor space. This suggests that either of the channels, but not both, should be used in the retrievals. This is in fact presently done in SOUNDER by using only channel 5.

The rms first guess temperatures vary from 4.1 to 20.4°C and the rms radiances vary from 3.1 to 24.9 ergs. The number of high correlations between the temperatures and between the radiances is significant and suggests that there is a great deal of redundancy in each type of predictor data. This conclusion is verified in the results presented in the sequel. The large number of cross-correlations between temperature and radiances implies that there is a great deal of redundancy between the two types of predictor data as well.

As discussed earlier, the data to be used as the dependent or "truth" set is the TTPACK data. Thus, our objective is to reduce the discrepancies between the first guess and TTPACK profiles. The means and covariances for the first guess errors (first guess - TTPACK) are given in Tables 4.5 and 4.6 for the 13 TTPACK levels. It can be seen that the assumptions used in the minimum information solution of equal diagonal elements and zero off-diagonal elements is subject to some question. Fleming and Smith[4.8] have compared the performance of the "full statistical" and the minimum-information methods and found that the "full statistical" method was superior. They attributed its superiority to the fact that it carries more information about expected statistical variations and correlations in the predictor data. It was also found that the minimum-information accuracy was highly sensitive to the accuracy of the first guess profile. This is not surprising since the minimum-information solution will generally be (uniformly) close to the first guess profile.

122

- values below diagonal are correlations x10
- negative values are indicated with overbar
- values along diagonal are rms values

Temperature

level													
1	8.3												
3	8	5.3											
4	0	4	4.8										
6	6̄	3̄	7	10.8									
7	4̄	1̄	7	9	6.6								
8	6	5	2	2	1	4.1							
9	8	5	3̄	8	5̄	7	8.5						
10	8	5	4	8̄	6̄	5	9	12.4					
11	8	5	4̄	9̄	7̄	5	9	9	13.4				
12	7	4	5̄	9	7	4	9	9	9	13.8			
13	7	5	4̄	9̄	7	4	9	9	9	9	15.5		
14	8	4	4̄	8̄	7	4	9	9	9	9	9	16.7	
15	8	5	3̄	7̄	5̄	6	9	9	9	9	9	9	20.4

σ(°C)

Radiance

1	9	7	1	5	3	5	7	6	6	6	6	6	7			5.5				
2	6	7	6	1	2	5	3	2	1	1	1	2	3		8		4.1			
3	4	7	8	3	5	6	2	1	0	1̄	1	0	2		6	9		3.1		
4	8	6	1	6	4̄	6	8	8	8	8	8	8	9		7	3	3		5.5	
5	3	5	3	8	5	6	9	9	9	9	9	9	9		7	2	2	9		10.8
6	8	5	3	8	5	5	9	9	9	9	9	9	9		7	2	1	9	9	14.9
7	8	5	3	8	5	6	9	9	9	9	9	9	9		7	3	1	9	9	9	24.9
8	8	5	3	7	5	5	9	9	9	9	9	9	9		7	2	1	9	9	9	9	16.6

σ N(ergs)

| channel → | mb: 10 | 30 | 50 | 100 | 150 | 200 | 250 | 300 | 400 | 500 | 700 | 850 | 1000 | | channel #: 1 | 2 | 3 | 4 | 5 | 6 | 7 | 8 |

Temperature Level   Radiance

TABLE 4.3

PREDICTOR CORRELATION MATRIX—WEEK #1

123

TABLE 4.4

PREDICTOR AND TTPACK MEANS-WEEK #1

Temperatures				Radiances	
Level	mb	Mean First Guess	TTPACK	Channel	Mean
1	10	-50.3	-48.0	1	53.861
3	30	-57.1	-57.7	2	43.885
4	50	-63.2	-62.3	3	40.895
6	100	-70.3	-71.9	4	51.601
7	150	-63.4	-62.5	5	68.514
8	200	-55.5	-55.1	6	81.787
9	250	-48.8	-48.8	7	99.341
10	300	-42.4	-42.4	8	112.239
11	400	-29.2	-29.0		
12	500	-19.0	-17.9		
13	700	-2.9	-2.2		
14	850	4.3	5.0		
15	1000	10.9	11.8		

Temperatures in ^{O}C

Radiances in ergs.

Mean First Guess Errors

Level #:	1	3	4	6	7	8	9	10	11	12	13	14	15
	-2.30	.58	-5.46	1.59	-.90	-.48	.03	-.02	-.20	-1.05	-.72	-.75	-.84

Error Covariance Matrix:

	mb	1	3	4	6	7	8	9	10	11	12	13	14	15
1	10	16.30												
3	30	11.30	17.17											
4	50	-4.72	-5.13	16.45										
6	100	2.57	7.17	-3.20	13.90									
7	150	-.60	2.65	-.16	2.97	8.04								
8	200	.70	.36	-3.44	-.19	2.20	8.51							
9	250	1.77	-.23	-4.41	-1.06	-.90	7.43	11.78						
10	300	2.42	2.12	-5.51	.01	-.05	4.35	9.10	14.55					
11	400	1.26	1.19	-1.85	.66	-.34	.65	1.60	3.98	4.54				
12	500	.81	.94	-.94	-.46	-.40	-.55	-.74	-.23	2.57	5.28			
13	700	1.09	2.85	-2.57	2.64	.21	-.62	-1.59	-.35	.86	2.58	6.50		
14	850	.12	-.62	-1.59	-.02	-1.40	-.29	-.56	-.54	.36	.95	4.30	8.29	
15	1000	.11	-.90	1.83	-3.70	1.04	1.10	-.81	-2.85	-1.46	-1.03	-1.92	2.09	4.22

Error = first guess - TTPACK ($^{\circ}$C)

TABLE 4.5

MEANS AND COVARIANCES OF FIRST GUESS TEMPERATURE ERRORS - WEEK #1

Mean First Guess Errors:

Level #:	1	3	4	6	7	8	9	10	11	12	13	14	15
	-1.75	-.06	-5.24	1.52	-1.28	-.38	-.25	-.81	-.51	-.85	-.37	-.29	-.57

Error Covariance Matrix:

Level #:	mb	1	3	4	6	7	8	9	10	11	12	13	14	15
1	10	10.22												
3	30	3.53	11.71											
4	50	-.38	-3.84	15.23										
6	100	.83	6.11	-1.78	11.98									
7	150	-.61	1.85	-1.04	.67	6.45								
8	200	.43	1.66	-1.66	.67	3.37	9.42							
9	250	.68	1.33	-1.80	.52	.95	7.57	11.02						
10	300	-.30	3.38	-5.44	1.40	1.69	3.99	8.11	14.35					
11	400	.56	.71	-.61	.12	-.56	-.36	.49	2.32	3.38				
12	500	2.35	-.44	1.37	-.50	-1.29	-1.52	-1.87	-2.18	2.22	6.34			
13	700	.94	1.86	-.94	1.89	-.63	-1.27	-1.33	-.90	.70	2.17	5.44		
14	850	.16	.15	-.68	.60	-.43	-.01	.26	.01	.29	.85	3.53	6.58	
15	1000	-1.81	-2.61	.05	-3.62	-.46	-.69	-1.96	-3.28	-1.19	-.88	-.07	2.63	4.95

Error = First Guess - TTPACK ($^{\circ}$C)

TABLE 4.6

MEANS AND COVARIANCES OF FIRST GUESS TEMPERATURE ERRORS - WEEK #2

4.4.2 Discussion of Inversion Methods

A series of experiments were carried out to evaluate the minimum-information solution, using the statistical data base described in detail in Section 4.3. The statistical analysis consisted of the following three essential steps:

(i) Develop linear regression models for predicting the temperature profiles from the first guess profiles and the measured spectral radiances. This provides a performance baseline for linear models. This includes important trade-offs involving the number and type of predictor (independent) variables and sensitivity to parameters, such as latitude and zenith angle.

(ii) Develop a hybrid inversion technique in which the minimum-information program is cascaded with a linear regression model. The regression model uses the minimum-information solution as part of the predictor set.

(iii) Analysis and comparison of techniques to determine information handling capabilities of the minimum-information method and to determine possible sources of modeling error.

The basic structure and information flow, in simplified form, of the retrieval methods studied is given in Figures 4.2 and 4.3. Figure 4.2 shows the information flow for either the minimum-information or regression method. The basic inputs required are the initial forecast field $T_0(p)$ and the spectral radiances $\tilde{r}(\nu)$. The output $\hat{T}(p)$ is the estimated temperature profile. The performance of the methods is evaluated by a statistical analysis of the retrieval error. In Figure 4.3 the information flow for the hybrid method employing both minimum information and regression methods is shown. The inputs to the regression model are the spectral radiances $\tilde{r}(\nu)$ and the differences between the initial forecast field $T_0(p)$ and the minimum-information retrievals $\hat{T}_{mi}(p)$. As with the other methods, the performance is analyzed by statistical analysis of the retrieval errors.

The structure and information flow for height retrievals is similar to that for temperature retrievals.

127
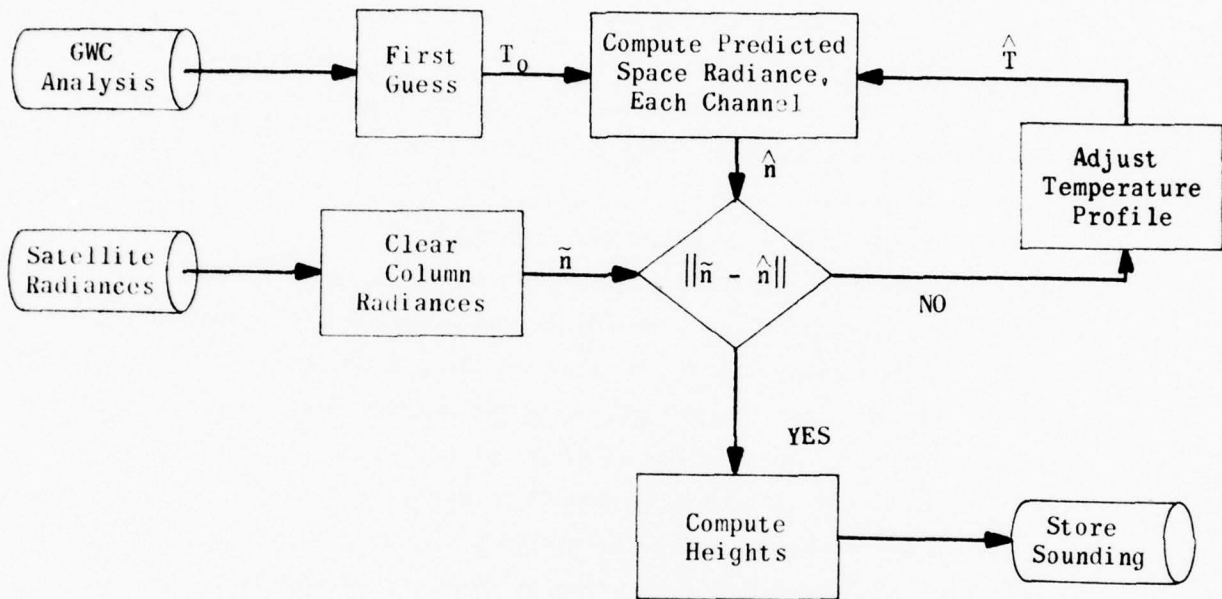
Figure 4.1 Information Flow For Minimum-Information Technique
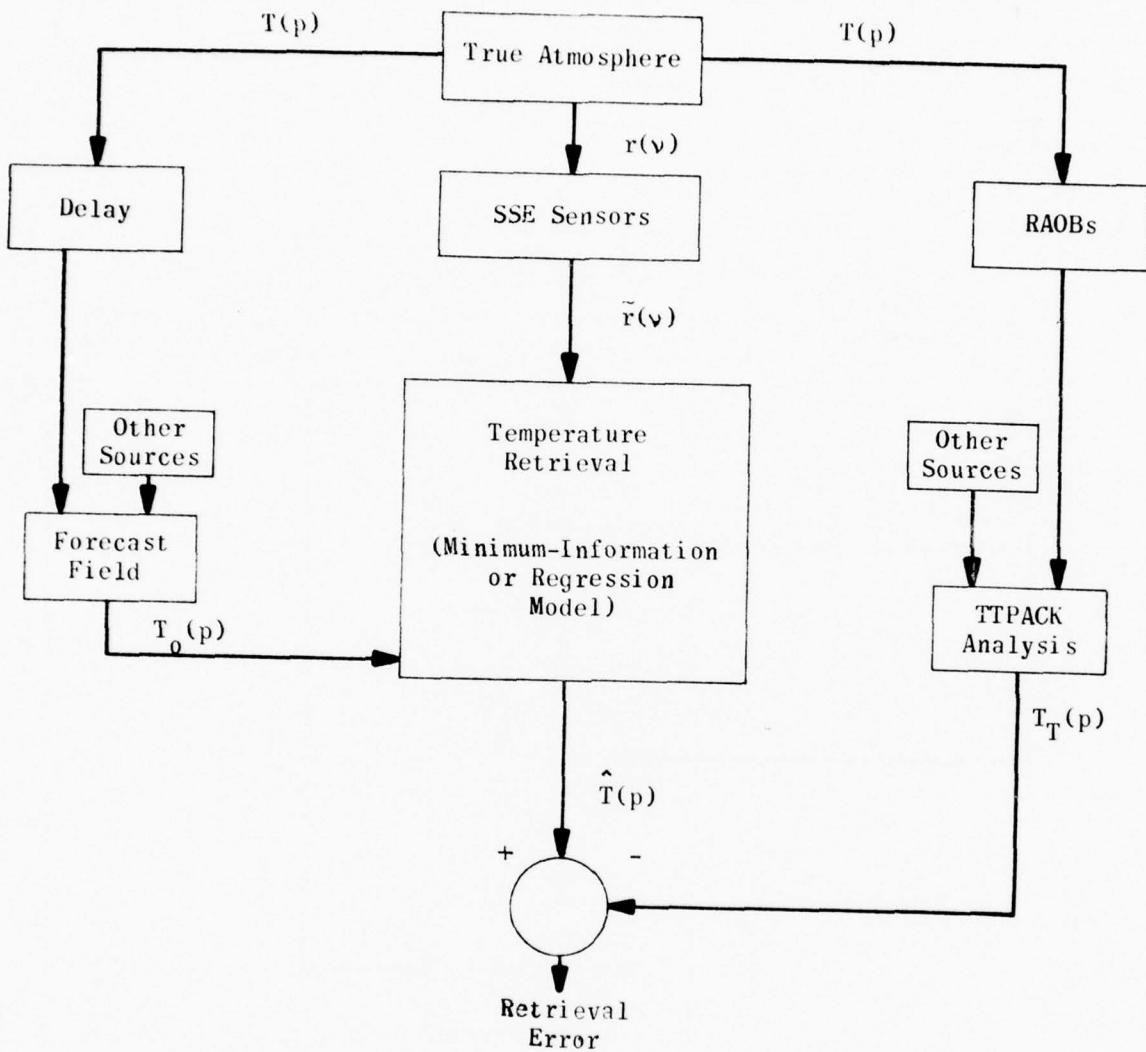
Figure 4.2 Information Flow For Analysis of Minimum-Information and Regression Methods
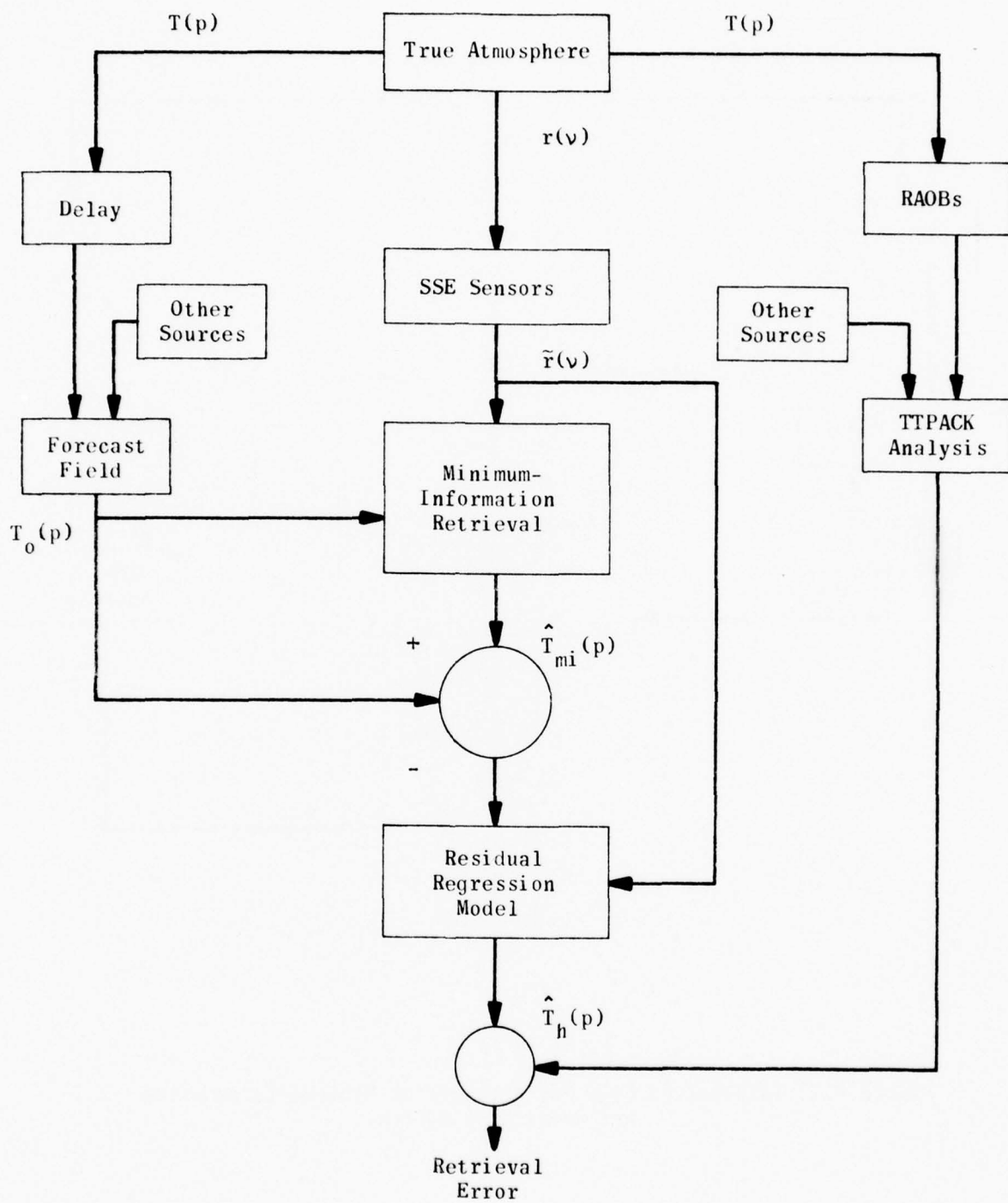
Figure 4.3 Information Flow for Analysis of Hybrid Method

130

The hybrid method was used in order to better analyze the minimum-information method. If the minimum-information method was a linear processor, then the performance of the hybrid and regression methods would be identical. Since the minimum information method is, in fact, a nonlinear processor, performance comparison of the hybrid and regression methods allows the efficiency of the nonlinear processing to be measured, at least in a qualitative way.

The coefficients for the regression and hybrid models were found using the stepwise regression method outlined in Section 4.2.3, using the TTPACK data as truth.

If the set of predictor (independent) variables is denoted by the vector x and the regression coefficients by the vector a, then the temperature estimate T for the $i\frac{th}{}$ level is

$$\hat{T}_i = a_i^T x + b_i$$

with b_i a constant. Denoting the TTPACK temperature by T_{Ti}, the regression error is

$$e_i = \hat{T}_i - T_{Ti}$$
$$= a_i^T x + b_i - T_{Ti}$$

The coefficients a_i, b_i are found to minimize the squared errors over the data base selected for study.

The temperature levels and spectral channels used in the DMSP analysis are given in Table 4.7. Only 13 of the 15 standard pressure levels were used in the analysis since TTPACK for 20 mb and 70 mb were not available. The window channel (835 cm^{-1}) is used in the SOUNDER program to provide an estimate of surface temperature and to aid in the cloud/no cloud decision process. The ratio of spectral radiance in channel 4 to channel 7 is used in determining whether clouds are present or not. Both channel 7 and channel 8 radiances were used in the regression models.

4.4.3 Statistical Analysis of Inversion Methods

The errors in the first guess temperature profiles are compared statistically with the errors in the minimum information retrievals in Table 4.8. The mean and standard deviations of errors are shown for both week #1 and week #2 data. The data show that the first guess is biased negatively

131

TABLE 4.7

TEMPERATURE LEVELS AND SPECTRAL
CHANNELS USED IN DMSP ANALYSIS

Temperature Level	p (mb)	CO_2 Channel	$\nu(cm^{-1})$	Approximate peak of Transmission Function (mb)
1	10	1	668	40
2	20[1]	2	677	60
3	30	3	695	150
4	50	4	708[2]	350
5	70[1]	5	725	700
6	100	6	747	1000
7	150	7	835[3]	
8	200	8	535[4]	
9	250			
10	300			
11	400			
12	500			
13	700			
14	850			
15	1000			

Notes: (1) not used in analysis (TTPACK data not available).

(2) reference frequency used in minimum-information solution.

(3) window channel

(4) water vapor channel

132

Level		Week 1				Week 2			
		First Guess		Final		First Guess		Final	
Number	mb	Mean	rms	Mean	rms	Mean	rms	Mean	rms
1	10	-2.31	16.30	2.92	5.75	-1.75	10.22	2.66	4.12
3	30	0.58	17.17	-2.34	5.43	-0.07	11.71	-1.51	4.34
4	50	-5.47	16.45	-2.54	3.91	-5.25	15.23	-1.86	3.39
6	100	1.60	13.90	-3.89	3.60	1.52	11.98	-3.28	3.39
7	150	-0.91	8.04	3.33	3.77	-1.29	6.45	3.92	3.91
8	200	-0.48	8.51	3.95	3.17	-0.38	9.42	3.61	3.69
9	250	0.04	11.78	3.02	3.42	-0.25	11.02	2.52	3.58
10	300	-0.03	14.55	2.27	3.61	-0.82	14.35	1.93	3.79
11	400	-0.21	4.54	0.99	2.96	-0.52	3.38	0.26	3.00
12	500	-1.05	5.28	0.61	2.67	-0.85	6.34	-0.12	2.97
13	700	-0.73	6.50	-1.04	2.94	-0.38	5.44	-1.11	2.99
14	850	-0.76	8.29	-1.41	2.94	-0.30	6.58	-1.45	3.12
15	1000	-0.85	4.22	0.68	4.12	-0.58	4.95	0.60	4.76

TABLE 4.8

COMPARISON OF DMSP FIRST GUESS AND FINAL ERRORS

at nearly all levels for both week one and two. The DMSP final errors at the same levels are significantly different: the bias at 10 mb stays at about the same magnitude but reverses sign, while the biases at 30, 50 and 100 mb are all negative (between -1.5 and -4°C) for both weeks. Since the minimum information iterations terminate on the basis of radiance matching criteria, this implies that colder than actual temperatures are required to match the measured and predicted spectral radiances. This problem could be caused by errors in the computed transmittance functions or propagation of tropopause errors. Between 150 and 300 mb, the performance is somewhat different. The mean first guess errors are generally less than one degree; however, the final errors are between plus 2 and 4 degrees. These errors could be due to compensation of the colder than actual estimates at higher altitudes in order to satisfy the radiance matching threshold. The data show that the rms error in the first guess, which generally varied between 7 and 16°C, was significantly reduced by the minimum information method above 300 mb. The rms DMSP final errors varied bewteen 3 and 6°C. Thus, use of the spectral radiances significantly reduced the variation from TTPACK for pressure levels less than 300 mb.

For pressure levels greater than 300 mb, the situation changes dramatically. The mean first guess errors are relatively small, although they appear negatively biased, and are generally less than 1°C. The mean DMSP final errors are essentially the same. The rms errors are reduced generally from a range of 3 to 8°C to a range of 3 to 4°C.

In order to test the statistical significance of the linear regression models, the data was partitioned into two sets. Set #1 includes all soundings from February 14 to February 21, 1975. Set #2 includes all soundings from February 22 to February 28, 1975. These two data sets were then used interchangeably as either training (dependent) or test (independent) sets. In the numerical results to be presented, the notation $a \rightarrow b$ is used to indicate that the regression model is derived from set #a, while the regression model is tested on set #b. All four possible combinations $(1 \rightarrow 1, 1 \rightarrow 2, 2 \rightarrow 1, 2 \rightarrow 2)$ are utilized.

The RMS regression errors obtained by using all 13 first guess levels and all eight spectral radiances are shown in Figs. 4.4 and 4.7 for the four different partitions of the data time set $(1 \rightarrow 1, 1 \rightarrow 2, 2 \rightarrow 1, 2 \rightarrow 2)$. Shown in each plot is the effect of the latitude and zenith angle partitions. The "all data" curves were used to determine a reasonable and useful bound on accuracy of temperature retrievals. That is, it should be possible in practice to realize this performance, since the temperature retrievals are made over smoothed data. The addition of structure which may be added via partitioning of the original data set (into, e.g., latitude and zenith angle bands) and efficient nonlinear processing would be expected to yield better performance since the variability of each of the subsets is less than the variability of the original data set. It is interesting, as will be subsequently shown, that this effect, though present, is not great enough to invalidate the "all data" model as a possible temperature inversion method. Several conclusions can be made from this data.

(1) performance is almost independent of which training and test sets were used. This implies that both weeks have essentially the same statistical variability and that regression models from either week can be used for accurate temperature inversions for the other week.

(2) RMS errors for all cases tended to be higher at 100 mb, 250 mb (near tropopause) and at 1000 mb. The increase at 100 mb could be explained by the lack of a weighting function which peaks nearby. 100 mb is approximately midway between the peaks at 60 mb (for the 695 cm^{-1} channel) and 150 mb (for the 708 cm^{-1} channel). The higher errors at tropopause are not
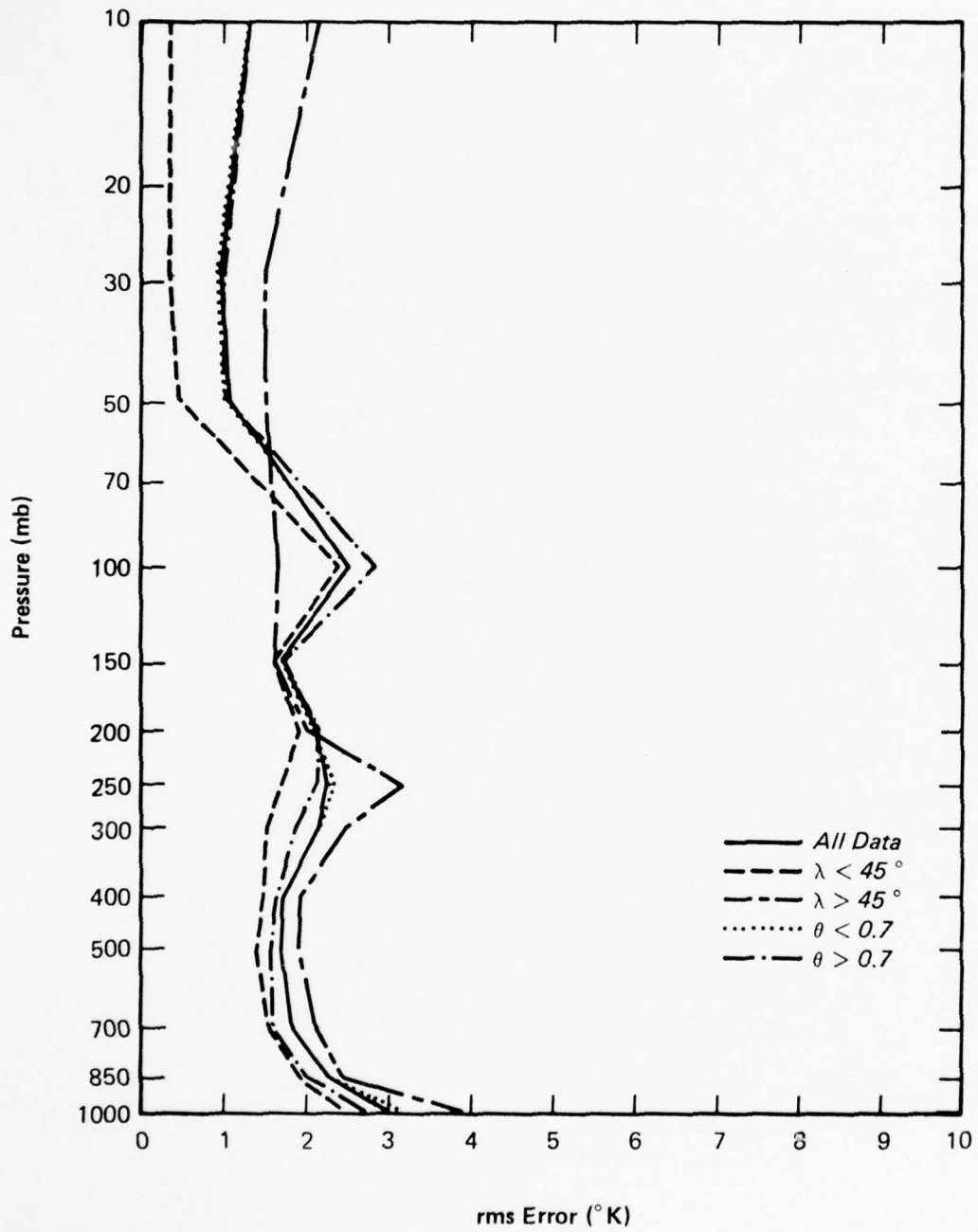
Figure 4.4   RMS Regression Errors (1→1)
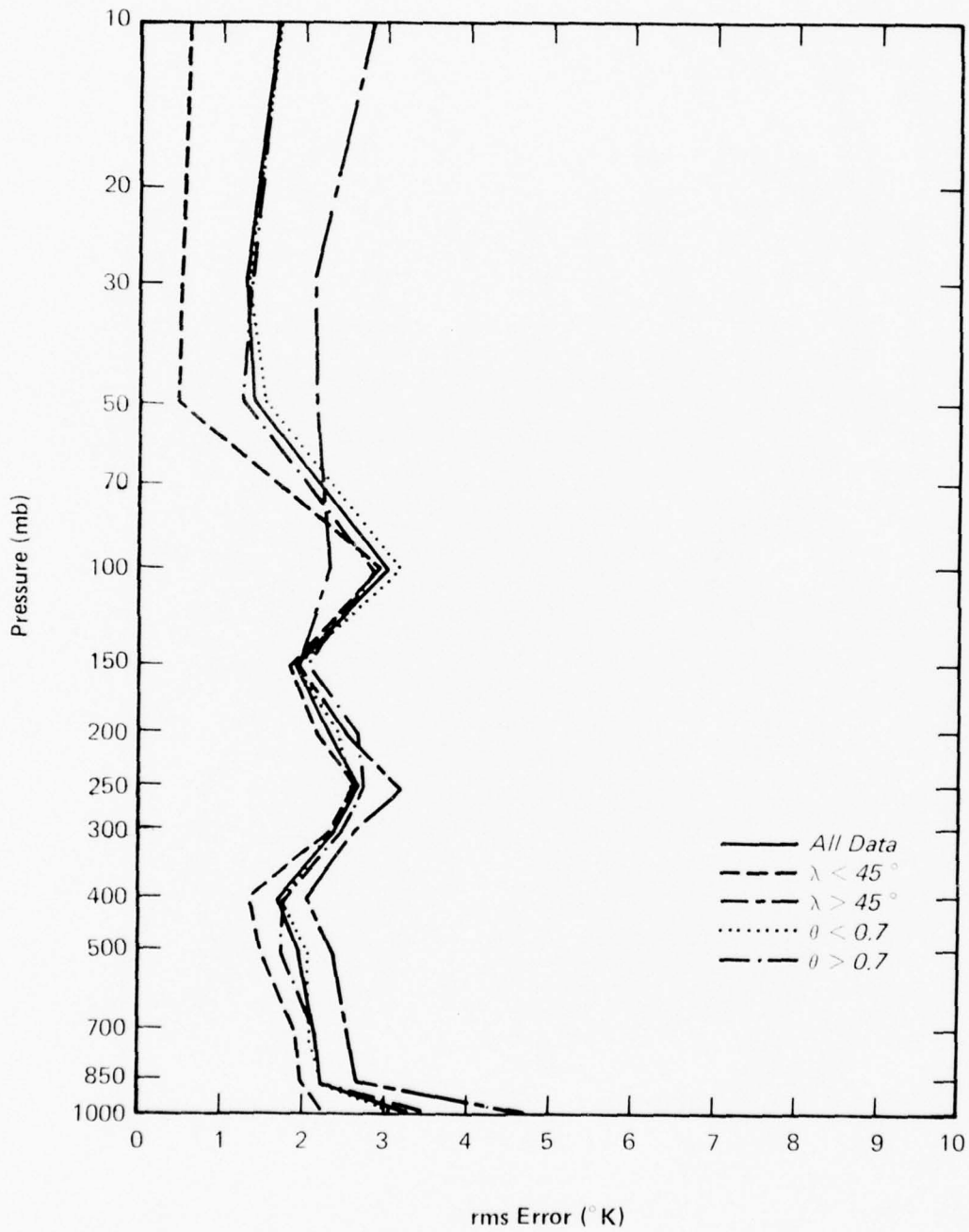
Figure 4.5 RMS Regression Errors (1→2)

137
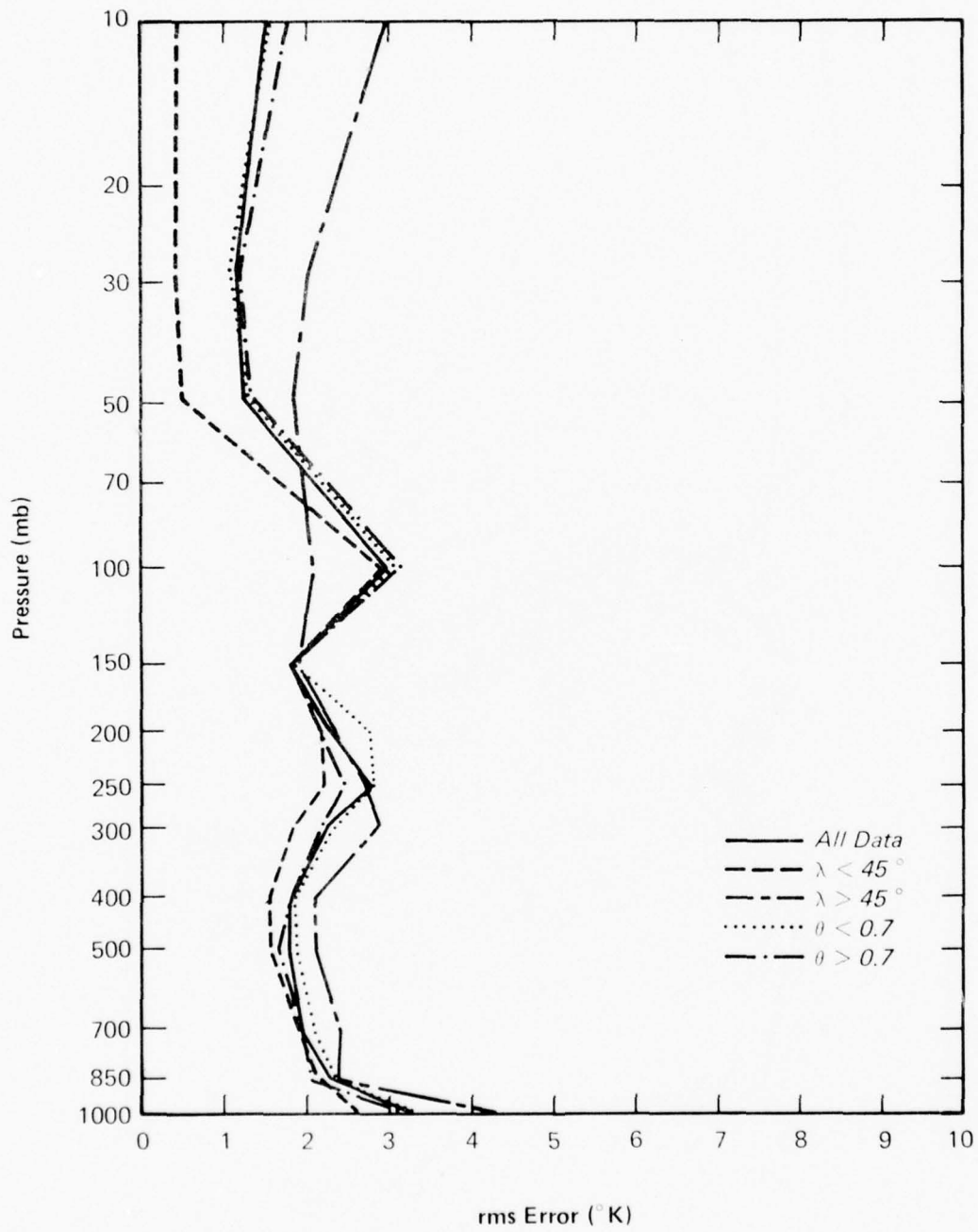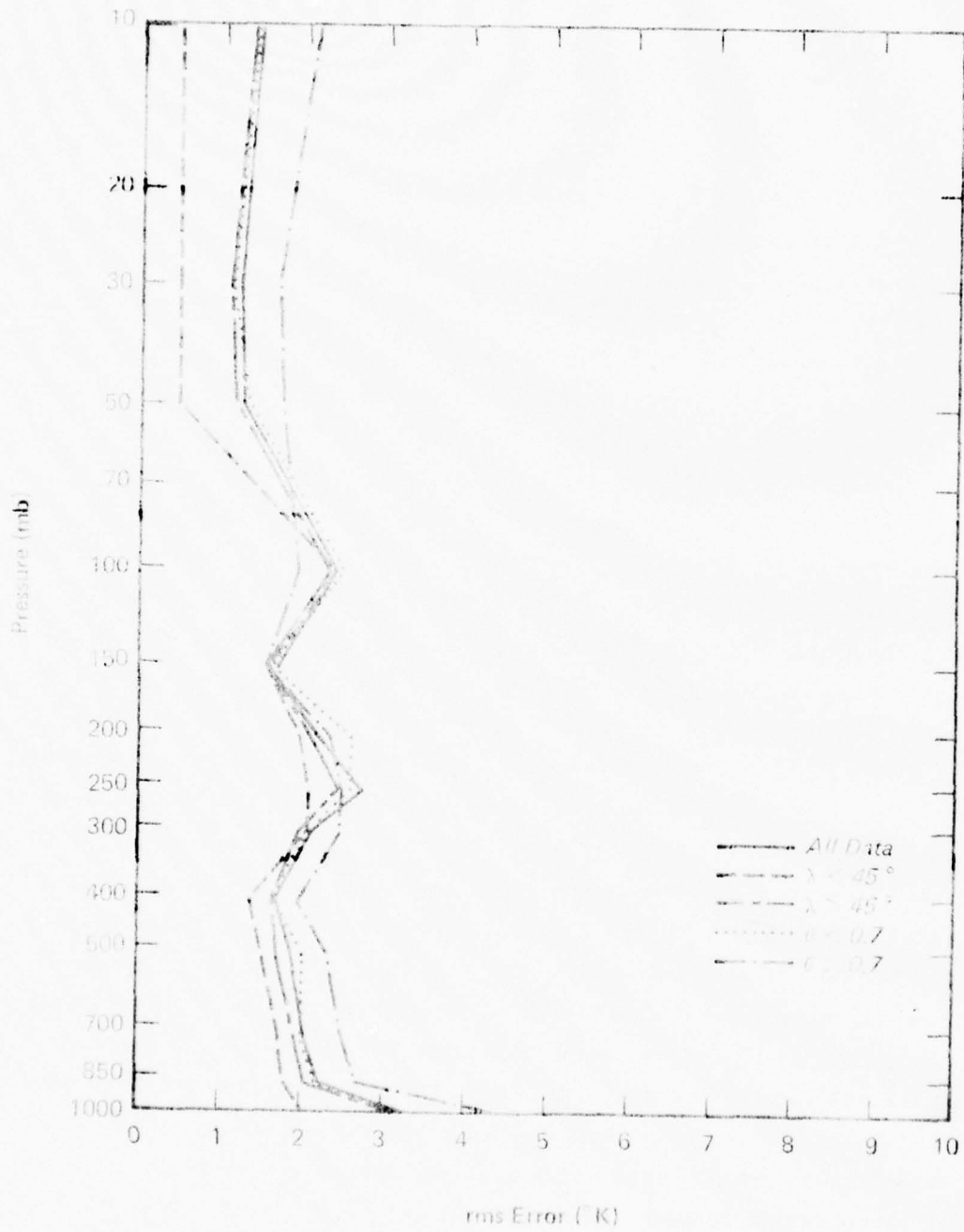
Figure 4.6   RMS Regression Errors (2→1)

138

Figure 4.7   RMS Regression Errors (2-2)

unexpected. The relatively high errors at 1000 mb
are probably related to the errors in estimating the
surface temperature.

(3) The sensitivity to latitude variations is much greater
than the sensitivity to zenith angle variations, especi-
ally at high altitudes. Regression errors are about 0.5°C
below 50 mb at low latitudes and rise to between 2.2°C and
3.2°C at the higher latitudes.

The regression coefficients for all week #1 data and all week
#2 data are plotted in Figs. 4.8 and 4.9. Continuous plots are shown rather
than just the points in order to better display the trends. The coeffi-
cients used correspond to the case where one first guess temperature, at the
same level, and all 8 spectral radiances were used in the independent data
set for estimating each level.

Examination of Figs. 4.8 and 4.9 reveals several things.
Channels 2,3 and 7 contribute most to the temperature below 30 mb. Note
that the channel 1 coefficient at these levels is negative, indicating a
compensation for the skirts of the transmission functions for channels 2
and 3. The first guesses, indicated by T_0, do not contribute significantly
to these estimates. Channel 4 contributes mostly to the temperature
estimates between 200 and 300 mb. Note that the channel 4 coefficient
between 50 and 150 mb is negative, indicating compensation for the skirts
of the transmission functions for channel 3. Note that the initial temperature
is significant in computing the 100 mb estimate. This may be obtained by the
fact that none of the transmission functions has a peak in this area, as
mentioned previously. Channel 5 contributes mostly to the region between
200 and 300 mb and also compensates for the channel 6 skirts. Channel 6
contributes to temperature estimates between 50 and 150 mb and compensates
for the skirts of the transmission functions for channels 4, 5 and 7.
Channel 7 contributes mostly in the region from 200 to 400 mb and at 1000 mb,
reflecting its usefulness at sensing the surface temperature. Channel 8,
the water vapor channel, does not strongly contribute to any level but has
a weak contribution between 200 and 400 mb.
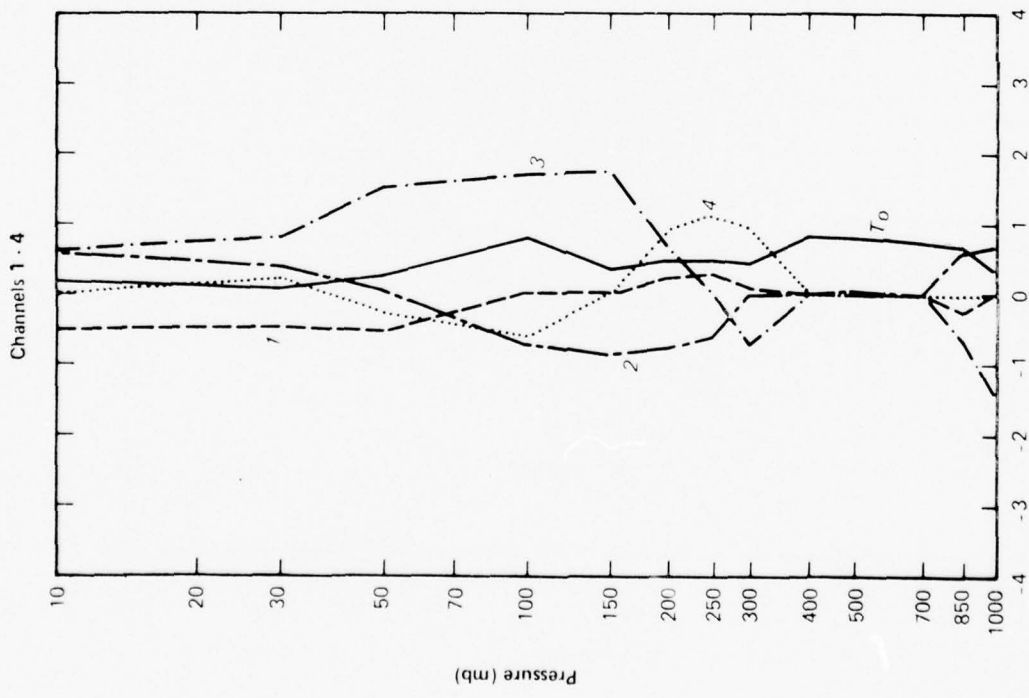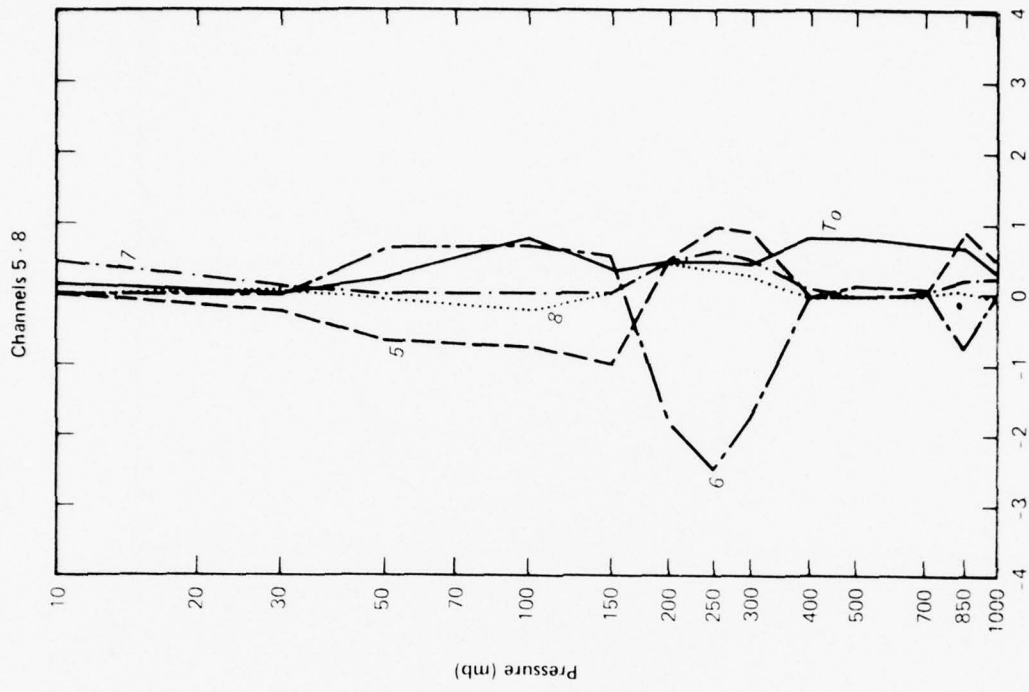
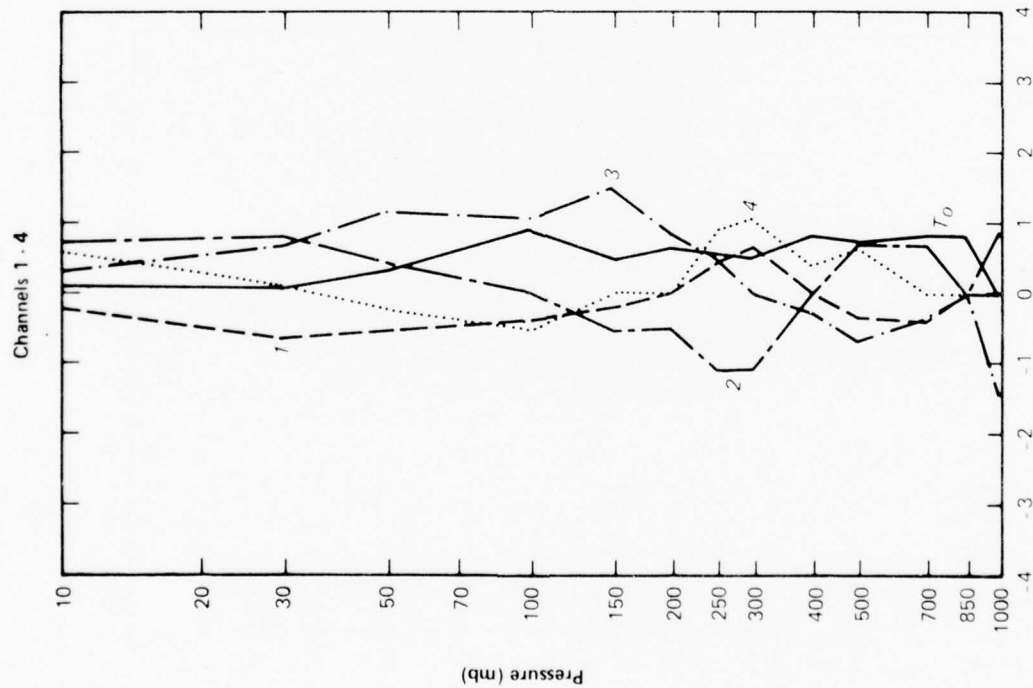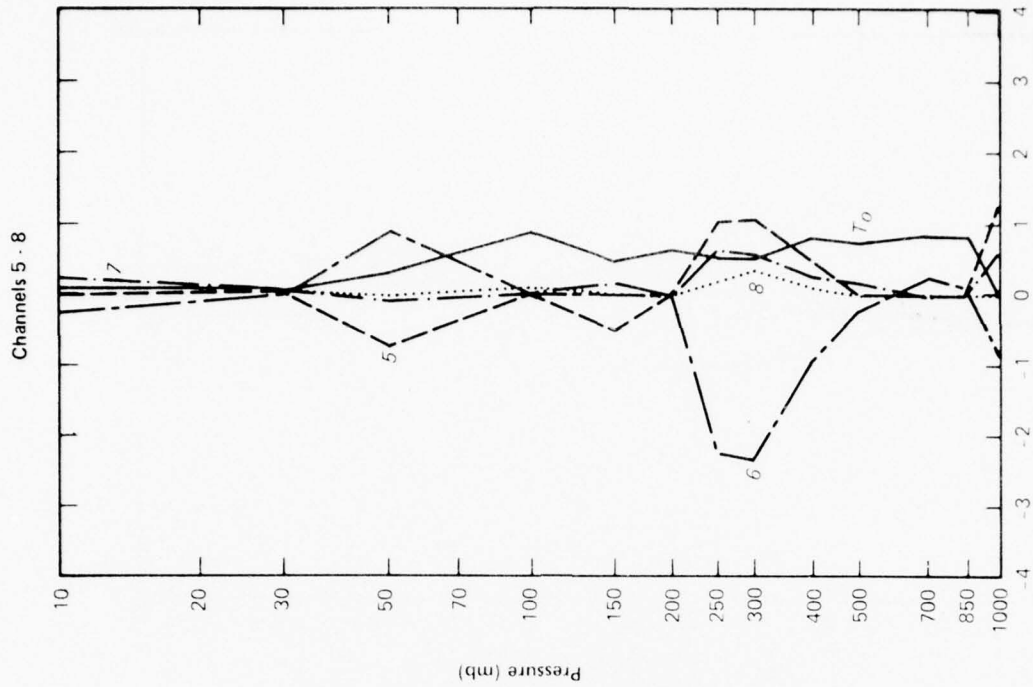Figure 4.8 Regression Coefficients;
Week 1; All Data

141

Figure 4.9 Regression Coefficients;
Week 2; All Data

142

The F ratios for the regression models given in Figs. 4.8 and 4.9 are given in Tables 4.9 and 4.10. Only those predictor variables which were significant at the 5% level were retained in the regressions. A zero value indicates that the variable was not significant at the 5% level. Examination of the data reveals several things. The first guess temperatures are relatively insignificant above 100 mb. Between 100 mb and 300 mb they are moderately significant, and are very significant between 400 mb and 850 mb. They are seen to be insignificant at 1000 mb.

Channel 1 is significant for temperature estimation at 30 mb, which is close to the weighting function peak. Channel 2 is not consistent but contributes at 100, 150 and 200 mb and weakly at 1000 mb. Channel 3 is quite significant from 30 to 150 mb and surprisingly significant at 1000 mb. Channel 4 contributes only moderately at the 250 and 300 mb levels. Channel 5 is significant at 150 mb, mostly due to its role of compensating for the skirts of the channel 3 transmittance function. Note that channel 5 also contributes at 1000 mb. Channel 6 contributes consistently at 50, 250, 300, 700, and 850 mb levels for both weeks. Channel 7 contributes significantly at 10 mb but only marginally at 1000 mb, where it should be contributing the most. However, Channel 7 contributes very significantly in the interval between 250 and 400 mb. Channel 8 (the water vapor channel) is seen to be relatively insignificant for use in temperature estimation at any level.

4.4.3.1 Sensitivity to Training and Test Set Data

The effect of using different training and test sets on regression performance was evaluated to determine the statistical significance and predictive power of the regression models. The results are summarized in Fig. 4.10. All four possible combinations of training and test sets (1→1, 1→2, 2→1, 2→2) were used. When the training and test sets were identical, the rms errors were generally less than 2°C. However, the errors at 100 mb and 250 mb were slightly larger, about 2.5°C. The largest errors occurred at 1000 mb, and were about 3.5°C. Note that both curves are almost identical, indicating that both the week 1 and week 2 data sets have the same statistical

143

Level	mb	T_0	Channel							
			1	2	3	4	5	6	7	8
1	10	58.6	73.8	50.0	117.9	0	0	0	907.0	0
2	20									
3	30	4.7	99.4	22.5	179.2	12.3	25.3	0	68.5	6.7
4	50	73.9	69.7	0	865.2	31.9	90.9	126.7	0	9.5
5	70									
6	100	483.4	0	50.3	73.6	19.6	16.2	22.1	0	6.0
7	150	159.7	0	208.5	263.3	0	141.7	86.1	0	0
8	200	122.1	5.5	33.5	35.7	83.6	13.5	100.4	127.0	36.9
9	250	211.7	12.4	42.9	0	106.5	31.2	108.8	130.5	48.2
10	300	310.0	4.0	0	94.8	72.6	28.5	71.9	103.7	35.0
11	400	2751.3	0	0	0	0	0	0	91.8	0
12	500	2162.4	0	5.07	0	0	0	92.1	0	0
13	700	1783.8	0	0	0	0	0	7.4	4.7	0
14	850	456.2	6.0	11.7	22.6	0	31.0	14.3	19.6	3.8
15	1000	23.6	0	54.5	140.9	0	66.9	0	11.0	0

TABLE 4.9

F RATIOS FOR REGRESSION MODEL - WEEK #1

· Use only one first guess temperature at each level.

TABLE 4.10

F RATIOS FOR REGRESSION MODEL - WEEK #2

Level	mb	T_o	Channel							
			1	2	3	4	5	6	7	8
1	10	12.8	9.1	41.6	13.1	88.8	0.	15.7	61.2	0.
2	20									
3	30	8.2	103.4	77.3	98.8	7.5	0.	0.	34.7	0.
4	50	98.0	71.2	18.4	302.3	14.3	44.5	47.8	16.9	8.4
5	70									
6	100	513.8	29.3	0.	64.6	63.5	0.	0.	0.	14.6
7	150	177.2	5.6	20.7	150.8	0.	170.9	0.	84.7	0.
8	200	303.8	0.	62.4	80.3	0.	0.	0.	0.	0.
9	250	272.9	10.8	38.9	13.8	47.3	20.2	66.1	93.7	16.6
10	300	355.7	38.2	95.1	0.	109.6	27.6	101.5	110.8	52.5
11	400	1515.7	0.	0.	28.1	30.8	11.7	28.7	37.1	20.1
12	500	900.1	15.4	24.4	30.1	63.3	0.	8.7	30.5	0.
13	700	1133.0	15.9	23.8	13.5	0.	0.	52.4	0.	0.
14	850	1214.0	0.	0.	0.	0.	0.	41.3	0.	0.
15	1000	0	0.	48.5	92.1	0.	28.1	7.7	63.6	0.

• use only one first guess temperature at each level.
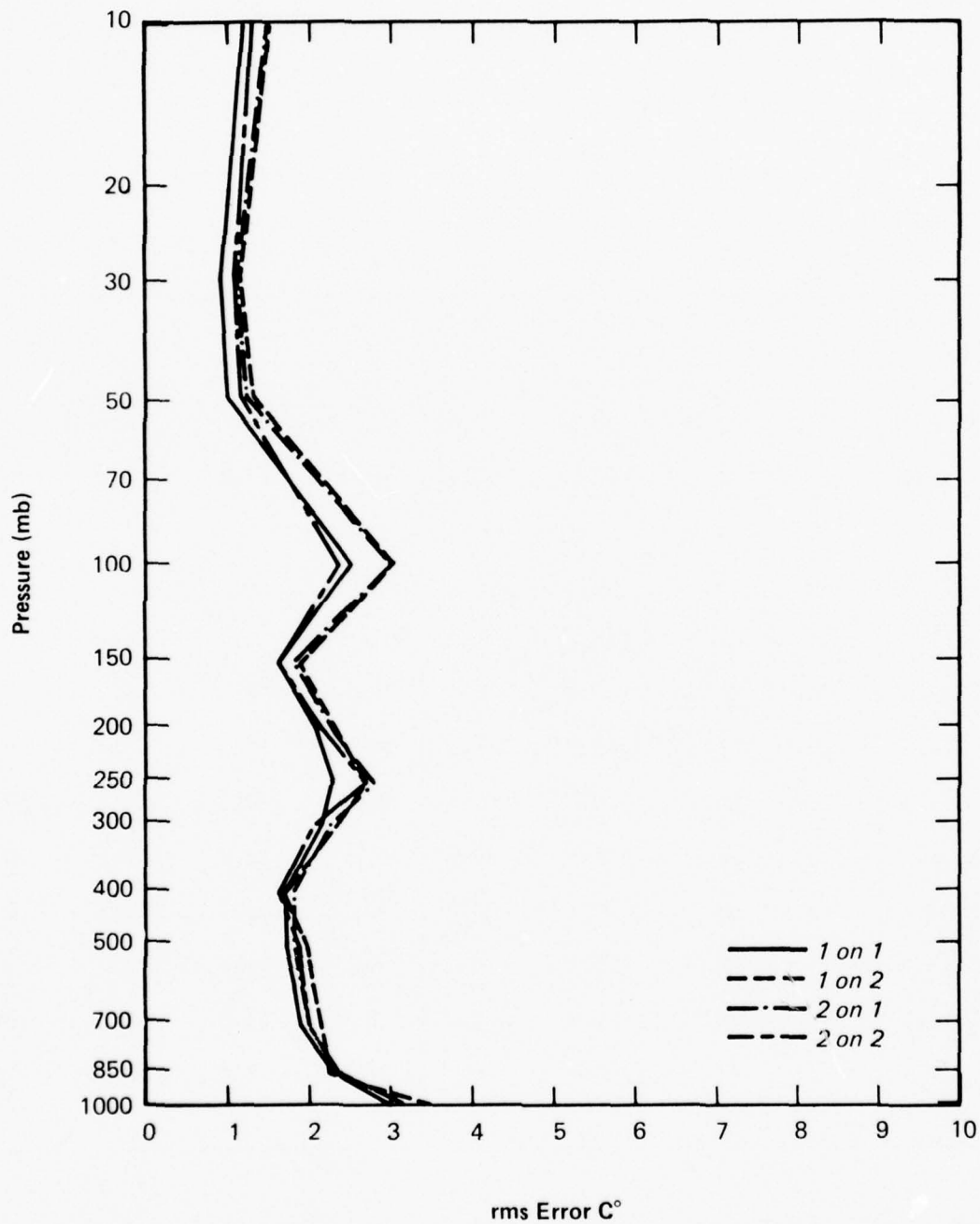
Figure 4.10   Effect of Using Different
Training and Test Sets; All Data

146

variability. When different training and test sets were used, the errors were slightly degraded. The maximum degradation in rms value is 0.6°C; however the degradation is generally less than 0.4°C. The shape of these curves is similar to that of the first two. The conclusions to be drawn from these results are:

> (1) Both week 1 and week 2 data sets are large enough to be statistically significant. That is, either one can form the basis for developing a valid regression model.

> (2) Either of the regression models may be used for accurate temperature retrievals for the other week.

4.4.3.2 Comparison of Retrieval Methods

A series of comprehensive tests were made on the minimum-information, regression and hybrid methods discussed earlier (cf. Section 4.4.2). The methods tested were:

> (a) minimum-information.

> (b) regression method, using the entire first guess temperature profile in the predictor set.

> (c) regression method, using only the first guess temperature at the level of interest in the predictor set.

> (d) hybrid method, using the entire first guess temperature profile in the predictor set.

The results of these tests are summarized in Figs. 4.11-4.32, in which the retrieval errors in °C are plotted for all data and the two latitude and zenith angle partitions. The most significant results may be summarized as follows:

> (1) The minimum-information retrievals are uniformly worse than the other three methods when the regression and tests are identical, with the exception of the $2 \rightarrow 2$ case for $\gamma > 45°$ at 250 mb.

> (2) More significantly, the minimum-information retrievals are uniformly worse than the other methods when different training and test sets are used, with the exception of the case $\gamma > 45°$ near 300 mb. The performance degradation is quite severe in many cases, especially above 100 mb, where it ranges generally from 2°C to 6°C. The degradation for pressures below 100 mb are generally about 1°C.

147

(3) The full regression method, using the entire first
guess profile (all T_0), is uniformly better than the other methods.[*]
This result is not unexpected when the training and test sets are identical.
However, this result holds also for the cases when the training and
test sets are different. The rms errors were generally about 1°C above
50 mb, between 2 and 3°C at 100 mb and 250 mb and between 1 and 2°C below
300 mb. Errors were, however, somewhat larger at 1000 mb, as high as 5°C.
This is apparently due to the way in which the clear-column measurements
are picked. Measurements may be made even when cloud cover is present.

(4) The effect of eliminating all but one first guess tempera-
ture level has little effect, generally 0.2°C or less. There were several
cases for which accuracy was significantly degraded - up to 1.5°C at 100 mb
($2 \rightarrow 2$, all data).

(5) Perhaps the most surprising result is that the performance
of the hybrid method, denoted "minimum-information residuals" was uniformly
worse than the regression method. The implication of this is that the
minimum-information method is nonlinearly processing the data in a non-
optimum manner. It appears that information is somehow lost in the minimum
information solution. As discussed previously, if the nonlinear processing
was efficient, the hybrid method would be expected to achieve the best
performance. The degradation of the hybrid method is quite striking in some
cases - often as high as 1°C and even reaching 2°C.

It should be noted that the rms errors for the hybrid solution
are quite sensitive to zenith angle above 200 mb, with significant
degradation from the optimal (regression) results appearing at large zenith
angles, but little degradation at low zenith angles. Since the zenith
angle computations are significant only for high values, this implies that
the zenith angle processing in the minimum-information method is degrading
the content of the data. Further, since the hybrid and minimum-information
performance is quite similar in this region at $\theta > 0.7$, minimum-information
appears to be doing a good job of linear data processing. Thus, the
implication is that the information is being lost in the nonlinear processing.
It is possible that program modifications to eliminate the zenith angle pro-
cessing would enhance the minimum-information solution performance.

[*]Slight exceptions such as for the case $\gamma > 45°$, $1 \rightarrow 1$ at 150 mb can be
attributed to the stepwise regression method and the way variables are
selected.

148

(6) The minimum-information rms errors are significantly larger, up to 6°K, above 100 mb at high latitudes than at low latitudes. This may be attributed to the larger variation in temperature profiles at high latitudes, the increased variability in the measurements due to cloud presence and the method in which the first guess profile is computed. For pressure levels above 10 mb and latitudes > 60°N only two guess profiles are used, one for summer and one for winter.

(7) The minimum-information errors are relatively independent of zenith angle, although they are somewhat larger between 50 mb and 200 mb for $\theta < 0.7$ radian.

(8) The regression rms errors vary somewhat with latitude. Below 45°N, the errors above 50 mb are small (about 0.5 K) but increase to between 2° and 3°K at 100 mb. Above 45°N, the errors are generally between 2° and 3°K at all levels. The increased error at 100 mb at low latitudes is probably due to the quiescent nature of the temperature profiles, which makes it difficult to obtain estimates in the middle of transmittance function peaks.

(9) The regression errors are insensitive to changes in zenith angle. The results obtained using: (1) all data, (2) $\theta < 0.7$ and (3) $\theta > 0.7$ are almost identical in all four cases. Since the zenith angle was not included in the regression model, this implies an essential independence of the information with respect to zenith angle. Thus the zenith angle does not appear to carry information relevant to the problem of temperature sounding. This also implies that the zenith angle computations in SOUNDER may not be required, although a more careful study of the interaction between θ and other internal program variables would have to be made to corroborate this conclusion.

Temperature Inversion Error Comparisons
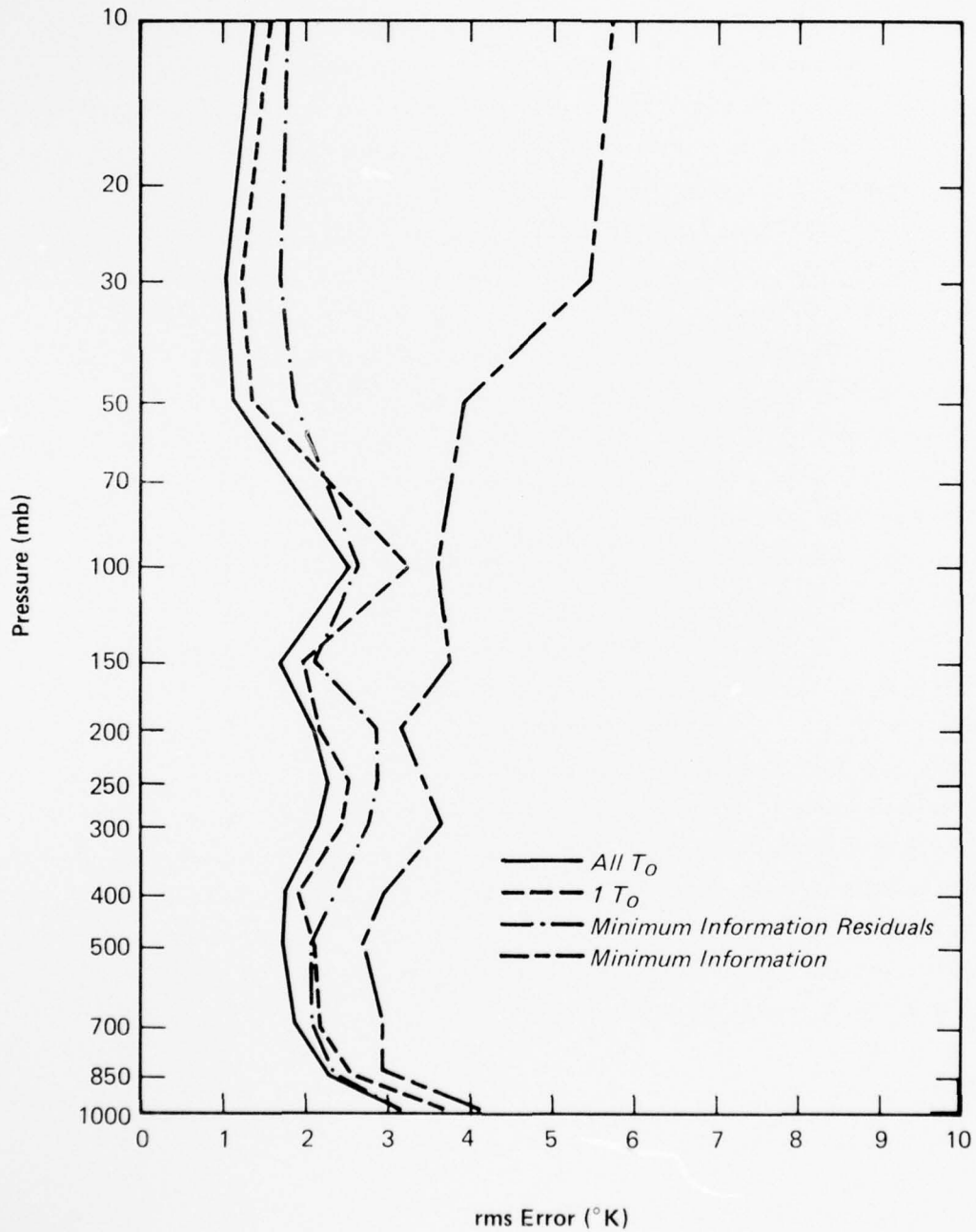
Figure 4.11   Temperature Inversion Error
Comparisons; All data(1→1)

Temperature Inversion Error Comparisons
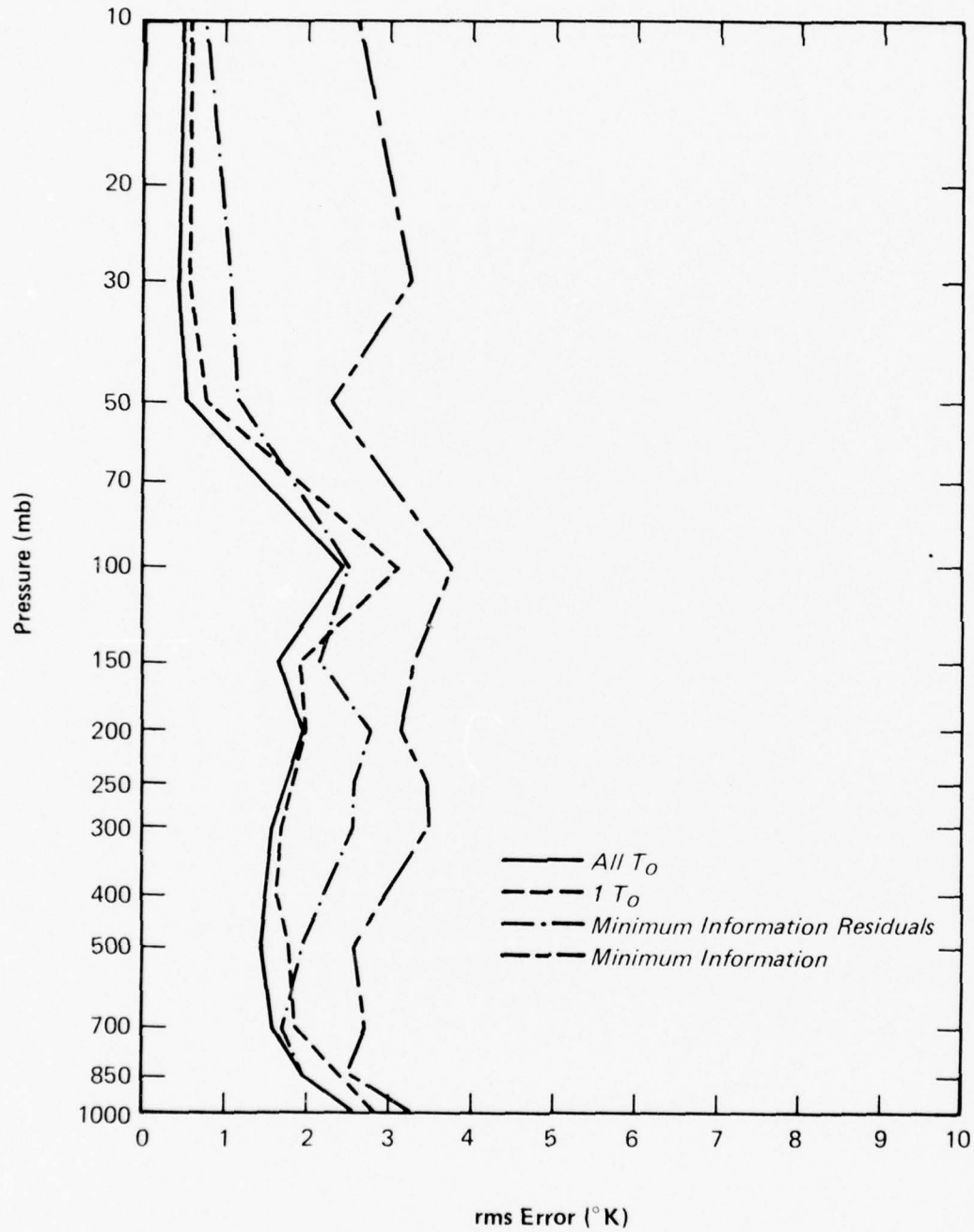
Figure 4.12 Temperature Inversion Error
Comparisons; $\lambda < 45°$ (1→1)

151

Temperature Inversion Error Comparisons

Figure 4.13 Temperature Inversion Error
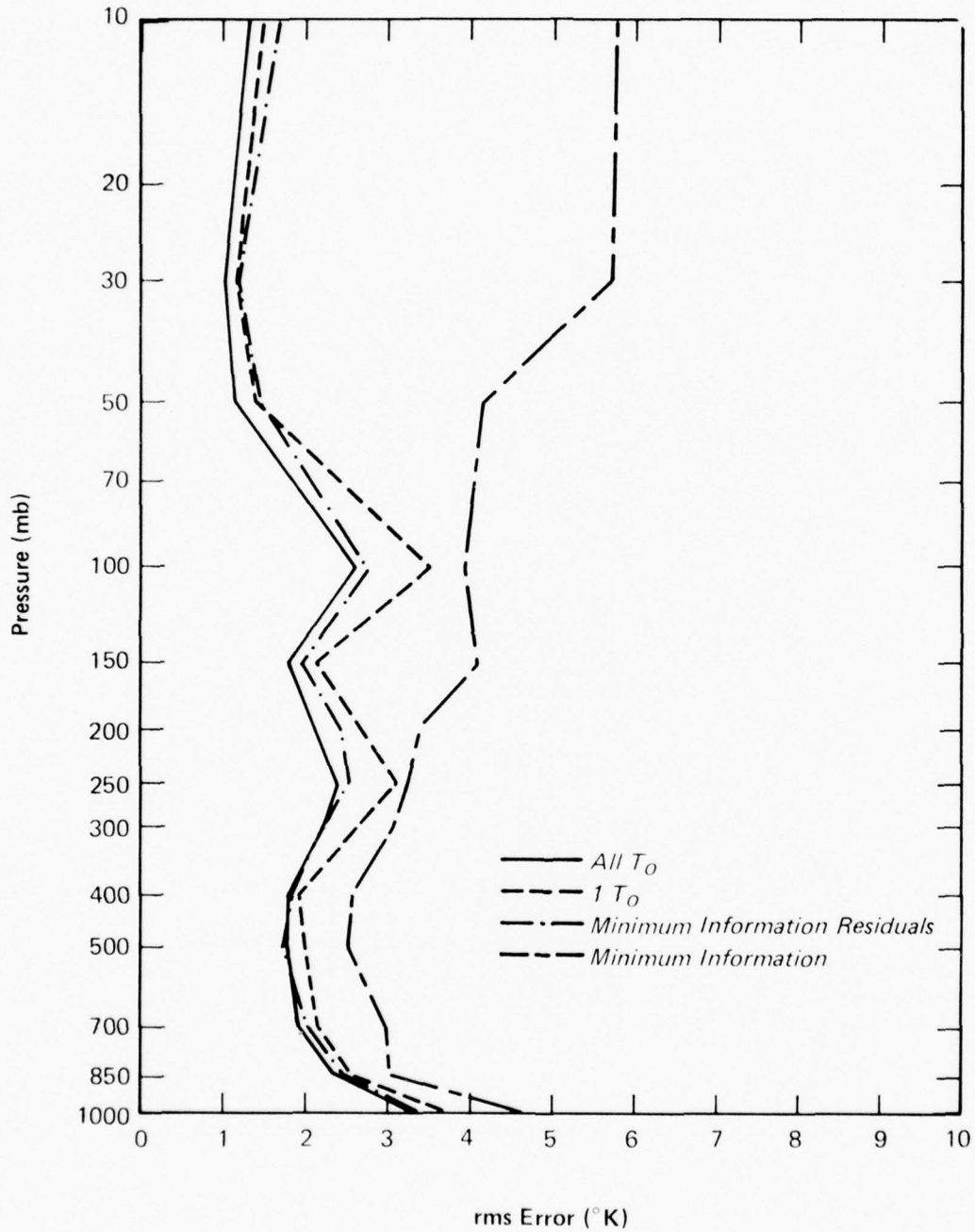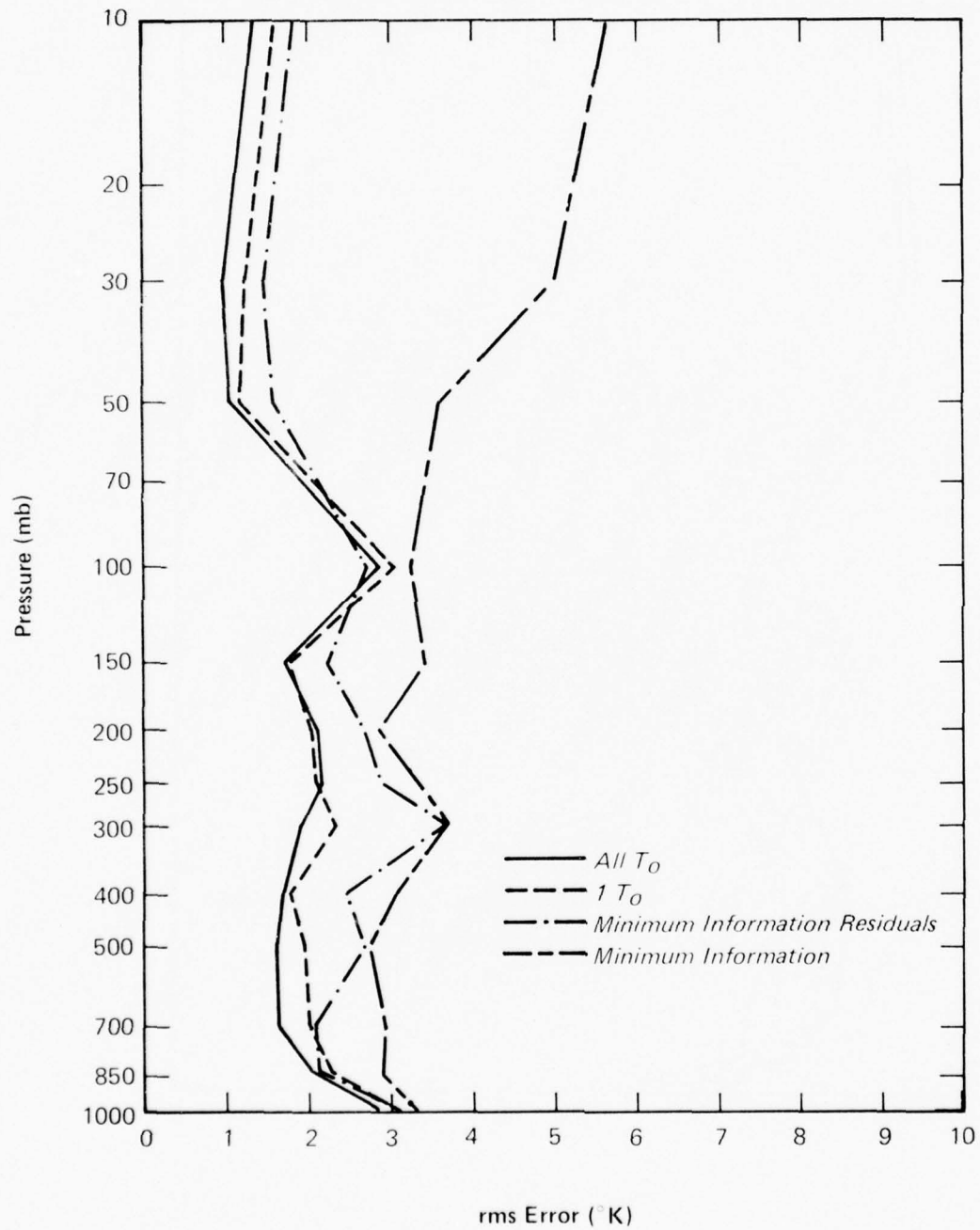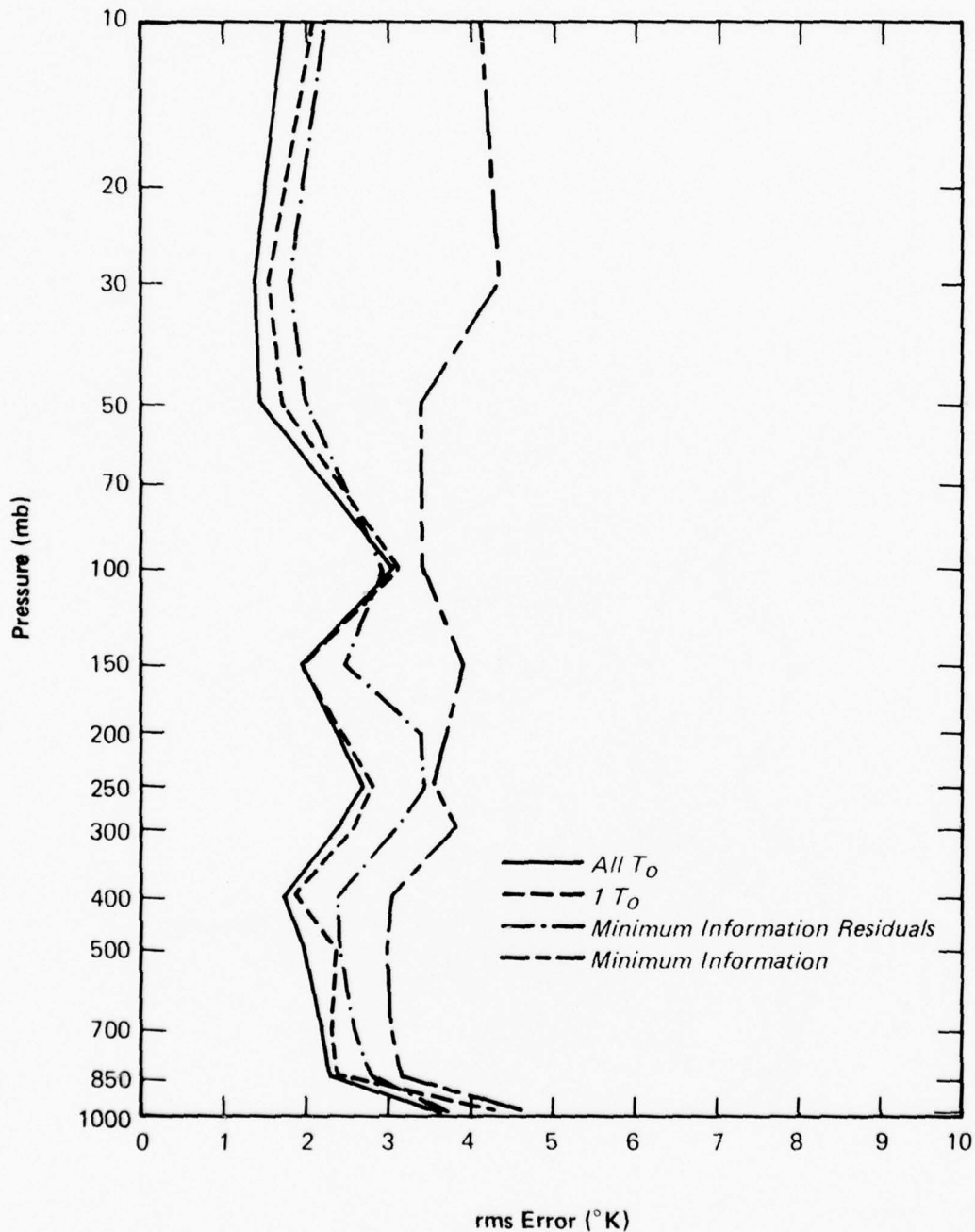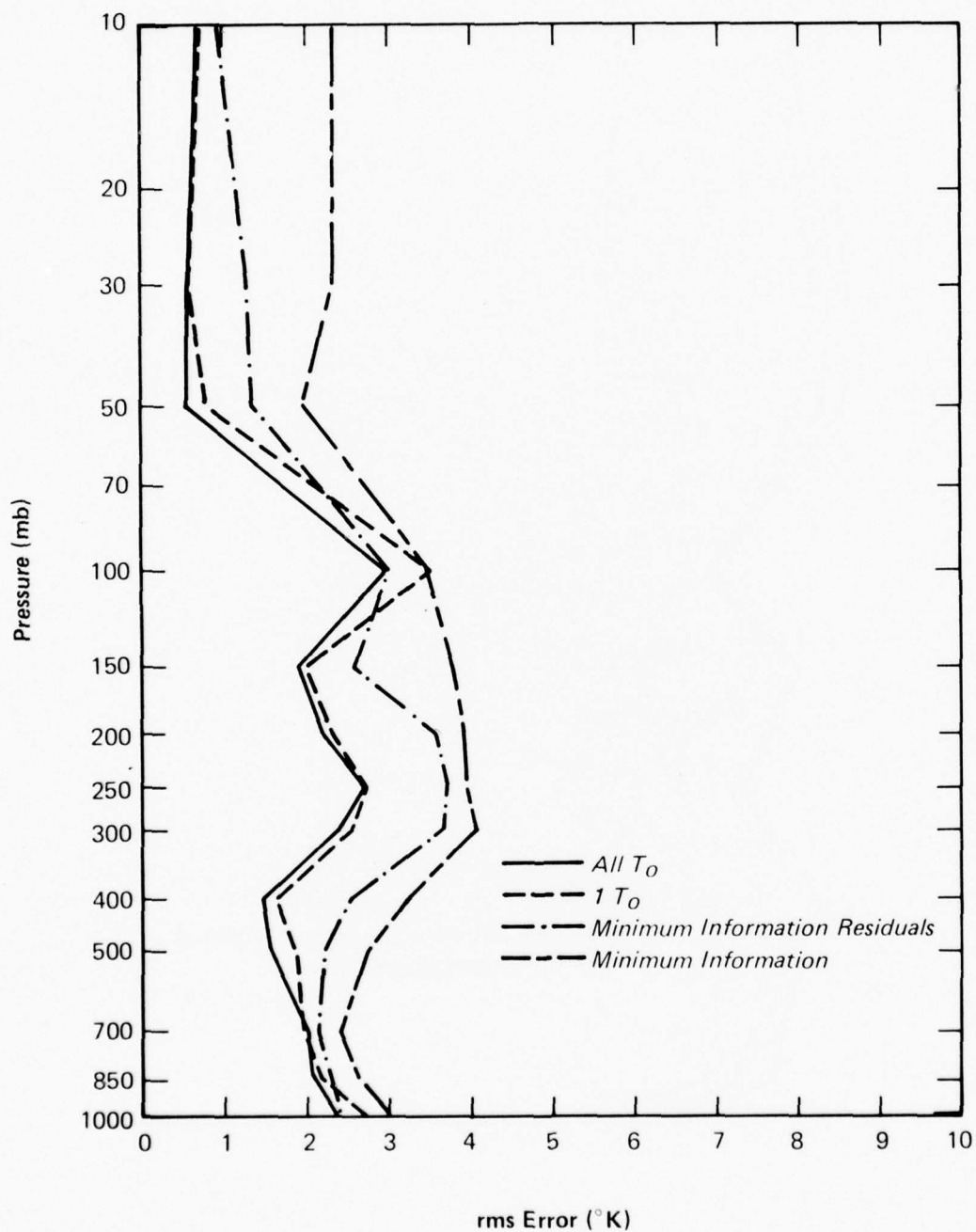Comparisons; $\lambda > 45°$ (1→1)

Temperature Inversion Error Comparisons
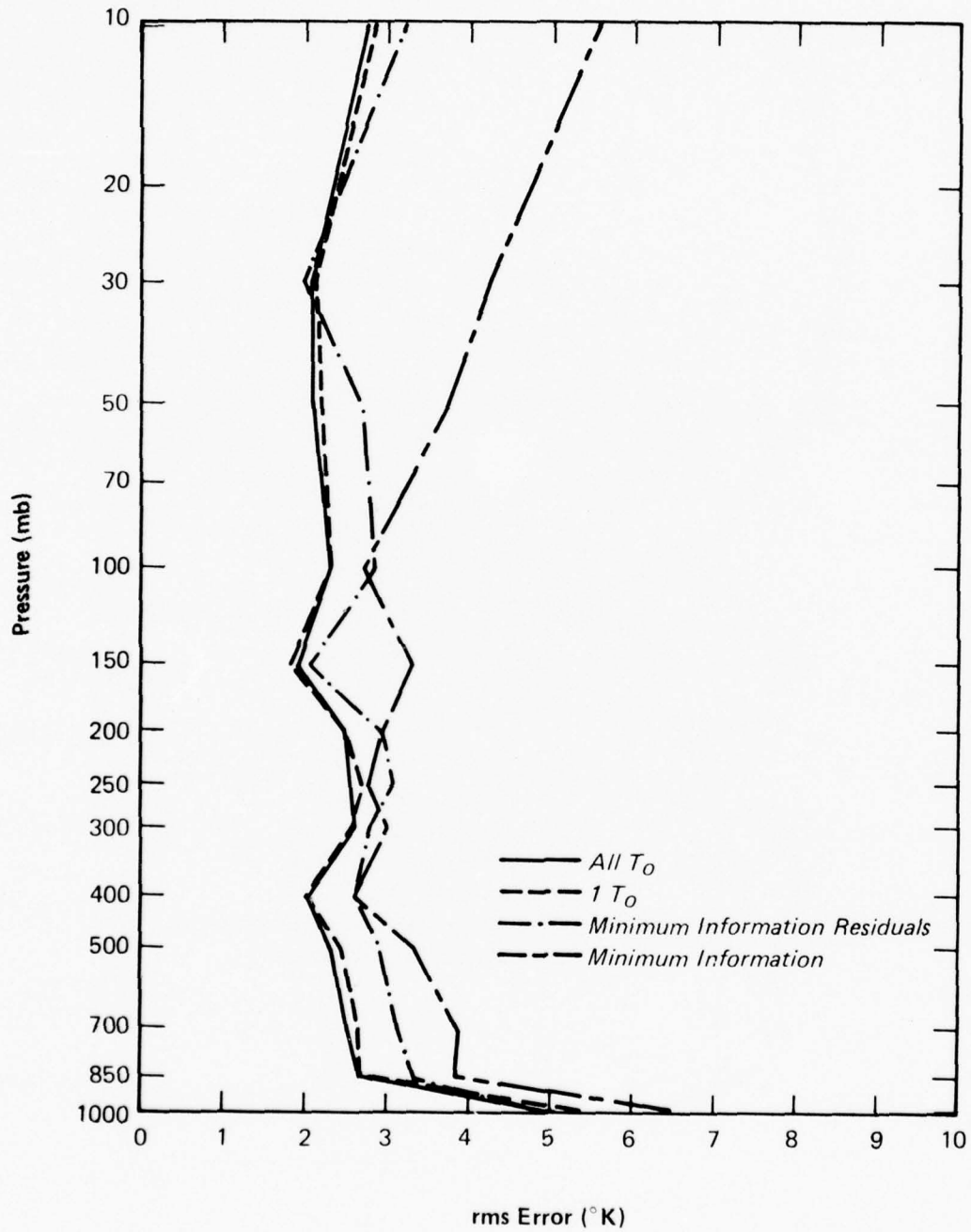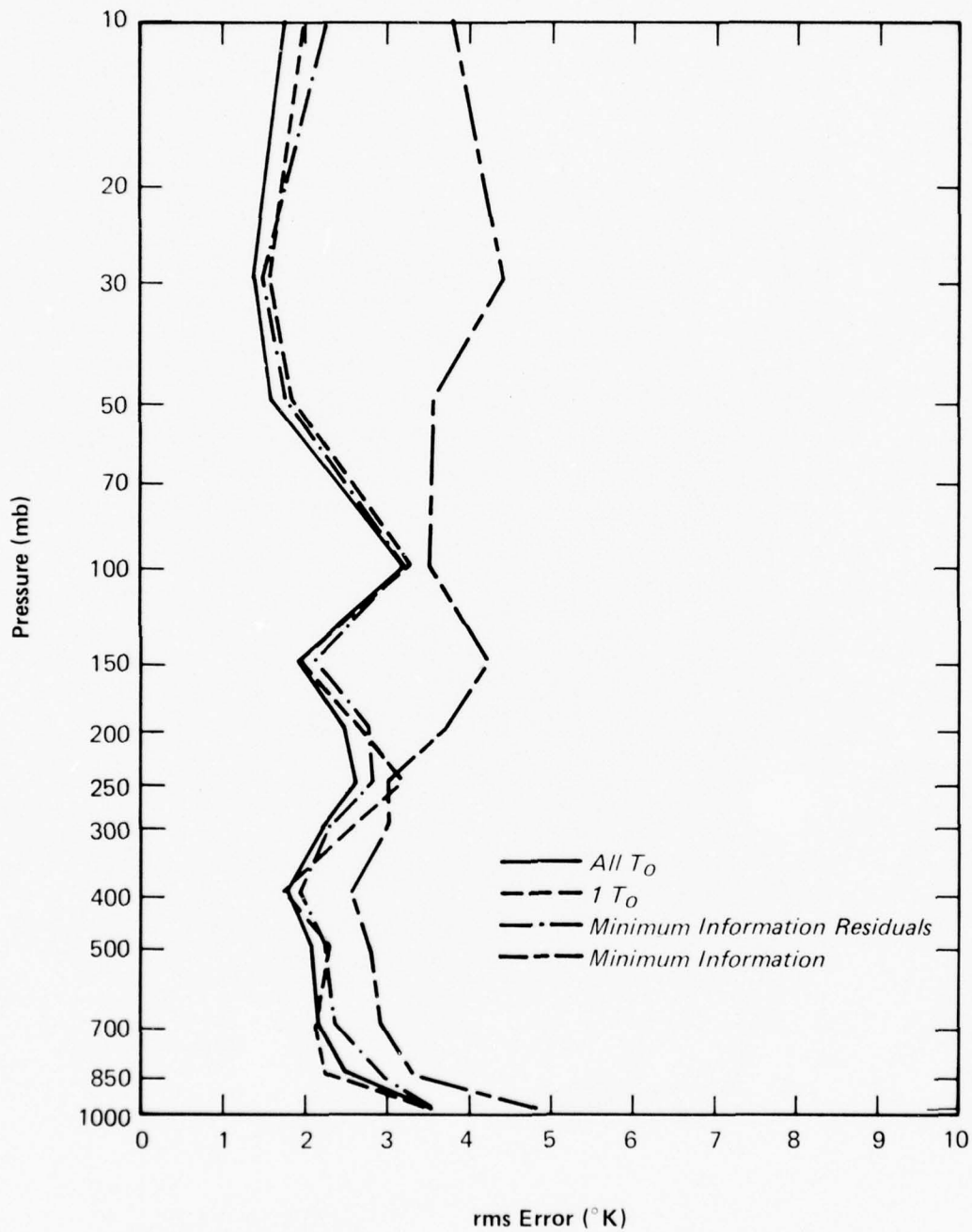

Figure 4.14   Temperature Inversion Error
Comparisons; $\theta < 0.7$ rad. (1→1)

153

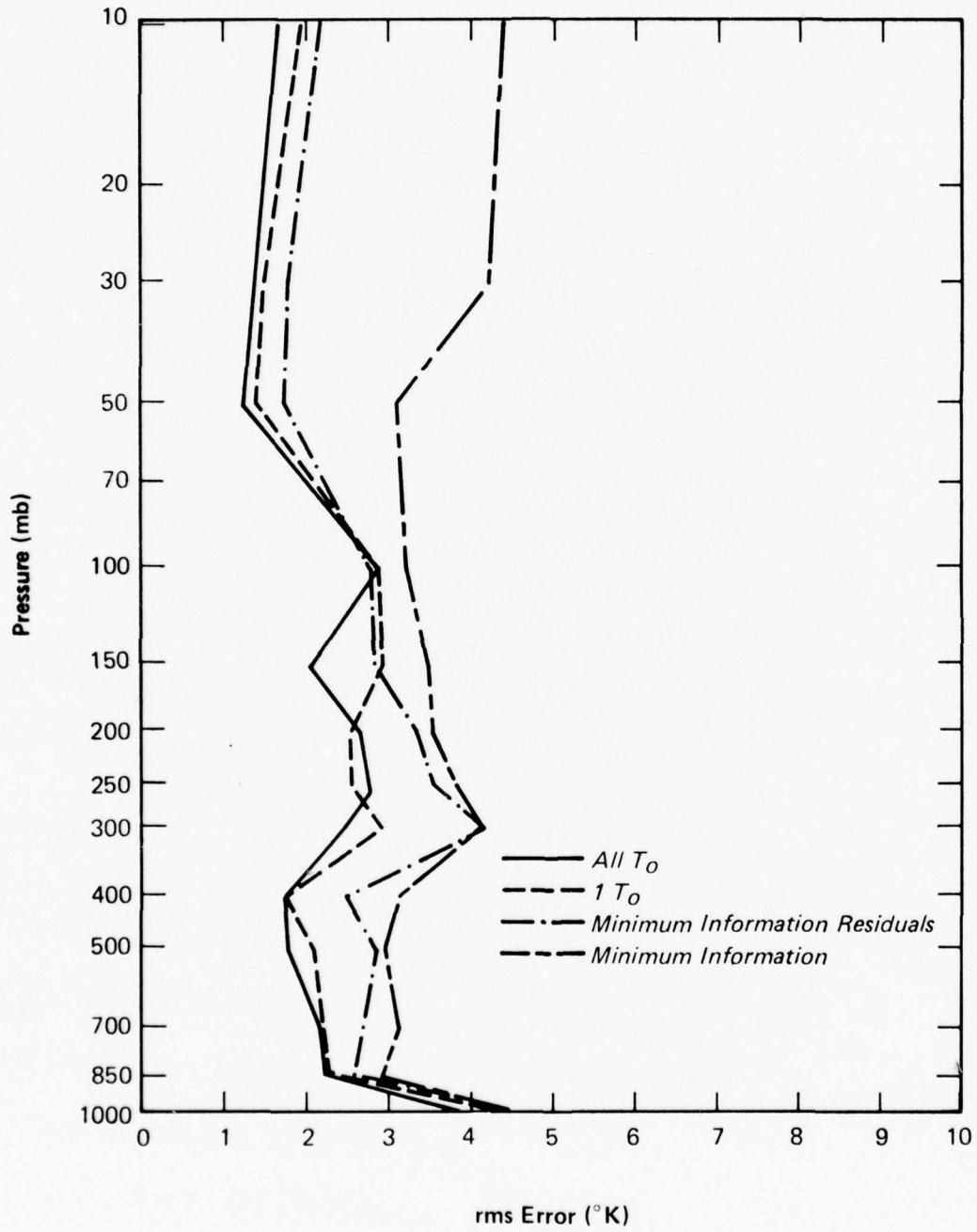Temperature Inversion Error Comparisons

Figure 4.15   Temperature Inversion Error
Comparisons; θ > 0.7 rad. (1→1)
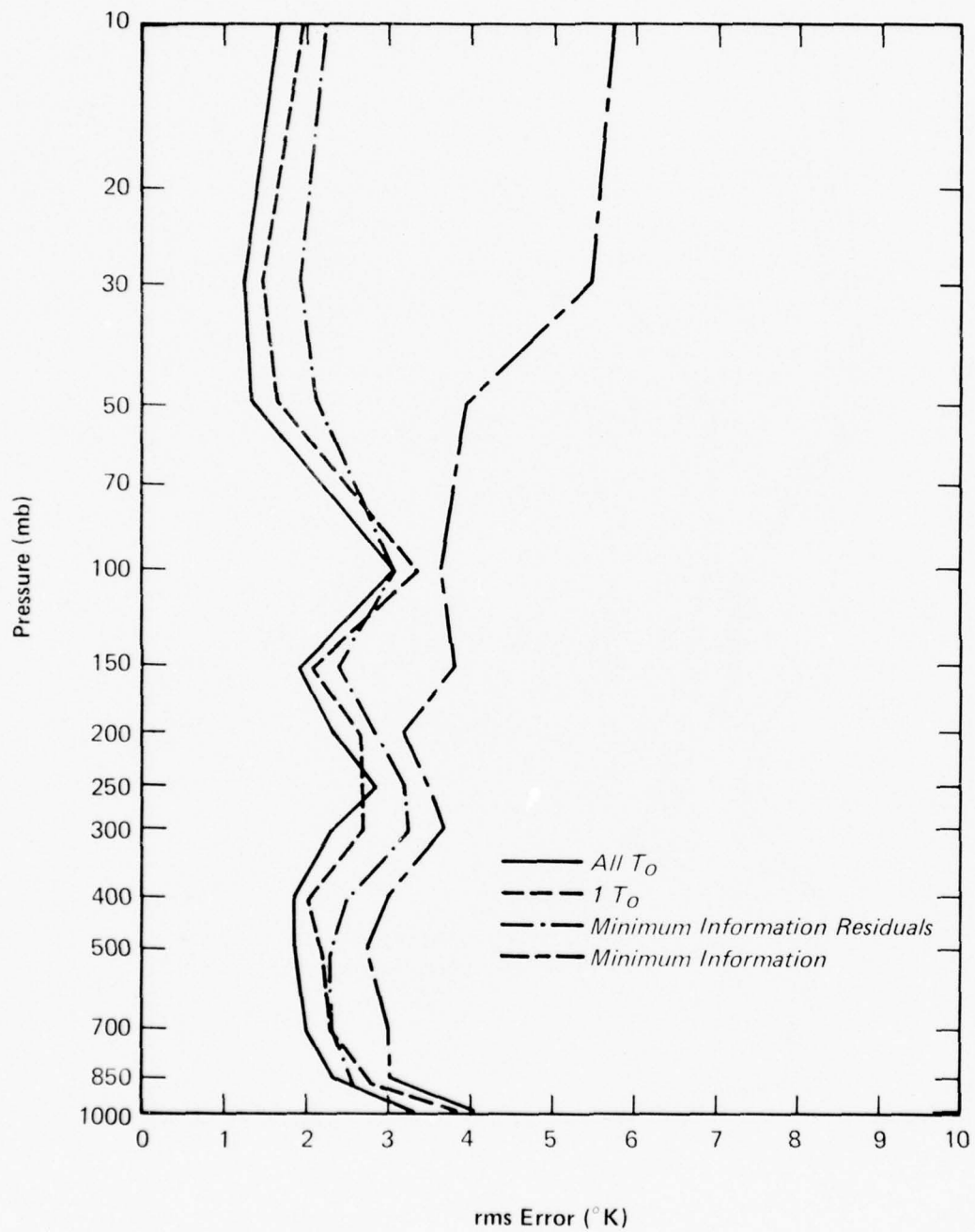
Temperature Inversion Error Comparisons

Figure 4.16 Temperature Inversion Error
Comparisons; All Data (1→2)
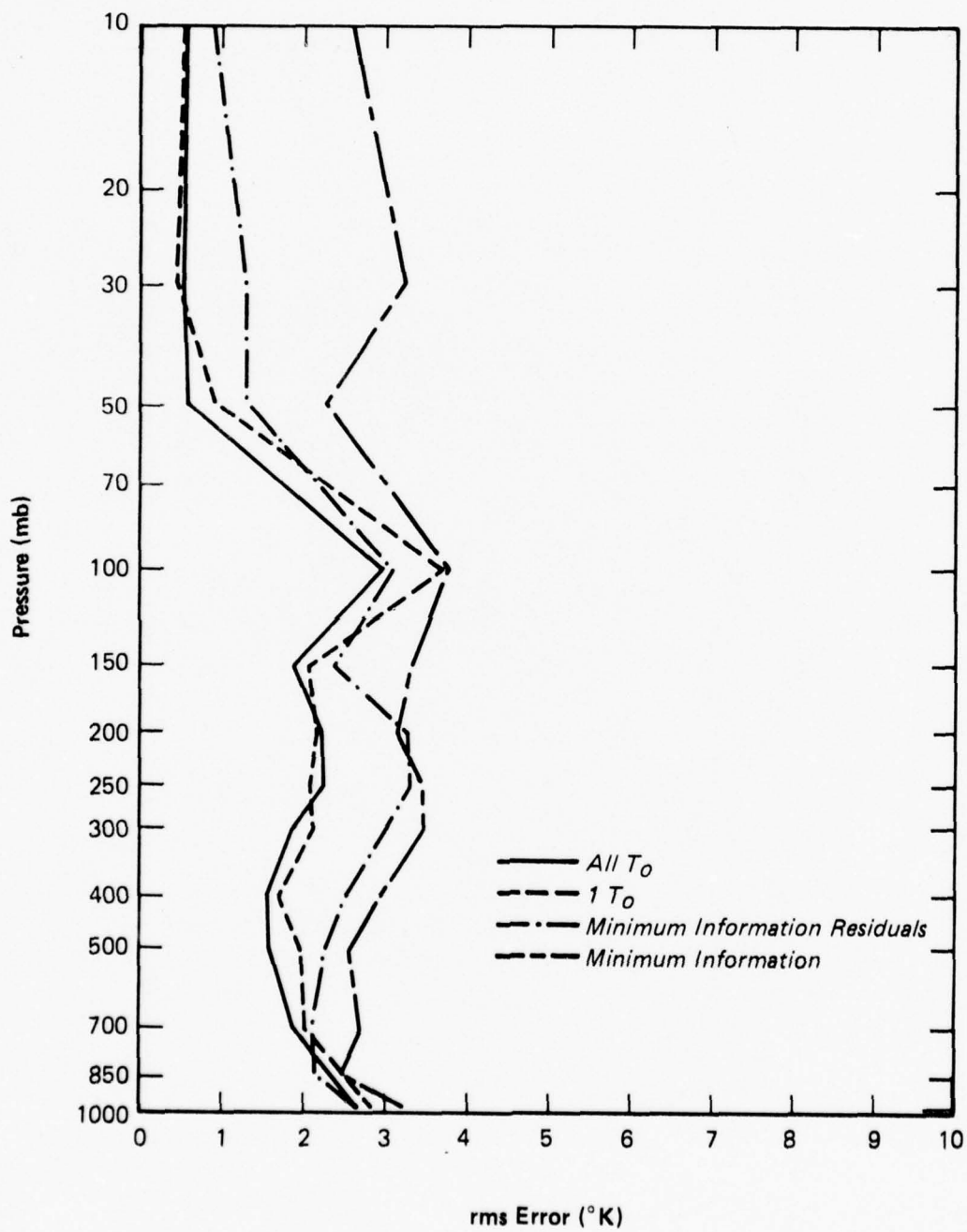
Temperature Inversion Error Comparisons

Figure 4.17 Temperature Inversion Error
Comparisons; $\lambda < 45°$ $(1 \rightarrow 2)$

156

Temperature Inversion Error Comparisons

Figure 4.18 Temperature Inversion Error
Comparisons; $\lambda > 45°$ (1→2)
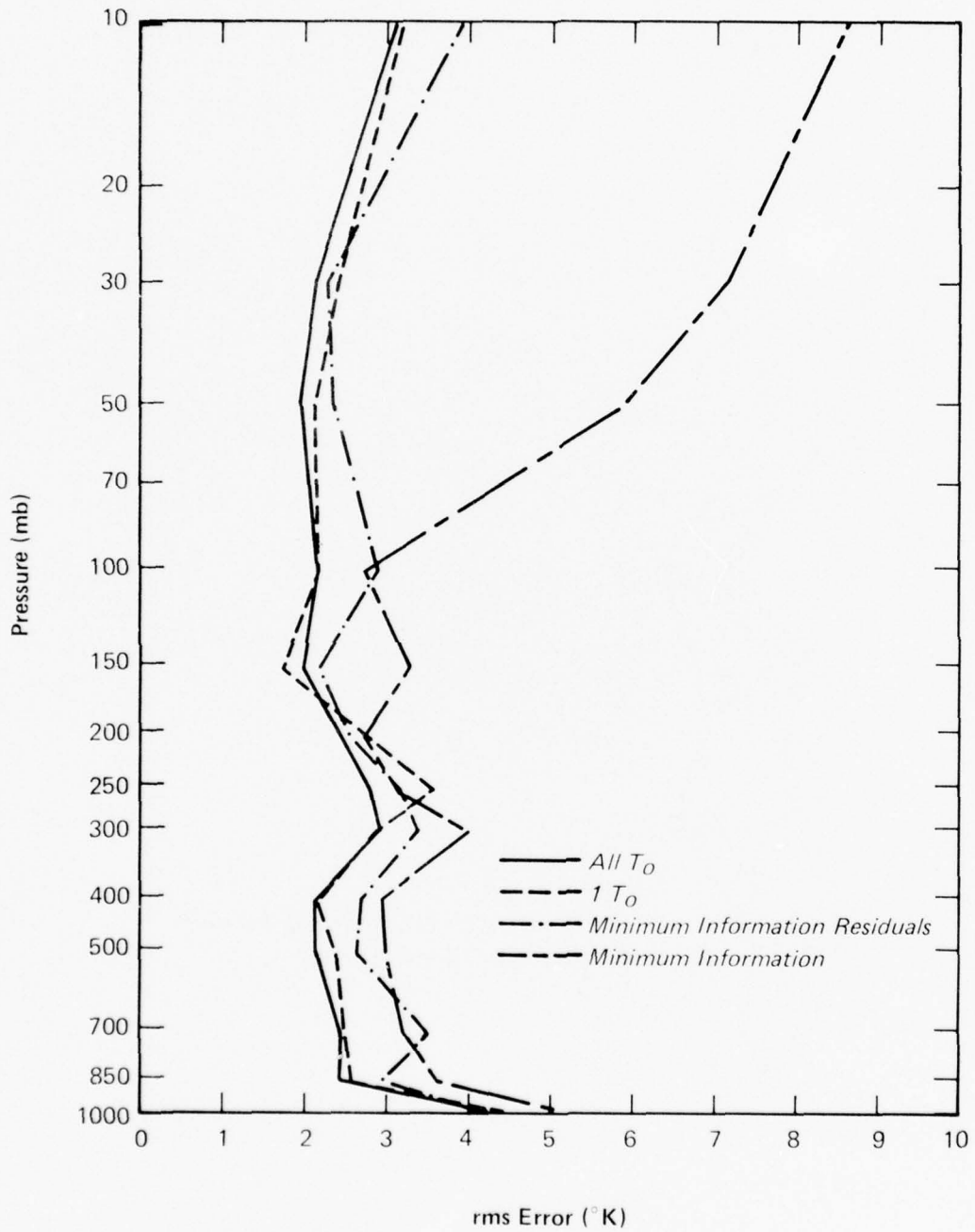
Temperature Inversion Error Comparisons

Figure 4.19 Temperature Inversion Error
Comparisons; $\theta < 0.7$ rad. (1→2)

Temperature Inversion Error Comparisons

Figure 4.20   Temperature Inversion Error
Comparisons; θ > 0.7 (1→2)

Temperature Inversion Error Comparisons

Figure 4.21 Temperature Inversion Error
Comparisons; All Data (2→1)

160

Temperature Inversion Error Comparisons

Figure 4.22 Temperature Inversion Error
Comparisons; $\lambda < 45°$ (2→1)

161

Temperature Inversion Error Comparisons

Figure 4.23 Temperature Inversion Error
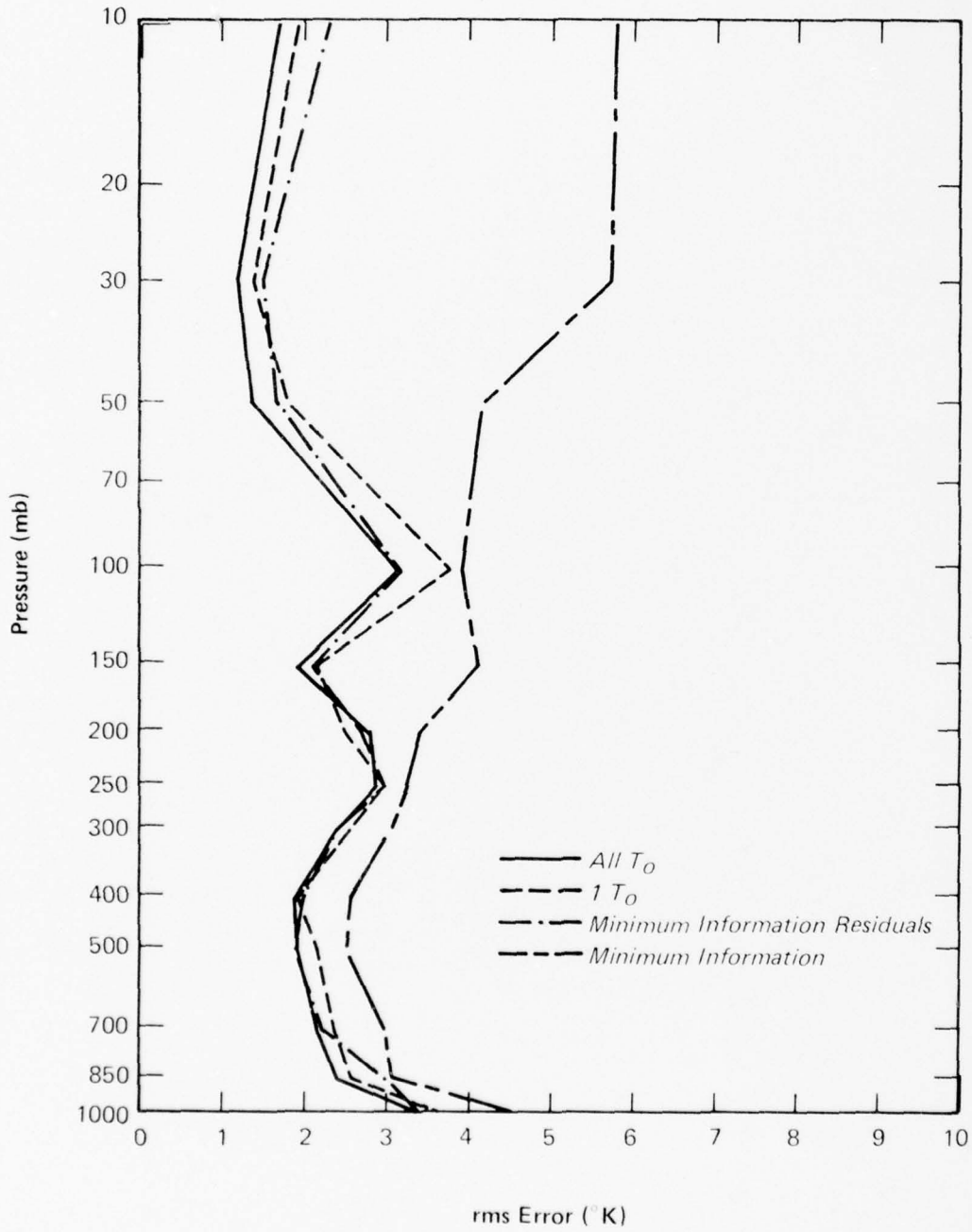Comparisons; $\lambda > 45°$ (2→1)

Temperature Inversion Error Comparisons

Figure 4.24   Temperature Inversion Error
Comparisons; θ < 0.7 (2→1)

163

Temperature Inversion Error Comparisons

Figure 4.25   Temperature Inversion Error
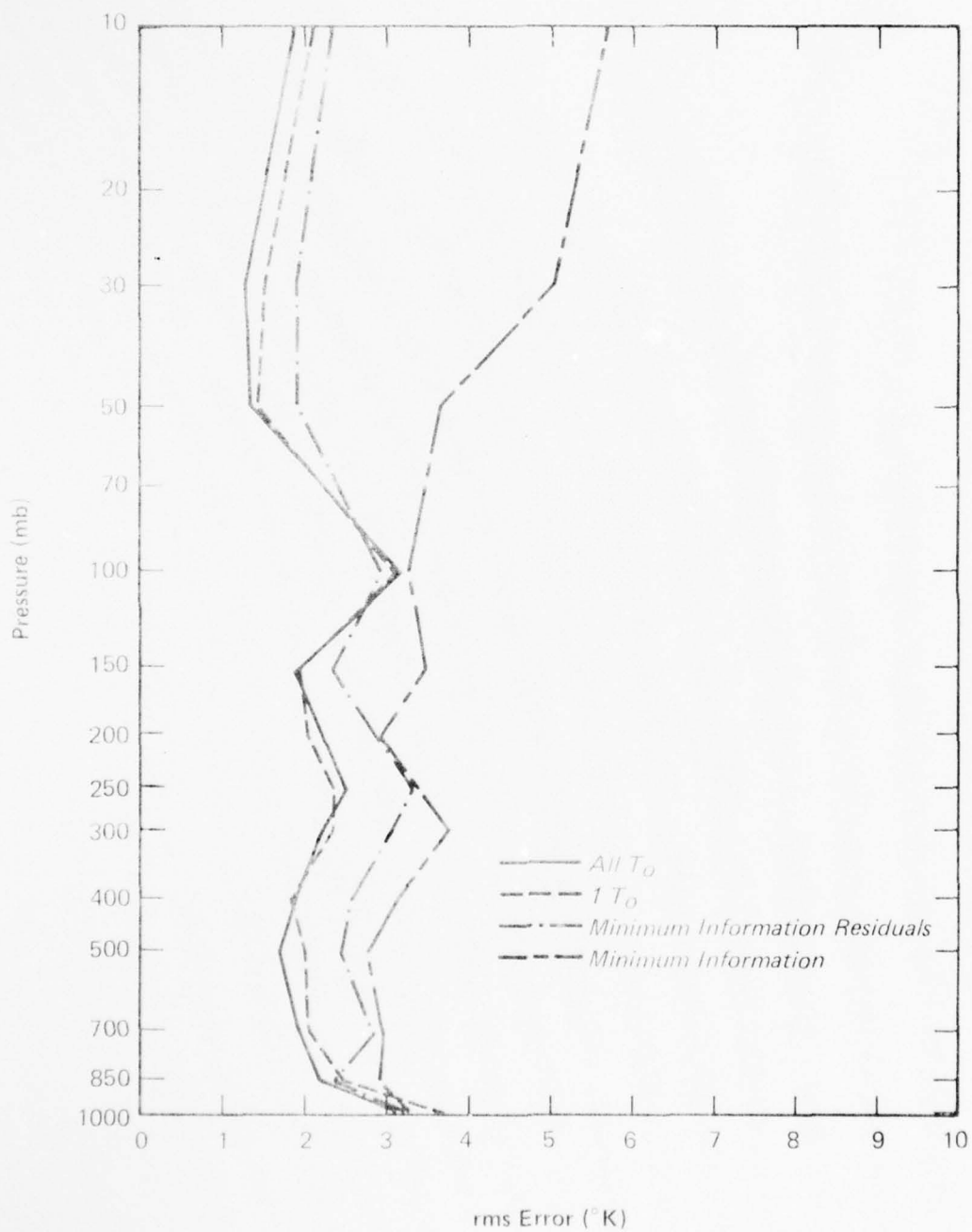Comparisons; θ > 0.7 (2-1)

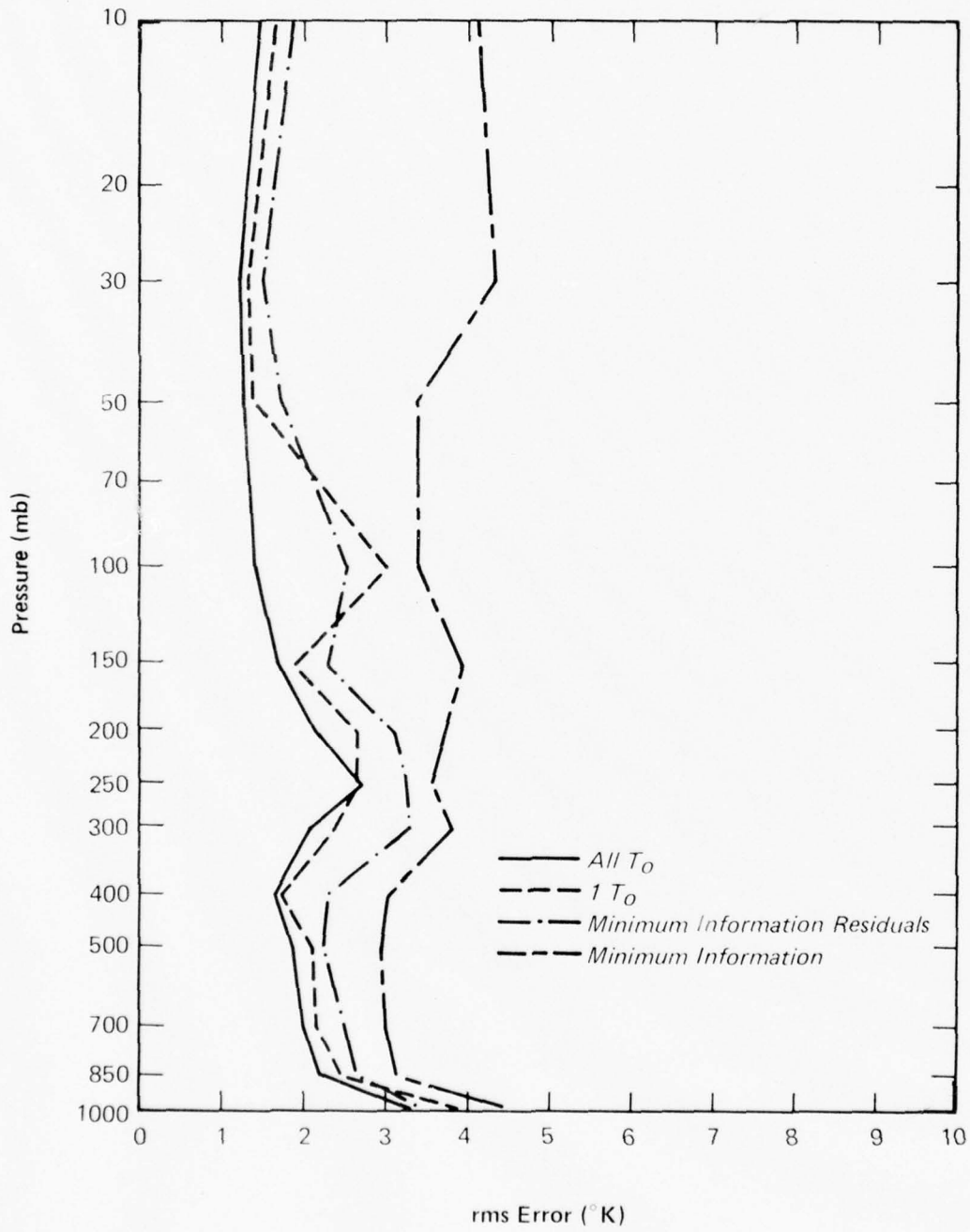## Temperature Inversion Error Comparisons

Figure 4.26 Temperature Inversion Error
Comparisons; All Data (2→2)

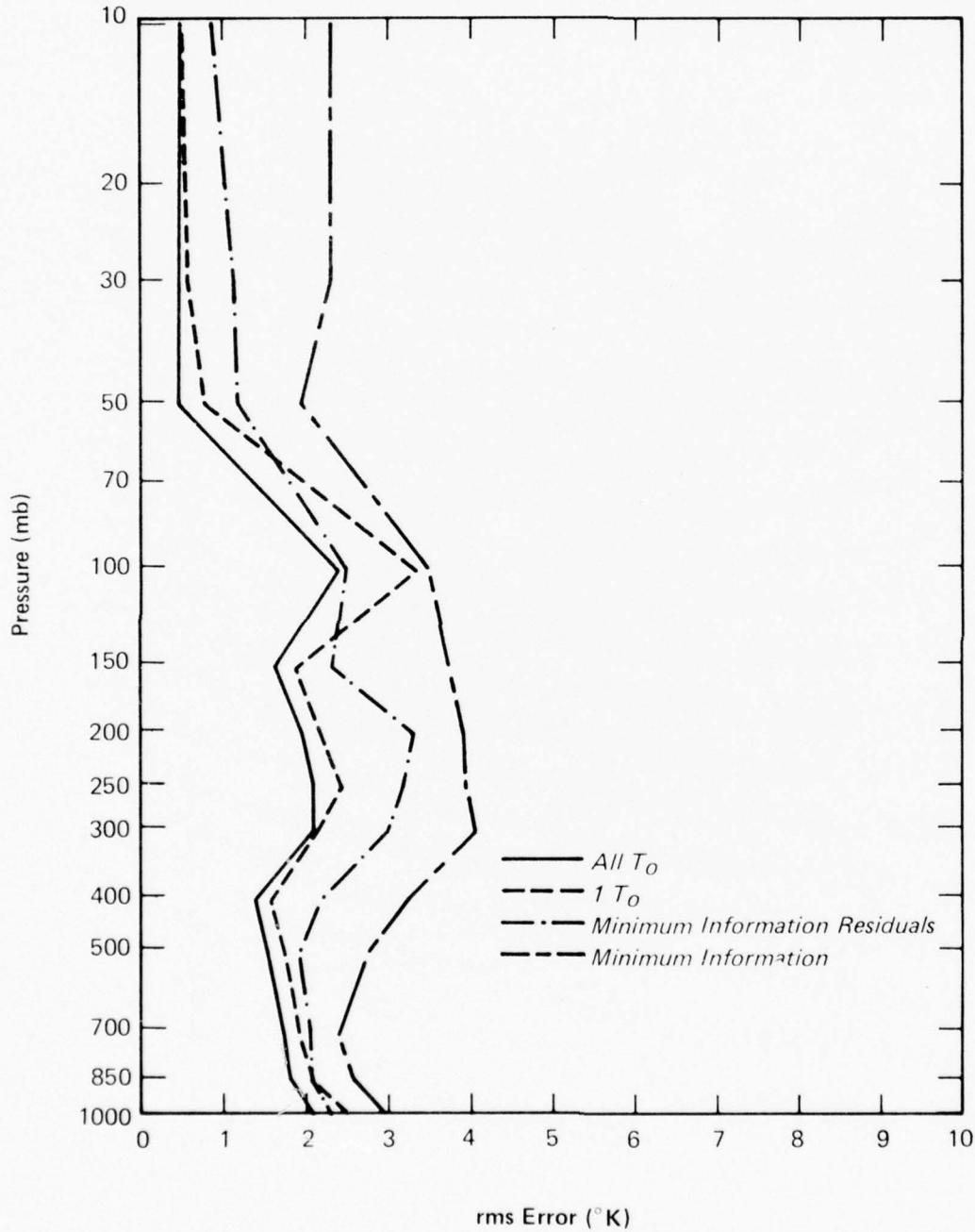165

Temperature Inversion Error Comparisons

Figure 4.27 Temperature Inversion Error
Comparisons; $\lambda < 45°$ (2→2)
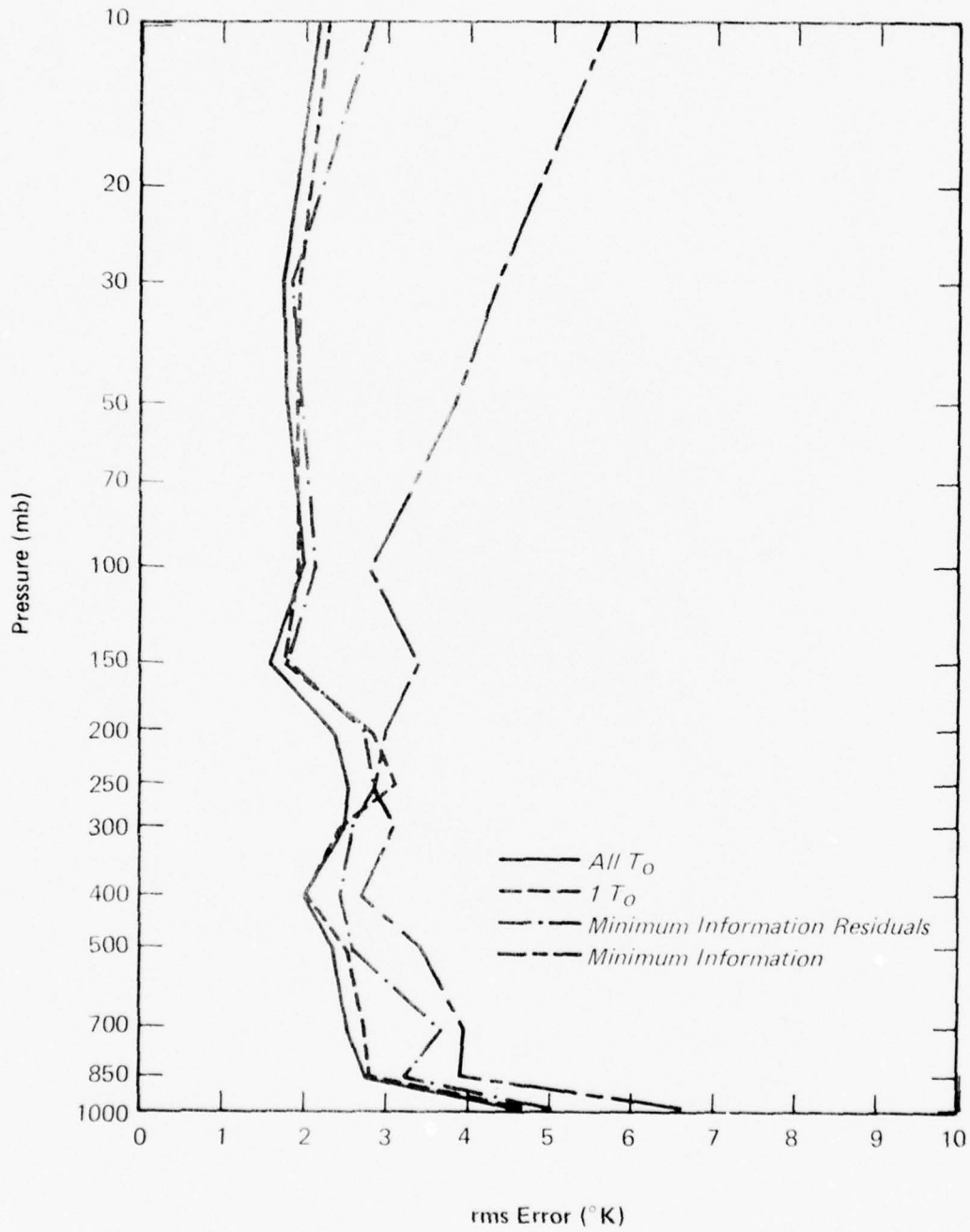
Temperature Inversion Error Comparisons

Figure 4.28 Temperature Inversion Error
Comparisons; $\lambda > 45°$ (2→2)

Temperature Inversion Error Comparisons

Figure 4.29   Temperature Inversion Error
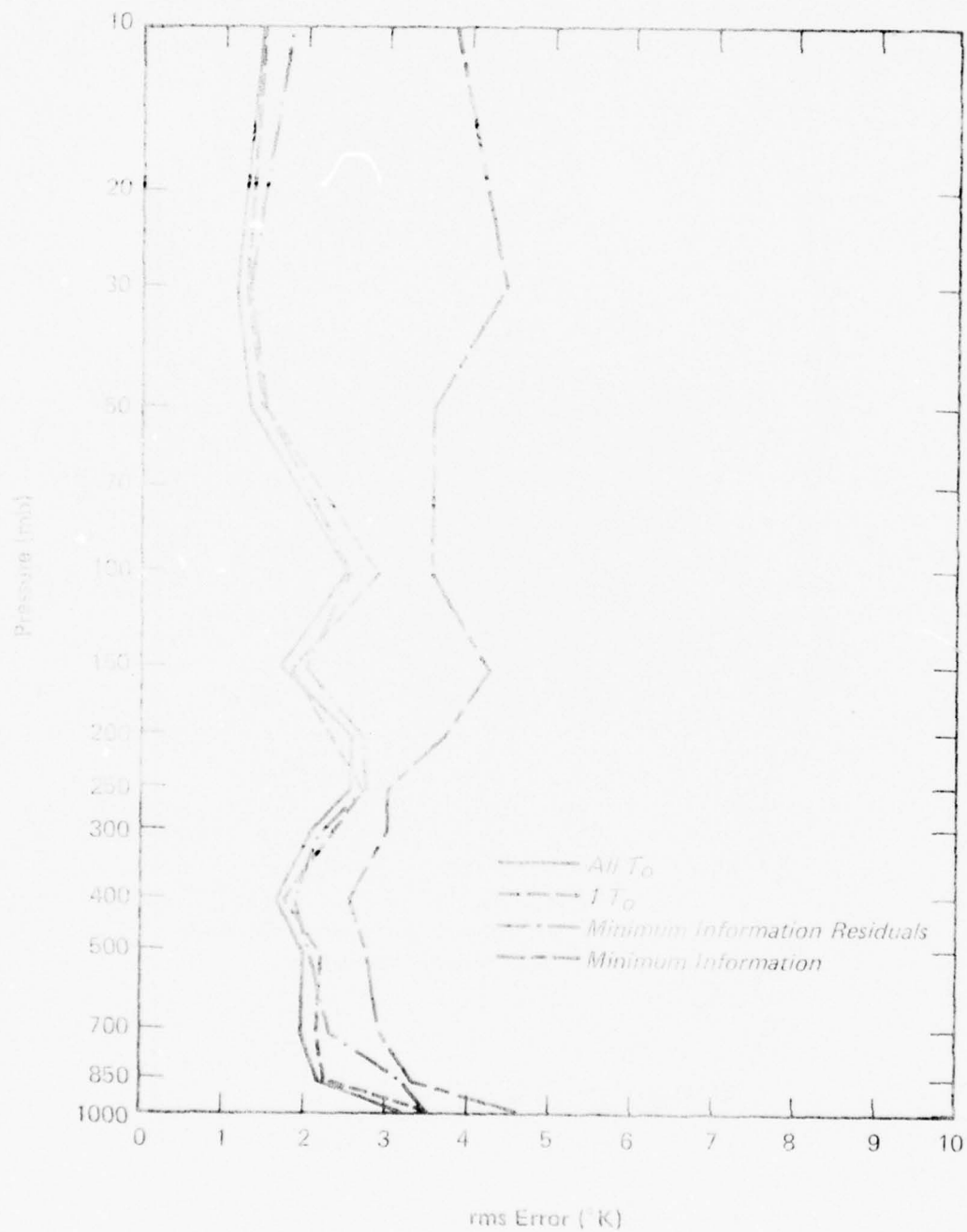Comparisons; θ < 0.7 (2>2)

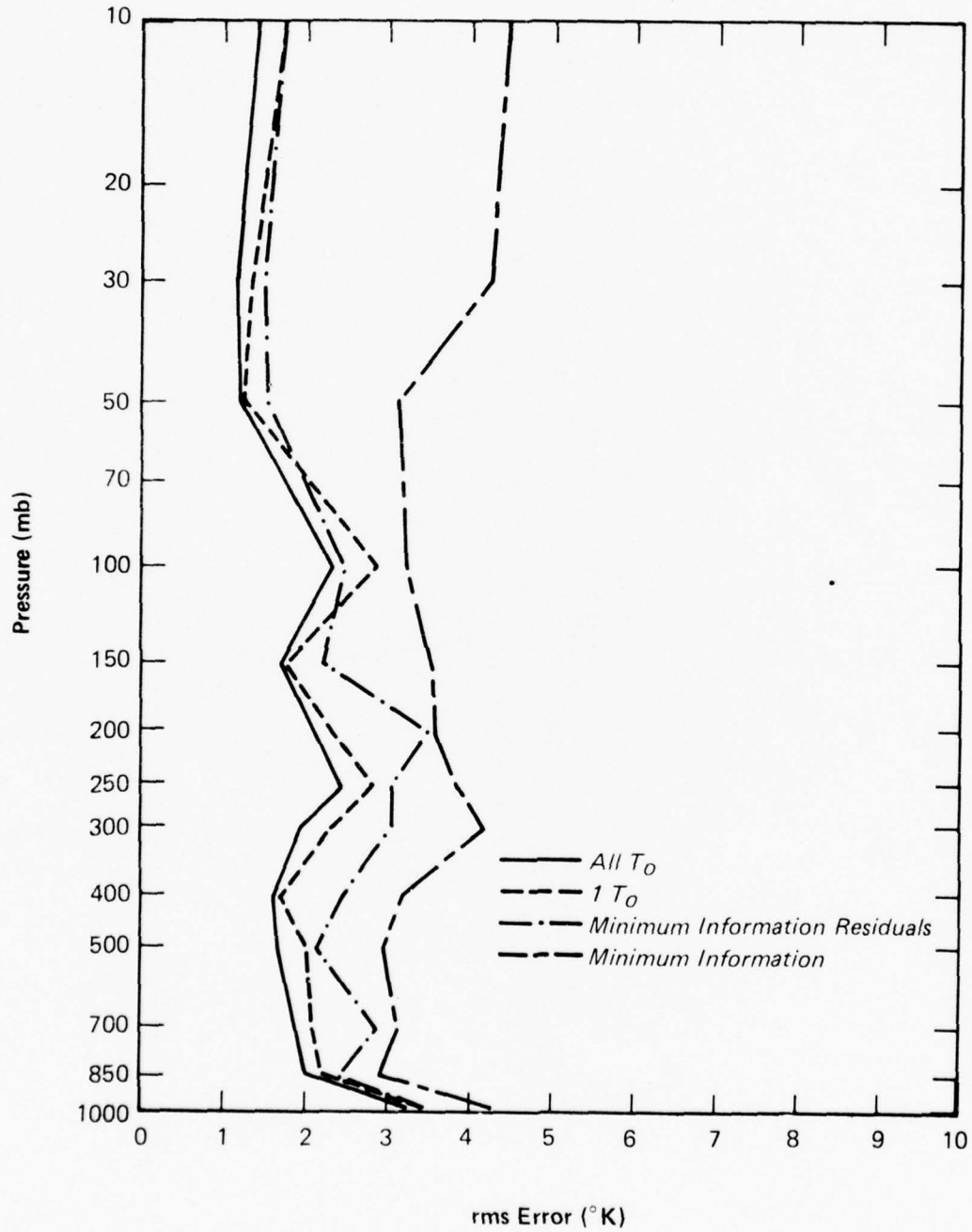Temperature Inversion Error Comparisons

Figure 4.30 Temperature Inversion Error
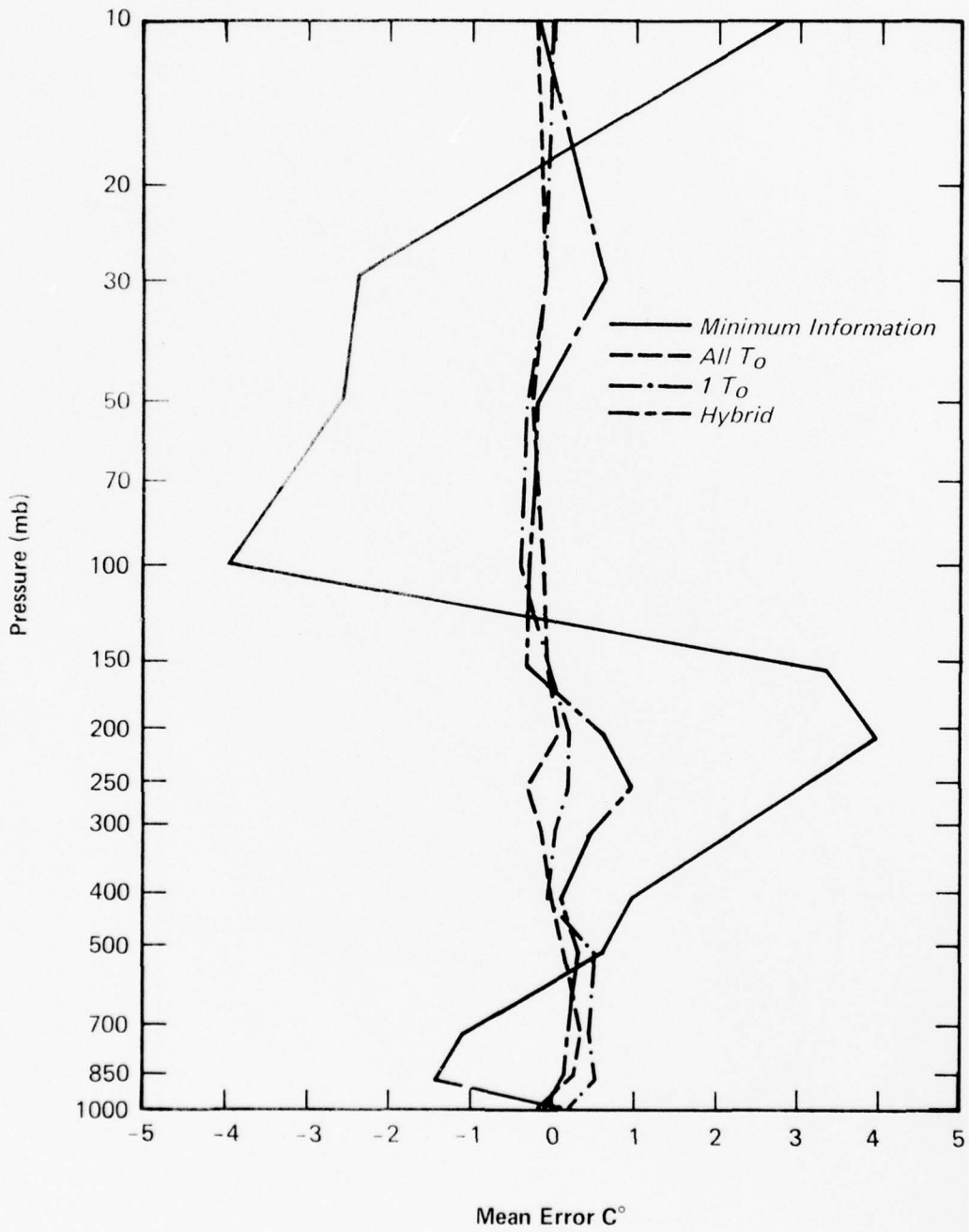Comparisons; $\theta > 0.7$ (2→2)

169

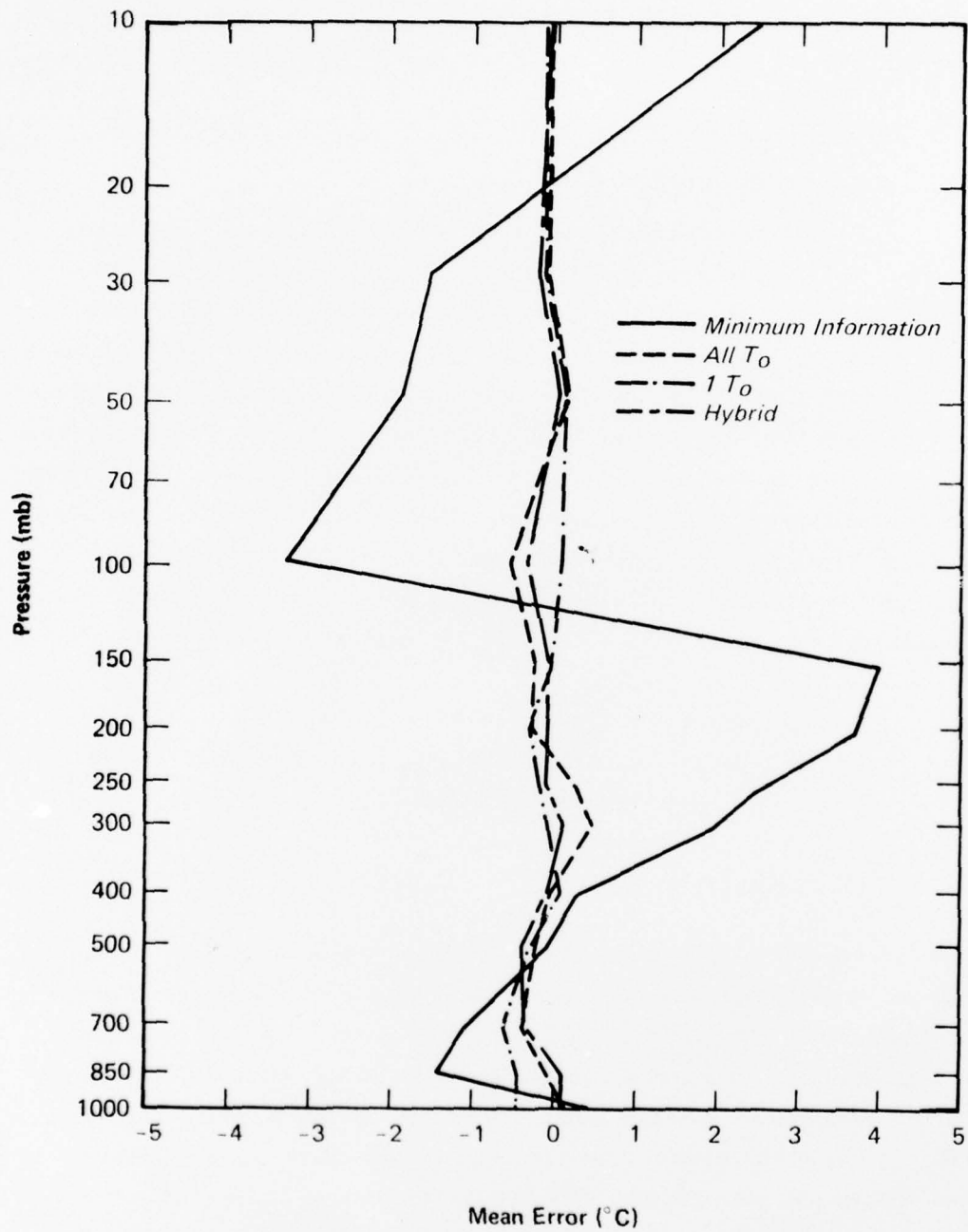Figure 4.31 Comparison of Mean Temperature Inversion Errors; All Data; Week 1

170

Figure 4.32 Comparison of Mean Tempera-
ture Inversion Errors; All Data; Week 2

4.4.3.3 Pressure-Height Inversion

Inversions were performed using pressure-height data for week #1. The data was identical to that used for temperature inversions. The results of performing stepwise regressions on the data, using all first guess temperatures and spectral radiances in the predictor set, are shown in Table 4.11.

4.4.3.4 Comparison of Temperature, Brightness Temperature and Height Inversions

Linear regression models were also generated for brightness temperatures and for pressure height data. The brightness temperature inversions were obtained by first converting the first guess and TTPACK profiles to brightness temperature via Planck's equation and then developing models to minimize the mean squared errors between them, using the brightness temperatures and spectral radiances as predictors. The retrieved brightness temperatures were then analyzed. The pressure-height data used corresponded exactly to the cases used for temperature inversions. An intercomparison of the three types of retrieval errors was made using the percentage of total variation explained, adjusted for the number of degrees of freedom. The results are shown in Table 4.12. The three types of predictands shown are

  (1) temperature (°C)
  (2) brightness temperature (ergs), obtained by converting
        temperatures to equivalent radiances via
        Planck's equation
  (3) heights (ft)

The results for the temperatures and brightness temperatures are quite similar and show a marked degradation around tropopause (200 mb). The height predictands show no degradation at this level since there is no sharp discontinuity in slope as is the case for temperature at tropopause. The height predictands explain about 99% of the variance between 100 mb and 500 mb, while the temperature predictands generally explain between 89% and 96% in the same region, except near tropopause where the value drops to about 70%. Note, however, that R^2 for heights drops below the temperature values below 700 mb. This is probably due to the decreased uncertainty in height, or thickness, first guess profiles near the earth.

172

TABLE 4.11

REGRESSION ANALYSIS FOR HEIGHTS - WEEK #1

Level	p(mb)	rms errors in ft.				
		all data	$\lambda<45°$	$\lambda>45°$	$\theta<0.7°$	$\theta>0.7°$
6	100	164	157	165	171	157
7	150	155	149	164	155	139
8	200	144	125	160	165	148
9	250	139	122	170	152	128
10	300	144	113	174	150	130
11	400	131	96	170	137	119
12	500	114	85	159	118	106
13	700	87	62	116	87	80
14	850	72	48	99	73	67
15	1000	62	46	86	62	63

TABLE 4.12
Percentage of Variation Explained (R^2) for Temperature, Brightness Temperature and Height Inversions
All Data - Week 1

Level	p(mb)	R^2		
		Temperature	Brightness Temperature	Height
1	10	.956	.957	
3	30	.895	.894	
4	50	.942	.948	
6	100	.960	.967	.991
7	150	.932	.933	.994
8	200	.712	.702	.995
9	250	.913	.915	.995
10	300	.959	.965	.993
11	400	.982	.983	.992
12	500	.985	.985	.990
13	700	.984	.985	.984
14	850	.981	.980	.968
15	1000	.975	.976	.929

4.4.4 Regression Coefficients

The regression coefficients for both week 1 and week 2 models are
given here. The models selected for display utilize only the first guess
temperature at the level being retrieved (the 1 T_o case), since these gave
essentially the same performance as using the full profile. Thus the predictor
set, before stepwise regression contained a single first guess temperature (in
degrees C) and eight spectral radiances (in ergs). The regression equation for
the ith level is

$$\hat{T}_i = \alpha_{ii} T_{oi} + \sum_{k=1}^{8} \beta_{ik} r_k + \gamma_i$$

$$i = 1, 2, \ldots, 13$$

with $\hat{T}_i$, T_{oi}, γ_i measured in °C and r_k measured in $\text{ergs}/(\text{cm}^2 \cdot \text{sec} \cdot \text{ster} \cdot \text{cm}^{-1})$.
The coefficients obtained using all data are displayed in Tables 4.13 and 4.14
for all 13 temperature levels. It is interesting that the regression models
are somewhat different for the two weeks although the same general trends are
present, as would be expected. The fact that both models yield quite accurate
retrievals for either week indicates that further reduction in the number of
predictors is probably possible with very little loss of retrieval accuracy.
Further work needs to be done in the area of model reduction. Possible
methods which should be explored include the statistical eigenvector method and
the use of coefficient shrinking techniques such as ridge regression and Stein's
method (see, e.g. Dempster, et al. [4.19]).

175

TABLE 4.13

REGRESSION COEFFICIENTS FOR WEEK # 1

Use One First Guess Temperature

Level	p(mb)	α_{ii}	β_{i1}	β_{i2}	β_{i3}	β_{i4}	β_{i5}	β_{i6}	β_{i7}	β_{i8}	Y_i
						Coefficients					
1	10	.173	-.542	.579	.597	0	0	0	.229	0	-82.6
3	30	.042	-.509	.393	.794	.193	-.226	0	.108	.043	-87.6
4	50	.218	-.567	0	1.503	-.329	-.671	.641	0	-.065	-61.6
6	100	.801	0	-.757	1.690	-.621	-.736	.675	0	-.127	-10.0
7	150	.357	0	-.859	1.736	0	-.995	.530	0	0	-48.4
8	200	.427	.213	-.792	.648	.901	.531	-1.804	.517	.229	-46.9
9	250	.438	.294	-.607	0	1.117	.976	-2.243	.608	.306	-52.5
10	300	.416	.087	0	-.714	.957	.905	-1.745	.511	.246	-47.3
11	400	.811	0	0	0	0	0	0	.080	0	-13.2
12	500	.815	0	.050	0	0	0	.159	0	0	-17.6
13	700	.767	0	0	0	0	0	.103	.048	0	-13.1
14	850	.688	-.263	.588	-.656	0	.914	-.759	.218	.080	-13.9
15	1000	.368	0	.668	-1.413	0	.533	0	.250	0	-25.1

TABLE 4.14

REGRESSION COEFFICIENTS FOR WEEK # 2

Use One First Guess Temperature

Level	p(mb)	Coefficients									
		α_{ii}	β_{i1}	β_{i2}	β_{i3}	β_{i4}	β_{i5}	β_{i6}	β_{i7}	β_{i8}	γ
1	10	.103	-.230	.714	.285	.570	0	-.234	.213	0	-104.8
3	30	.074	-.624	.786	.628	.095	0	0	.054	0	-90.2
4	50	.296	-.587	.411	1.179	-.235	-.770	.893	-.128	-.076	-64.8
6	100	.871	-.390	0	1.061	-.514	0	0	0	.092	-16.4
7	150	.456	-.215	-.557	1.463	0	-.534	0	.163	0	-37.0
8	200	.625	0	-.515	.825	0	0	0	0	0	-31.7
9	250	.556	.424	-1.083	.464	.868	1.034	-2.223	.634	.213	-36.9
10	300	.497	.655	-1.036	0	1.038	1.089	-2.310	.594	.322	-45.4
11	400	.810	0	0	-.244	.405	.503	-.891	.237	.143	-17.3
12	500	.768	-.384	.695	-.664	.634	0	-.225	.192	0	-19.9
13	700	.820	-.390	.686	-.350	0	0	.221	0	0	-13.1
14	850	.820	0	0	0	0	0	.167	0	0	-12.7
15	1000	0	0	.867	-1.423	0	1.373	-.857	.689	0	-60.6

5 CONCLUSIONS

1. On the average, radiances measured at all latitudes and longitudes for Bird 8531 correspond closely with those from Bird 9532.

2. Radiances measured at all Bird 8531 channels, except 4, are greater (warmer) than those from Bird 9532.

3. Criteria used to insure clear column viewing by discriminating against low clouds and hot surfaces (CLDDIF and HOTSF) are far more restrictive in today's operations at AFGWC. Results show that the present SOUNDER accepts only 1/4 as many cases for completing an inferred profile as it did in the 1975 research data set. In fact, out of 10 cases with nearly coincident satellite and RAOB soundings only one case could be retrieved using present-day criteria. Many of the most significant meteorological temperature profiles are being eliminated.

4. Signal to noise ratio and the epsilon value (SNOIS and EPS) are used to control convergence for a solution and to monitor the maximum difference allowable between calculated and measured radiance from any channel. Wide variations in SNOIS and EPS produced insignificant differences in the retrieved temperature profile. The additional computer time required to obtain convergence of a solution was not warranted by the use of the more restrictive values of SNOIS and EPS.

5. Variations in the water vapor profile produce insignificant effects on retrieved temperatures in high latitudes but become dominant for mid-latitude and tropical regions. Errors due to water vapor effects are most pronounced on 850 and 700 mb retrieved temperatures.

6. Underlying surface effects influence the measured radiances at all channels, even those whose weighting functions are near zero at the surface. Accounting for the underlying surface effects is more important than water vapor effects in the mid-and high-latitudes. The type and intensity of the surface effects are highly dependent upon the low level air temperature profile. In fact, a good correlation (0.912) exists between the low level air temperature gradient derived from the forecast data and the retrieved temperature errors at 1000 mb level. It appears that significant improvements in retrieval of 1000 mb air temperatures are attainable.

7. Detailed statistical analysis of DMSP minimum-information retrievals has been made using AFGL data from February 14-28, 1975, with TTPACK data used as truth.

8. A series of linear regression models were developed using forward stepwise regression on TTPack data as the truth model. First guess temperatures and spectral radiances from eight DMSP SSE channels were used in the predictor set.

9. Regression method yields significantly lower mean and rms errors than the minimum information technique over the entire Northern Hemisphere and at all zenith angles.

10. Minimum-information method appears to degrade information during nonlinear processing of input data. (e.g., temperature dependence of water vapor transmittance, CO_2 transmittance function dependence on zenith angle).

11. Zenith angle does not appear to be a significant predictor.

12. It appears that simple regression models may be fitted on weekly data and used for accurate temperature retrievals for the following week. This implies that the data base contained enough statistical variation to yield statistically significant results. More importantly, the results indicate that the regression models might be used operationally for temperature retrievals.

6 RECOMMENDATIONS

1. The acceptance criteria to distinguish between cloudy or hot surfaces, CLDDIF and HOTSFC, need to be reviewed because underlying surface effects appear to be causing vertical soundings to be discarded for low nadir angles and for the most significant types of meteorological profiles.

2. Underlying surface effects must be defined and incorporated before significant analytical or statistical operational improvements can be expected in any satellite temperature retrieval near the earth's surface.

3. A study should be performed using the ALLRADIANCE data to investigate cloud effects and reduce their effect on temperature inversion errors.

4. The effects of sensor center frequency shifts, water vapor uncertainties, and transmission function variations needs to be thoroughly studied.

5. GAC's Research version of SOUNDER is an effective tool that should be used to define more precisely the effects on and improvements to the AFGWC operational version for retrieving temperature profiles from DMSP.

6. Use of statistically-based models should be investigated further for other seasons and with a larger data base.

7. The effect of zenith angle on temperature inversion should be thoroughly investigated.

8. Based on this study, statistical models should be strongly considered for implementation at AFGWC.

9. The use of additional data, such as microwave, and sea surface temperatures should be considered for the temperature inversion problem.

1 L.D. Kaplan, "Inference of Atmospheric Structure from Remote
   Radiation Measurements", Journal of the Optical Society of America,
   Vol. 49, No. 10, 1959, pp. 1004-1007.

2 W.L. Smith, H.M. Woolf and H.E. Fleming, "Retrieval of Temperature
   Profiles from Satellite Measurements with Dynamical Forecasting",
   J. Applied Meteorology, Vol. II, No. 1, Feb. 1972, pp. 113-122.

3 M.T. Chahine, "Inverse Problems in Radiative Transfer: Determination
   of Atmospheric Parameters", Journal of the Atmospheric Sciences,
   Vol. 27, 1970, pp. 960-967.

4 W.L. Smith, "Iterative Solution of the Radiative Transfer Equation
   for the Temperature and Absorbing Gas Profile of an Atmosphere",
   Applied Optics, Vol. 9. No. 9, 1970, pp. 1993-1999.

5 W.L. Smith and H.M. Woolf, "The Use of Eigenvectors of Statistical
   Covariance Matrices for Interpreting Satellite Sounding Radiometer
   Observations", J. Atmos. Sciences, Vol. 33, No. 7, July 1976, pp. 1127-1140.

6 S. Fritz, et al., "Temperature Sounding from Satellites", NOAA
   Technical Report NESS 59, Washington, D.C., July 1972.

7 M.P. Weinreb and H.E. Fleming, "Empirical Radiance Corrections:
   A Technique to Improve Satellite Soundings of Atmospheric Temperatures",
   Geophysics Research Letters, Vol. 1, No. 7, November 1974, pp. 298-301.

8 H.E. Fleming and W.L. Smith, "Inversion Techniques for Remote Sensing
   of Atmospheric Temperature Profiles", Presented at 5-th Symposium on
   Temperature, Washington, D.C., June 21-24, 1971.

9 M.T. Chahine, "Determination of the Temperature Profile in an Atmosphere
   from the Outgoing Radiance", Journal of the Optical Society of America,
   Vol. 58, No. 12, 1968, pp. 1634-1637.

10 D.S. Crosby and M.P. Weinreb, "Effect of Incorrect Atmospheric Statistics
    on the Accuracy of Temperature Profiles Derived from Satellite Measurements",
    J. Statist. Comput. Simul., Vol. 3, 1974, pp.

11 M.S. Malkevich, V.P. Kozlov and I.A. Gorchakova, "On Application of
    the Statistical Method for Determination of Atmospheric Temperature
    Profiles from Satellites", Tellus, Vol. 21, No. 3, 1969, pp. 389-394.

12 W.D. Klein, T.H. Kyle and W.C. Smith, "Special Sensor H Data
    Processing at AFGWC: Preliminary Results", November 1976.

13 W.G. Smith, "The Impact of Measurement Noise on SSE/SSH Vertical
    Temperature Profiles", presented at METSAT Mtg., AFGL., Spring, 1977.

14 R.E. Kalman, "A New Approach to Linear Filtering and Prediction Problems",
    Transactions ASME, Ser. D: Journal of Basic Engineeering, Vol. 82,
    1960, pp. 35-45.

15 M.R. Foster, "An Application of Weiner-Kolmogorov Smoothing Theory to Matrix Inversion", Journal of the Society for Industrial and Applied Mathematics, Vol. 9, No. 3, 1961, pp. 387-392.

16 S. Twomey, "On the Numerical Solution of Fredholm Integral Equations of the First Kind by the Inversion of the Linear System Produced by Quadrature", Journal of the Association of Computing Machinery, Vol. 10, 1963, pp. 97-101.

17 G.E. Backus and J.F. Gilbert, "Numerical Applications of a Formalism for Geophysical Inverse Problems", Geophysical Journal of the Royal Astronomy Society, Vol. 13, 1967, pp. 247-276.

18 N.R. Draper and H.Smith, Applied Regression Analysis, New York, Wiley and Sons, 1966.

19 A.P. Dempster, M. Schatzoff and N. Wermuth, "A Simulation Study of Alternatives in Least Squares", Journal of the American Statistical Association, Vol. 72, No. 357, 1977, pp. 77-106.